MSc Thesis report

Installation Limits of Large Diameter Cold Water Pipes in Deep Water for Land-Based OTEC Plants

August 5, 2015

Author

K. Keesmaat

Thesis committee

Prof. dr. ir. R.H.M. Huijsmans
Dr. ir. S.A. Miedema
Dr. ir. A. Romeijn
Ir. B.J. Kleute

Faculty of Mechanical, Maritime
and Materials Engineering
Delft University of Technology

TU Delft Delft University of Technology

Bluerise harnessing the ocean's power

"The secret of happiness is this: let your interests be as wide as possible, and let your reactions to the things and persons that interest you be as far as possible friendly rather than hostile."
– Bertrand Russell

Acknowledgements

Working on this thesis for the past nine months has been a very valuable and enjoyable time. Being able to completely schedule my own time and work, due to the large freedom provided by Bluerise, has proven to be both challenging and convenient for me. Challenging, due to the fact that motivation can sometimes be hard to muster when working on the same topic for several months, with no finish line yet in sight, especially when the world has to offer such a wide range of interesting things. Taking that into consideration, I am very happy that I was able to finish this thesis within a very reasonable timespan, with for me very satisfying results and surprisingly with significantly less deadline stress than I had initially expected. This would not have been possible without the following people;

First of all, I would like to thank the nice people at Bluerise. Their support and interest was very motivating and gave me the feeling of being a valued member of the team. Being in a room with multiple graduate students also enriched my overall experience of working on this thesis. As we could often help each other out, learn about other cutting-edge topics, share experiences and off course play a game of table tennis to relax. Special thanks go to Berend Jan Kleute, who has been my daily supervisor at Bluerise. He was able to find me a topic that truly suited me well, helped me with brainstorming, coached me in writing a well-structured thesis and has often motivated me to just take a step further.

Second, I would like to sincerely thank the Delft university members of my graduation committee, Professor René Huijsmans, Arie Romeijn and Sape Miedema for their time, support and valuable input, which I took to heart to improve this thesis. You have helped me decide the direction of this thesis at some crucial points, where I was unsure about how precisely to continue and pointed me at what was truly interesting to research.

Finally, I would like to thank my friends and family for providing perfect circumstances for me to work on this thesis. Thanks Mom and Dad, for always supporting me and indulging me with so much unforced free time, which enabled me to complete my study quickly yet laid-back. Thank you Kim, my sweet and loving girlfriend, who has always believed in me, supported me and gave me valuable advise. Without you my life would have been much less enjoyable and the luxury of working on my thesis in the nice city of Antwerp from time to time, provided by you, kind of made large parts of the past nine months feel like a holiday.

Kevin Keesmaat
Delft, August 2015

Abstract

The growing worldwide demand for clean, sustainable electricity generation and energy efficiency offers a valuable opportunity for the large scale implementation of OTEC and SWAC. One of the remaining technological challenges for large scale land-based OTEC and SWAC is the installation of the very large diameter (>2.5 m) cold water pipelines (CWPs) in water depths close to 1000 m, which provide the required cold deep seawater supply.

Therefore, the aim of this thesis is to find and expand the limits of the installation of very large diameter deep water CWPs.

Currently, the largest diameter CWP installed in deep water is a HDPE pipe with a diameter of 1.4 m. The first part of this thesis analyses the limits of the conventional installation method for marine large diameter HDPE pipes. This is done with both an analytical natural catenary model as well as with a FEM Orcaflex model. From this analysis, it can be concluded that the largest HDPE pipe which can be installed using this conventional installation method has a diameter of around 2.3 m (No significant safety factors were included). This is not big enough for large scale OTEC.

To expand this limit, some adjustments are proposed for the conventional installation method, which might slightly increase the installation capabilities. For a significant increase, alternative pipe materials for use with the conventional installation method and completely different installation methods are proposed.

Two alternative pipe materials show promising results to expand the limit of the maximum pipe diameter which can be installed. Especially the very flexible elastomer TPU might provide an almost unlimited increase in installation limit. Further analysis of the materials is however required, to determine whether they are truly suitable for a deep water CWP. Additionally, the higher price and the poor availability in large diameter pipe of alternative materials can limit feasibility.

Four very different alternative installation methods are proposed to increase pipeline installation capabilities. Although these methods are all very promising, detailed analysis is required to assess the true feasibility.

This thesis should suffice as a solid base for future research aiming to establish a reliable method for the installation of very large diameter CWPs. Therewith, hopefully yet another challenge, left for the large scale implementation of OTEC and SWAC, can soon be met.

Contents

List of Tables

List of Figures

"Saving our planet, lifting people out of poverty, advancing economic growth... these are one and the same fight. We must connect the dots between climate change, water scarcity, energy shortages, global health, food security and women's empowerment. Solutions to one problem must be solutions for all."

Ban Ki-Moon, United Nations Secretary General

1 Introduction

Increasing energy use has long been linked strongly to economic growth, often accompanied by a rising standard of living [1]. To be able to continue this line and also provide a high standard of living for people in developing countries, a large, stable and sustainable energy supply will have to be created. An example of expectations considering the world's future development is given in figure 1.1.

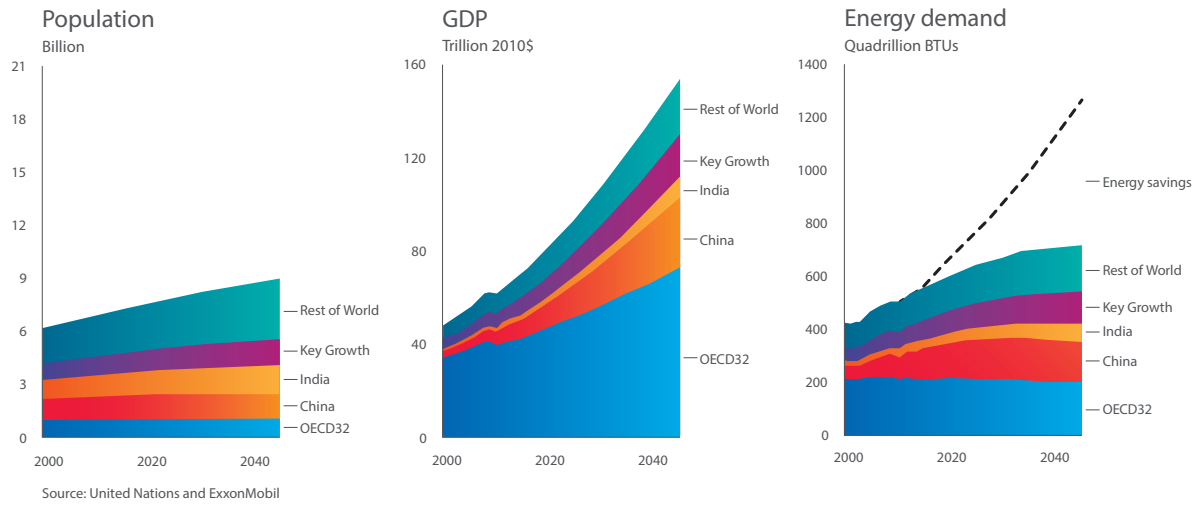

Figure 1.1: ExxonMobil Energy Outlook Expectations [2]

The current large scale use of fossil fuels is not suitable as a big part of this future energy supply. Firstly because fossil fuels will eventually run out and are therefore by definition not sustainable. Secondly fossil fuel production and energy generation comes paired with greenhouse gas emissions. These greenhouse gas emissions are expected to become a problem even before we run out of fossils fuels to burn, as they cause climate change and global warming. Studies have shown that, to prevent catastrophic climate change fossil fuel use will have to be decreased strongly, instead of increased [3].

To fulfil the strongly increasing demand for energy in the future we will therefore need different sources. Sources which don't contribute to climate change, can supply large amounts of energy and are by definition sustainable, to provide for many generations to come.

Wind and solar energy are such sources and have been known for a long time. An additional energy source which is enjoying renewed attention is the ocean. Ocean energy has many disciplines which have promising potential to provide for a large part of the future energy supply [4]. One especially promising technique for harvesting sustainable ocean energy is ocean thermal energy conversion or OTEC. This technique is not commercially available yet and requires additional research and development to achieve commercial large scale.

An additional method to make sure enough energy is available for the future is by decreasing the correlation of energy use with economic growth. This can be done by increasing the energy efficiency of our societies, thus doing more with less.

A measure to be much more energy efficient is to use sea water air conditioning, or SWAC, instead of electric air conditioning. With SWAC the electrical energy demand for cooling can be offset by 75–85%, compared to conventional electric air conditioning [5].

1.1 Ocean Thermal Energy Conversion

OTEC utilizes the difference in seawater temperature between the upper and deep ocean layers to generate electric energy in a thermodynamic cycle. Indirectly OTEC is a form of solar energy, as the sun heats the oceans from which OTEC harvests thermal energy. Since the seawater temperature in different layers of water is relatively stable OTEC can supply base load power; a stable source of sustainable energy 24 hours per day, only fluctuating mildly during the seasons of the year. This results in a very high capacity factor. An additional benefit of OTEC is that in a certain configuration it is able to produce fresh water aside from electricity.

The main process which is used to transform the temperature difference into electric energy is based on a simple Rankine Cycle. In a Rankine Cycle a working fluid is used comparable to the type of fluids used in heat pumps such as household refrigerators. This working fluid is first pressurized as a fluid by an electrically driven pump. Then the pressurized working fluid is heated in a heat exchanger (the evaporator), using the warm seawater from the upper surface layers. This results in a pressurized vapour as the working fluid evaporates at temperatures even below the relatively low temperature of the warm seawater. The pressure and temperature are then decreased by letting the working fluid expand through a turbine. This turbine is coupled to a generator and in this way electric energy is generated. The working fluid is now a vapour at low pressure. Finally the working fluid is condensed into a low pressure liquid state using another heat exchanger (the condenser), which is being cooled by the cold seawater from the deep sea. After this final step the working fluid can be pressurized again by the pump and the cycle starts all over. This process is illustrated in figure 1.2.

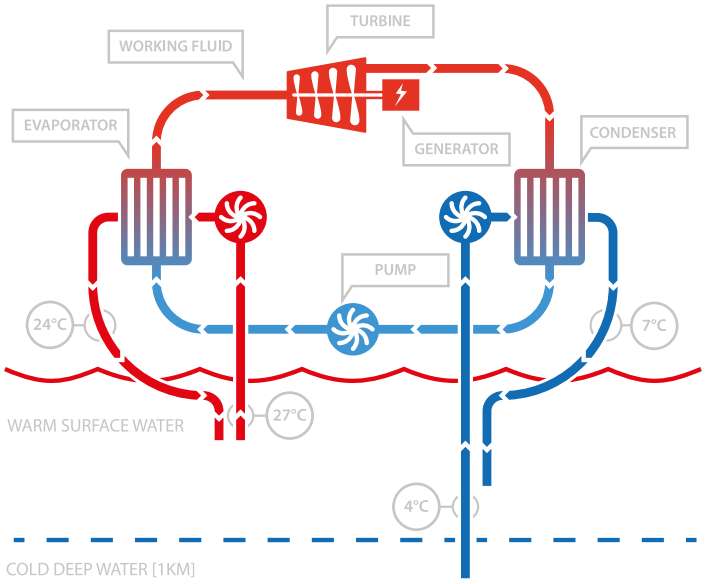

Figure 1.2: OTEC Basic Working Principle [6]

Areas currently enjoying attention for the development of OTEC are situated in the sub-tropics and tropics with nearby access to deep water (>1000 m). Examples of such areas are the islands of Curaçao and Hawaii but also coastlines of countries such as India and China [7].

Surface water in tropical areas can reach temperatures in excess of 25°C. Going down through the water column seawater temperatures decrease quickly. Water masses useful for the cold water intake of OTEC installations are found at depths of 800–1000 m and have temperatures as low as 4–5°C. This temperature difference of 20°C and more is suitable for OTEC to operate [8].

OTEC installations can be divided into two categories; floating/offshore installations and land-based/onshore installations. These two categories are illustrated in figure 1.3. An additional category can be identified as a hybrid between floating and land-based OTEC, although showing more similarities with land-based OTEC; shelf-mounted OTEC.

In the first case a floating OTEC platform is installed at sea, from which pipelines are suspended vertically to collect warm and cold water. The second case features an OTEC installation on land, near the shore. From this installation pipelines run over land and into the ocean to collect the warm and cold water. These pipelines follow the decline of the seabed shelf and slope down into the sea. For land-based OTEC a steep seabed shelf and slope are desired to minimize the length of pipeline required. Shelf-mounted OTEC does at this point in time not enjoy too much attention. It is installed at sea on the seabed shelf, which decreases the length of required pipeline but makes maintenance much more difficult and installation more expensive. Shelf-mounted OTEC should be considered when installing land-based OTEC in an area with a very long seabed shelf, which only declines slowly.

Aside from the hot and cold water intake pipelines, one or more (possibly mixed hot and cold) water outlet pipelines are in position. These pipelines transport the used seawater back into the ocean at a depth corresponding roughly with its temperature, density and

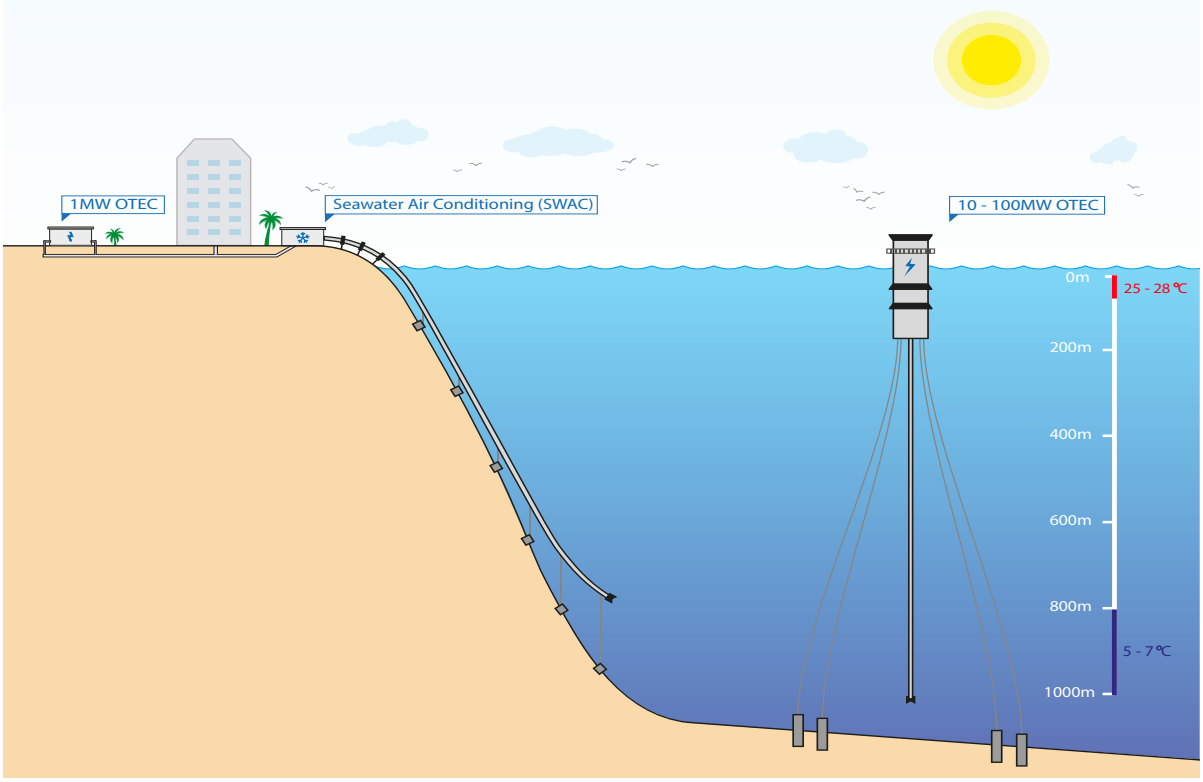

Figure 1.3: Artist Impression of Different OTEC Implementations [9]

salinity. This depth will also ensure that no excess algal growth will occur due to the nutrient rich water.

All three variations of the OTEC technology pose interesting challenges for an offshore engineer. For floating OTEC we can think of the design of the offshore platform or the dynamics of the suspended pipeline. Land-based and shelf-mounted OTEC both require the installation of a large diameter, long length pipelines in deep water. The design of an offshore shelf-mounted OTEC platform (tower) is also an interesting aspect.

1.2 Sea Water Air Conditioning

Seawater air conditioning or SWAC is a technology in which cold seawater is used to generate cooled air for air conditioning. Utilizing the cold seawater to produce chilled water for air conditioning units has the potential to save large amounts of energy, usually required to create chilled water electrically. This can result in great environmental as well as financial costs savings [5].

This technology is especially suitable for areas where lots of cooling is required, that are close to the shore and with nearby access to deep sea water. Alternatively this technology is used with cold lake or river water for appliances located near a large and deep lake or big river.

SWAC is predominantly installed as a land-based facility with cold water intake and output pipelines running into the deep ocean. The SWAC facility primarily houses

heat exchangers, which are used to create chilled fresh water using the cold seawater. From this facility the chilled water is distributed to the customers being for instance cities, resorts, offices, factories or data centres. The chilled water is not always just used for air conditioning but for instance also for direct cooling of factory processes. An alternative appliance for sea water cooling are offshore vessels requiring large amounts of cooling. In particular Floating Production, Storage and Offloading vessels for oil production (FPSOs) use long vertical pipelines suspended from the vessel, to collect cold seawater for the cooling of several processes.

At this point in time land-based OTEC is often combined with SWAC to increase the economic feasibility of these projects. In this way the expensive pipelines to the deep sea can be shared. Similarly ocean ecoparks can be added to further increase economic feasibility. These ocean ecoparks benefit especially from the nutrient-rich deep seawater, which can for instance be used to grow a wide range of marine species.

1.3 Research Objective

Research on land-based OTEC can often be used for a wide range of other appliances such as SWAC and aquaculture. Besides, land-based OTEC is often seen as the first step towards full scale commercialization of OTEC. This is especially true for small energy dependent islands in the tropics, which are at the moment the main target areas for OTEC development [10][11]. Furthermore, currently planned land-based OTEC projects, like on Curaçao, and future projects could directly benefit from more knowledge. Therefore, the focus of this thesis is on research required for the further development of land-based OTEC. Additionally, knowledge gathered from research on land-based OTEC might also prove valuable for shelf-based and even floating OTEC.

Further narrowing down the research topic, it can be concluded that the most challenging aspect of land-based OTEC is the design and installation of the cold water pipe [12][13]. This is especially true from an offshore engineering perspective, which is the context in which this thesis is performed. The cold water intake pipe is specifically targeted as it has to be installed in a much greater depth and has a much longer length compared to the warm water intake and cold/warm/mixed water outlet pipes. Therefore, it will likely be the hardest pipeline to install. Furthermore, CWPs of the size required and in the great depth required for large scale OTEC, capable of commercial power production (multiple MWs scale), have never been installed. From these observations the research objective is set;

Research Objective

To investigate how a very large diameter Cold Water Pipe can be designed and installed for large scale land-based OTEC appliances

This will be done by first establishing a clear picture of the history and current state-of-the-art of deep water large diameter pipeline installations. Both analytical and numerical methods will be used to initially try to expand these established abilities. If these prove insufficient to achieve the required pipeline diameter and depth for large scale OTEC, alternative pipeline designs and installation methods will be investigated. The final

results of this thesis shall offer insights in how to design and install a large diameter cold water pipe suitable for a large scale land-based OTEC plant.

1.4 Thesis Structure

The core structure of this thesis is shown in figure 1.4, to provide a clear insight in the way it is composed. As can be seen from the figure, this thesis starts with an informative section. This is followed by a large modelling theory and results core section. Continuing are hands-on practical sections, providing engineering solutions. Finally the report is concluded and recommendations are given.

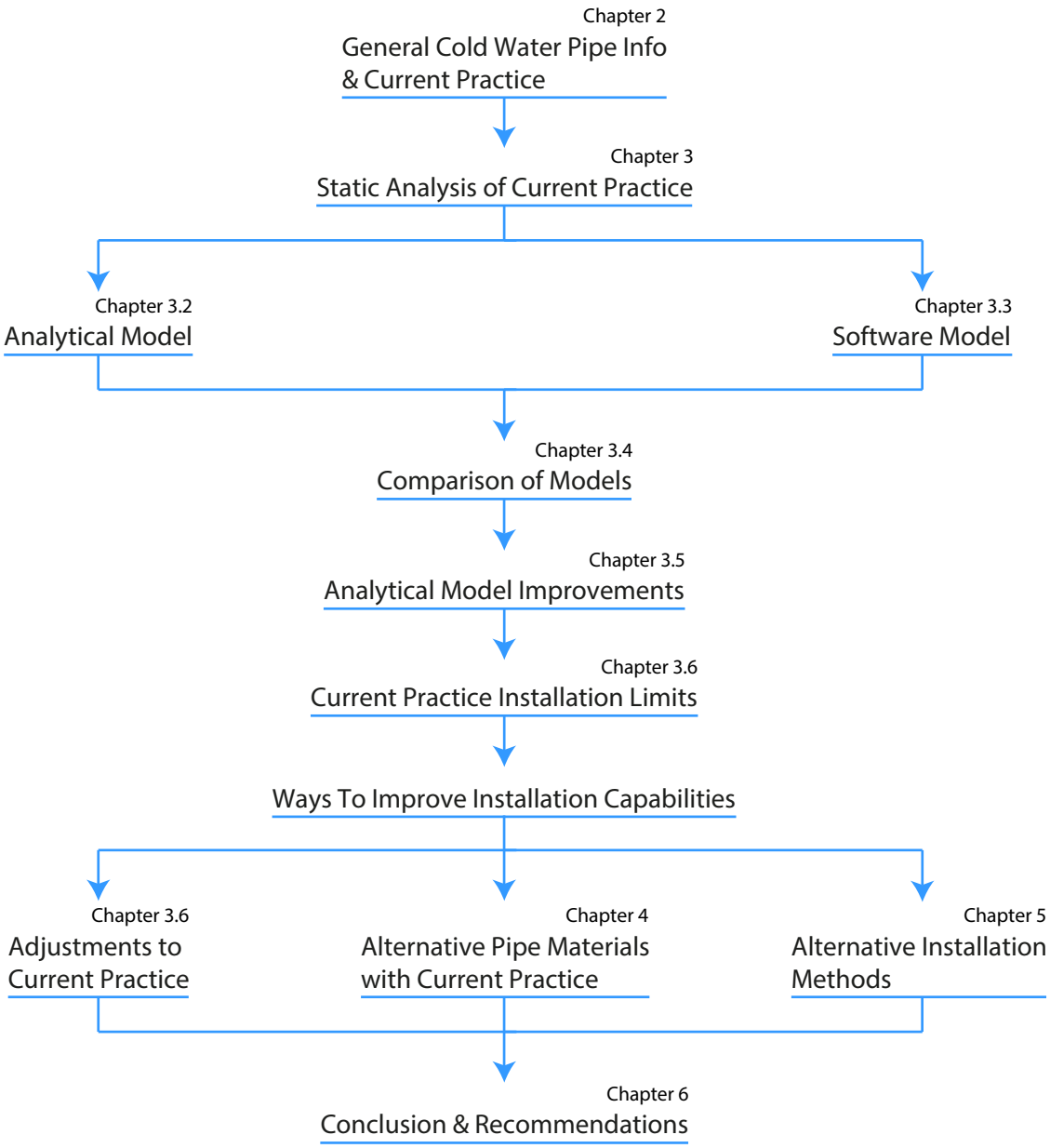

Figure 1.4: Thesis Structure

"Two lessons from the Claude era. First: never underestimate the difficulties of a cold-water pipe. Second: don't let enthusiasm override judgement."

J.R. Chiles on the french OTEC pioneer Georges Claude [14]

2 Cold Water Pipelines

The cold water pipeline (CWP) design and its installation remain among the most expensive and challenging aspects of the successful implementation of OTEC and SWAC [12]. To be able to upscale OTEC and SWAC to a large scale for significant power production/saving, big diameter pipelines are required to provide large quantities of cold water at energy efficient low flow velocities. An example indicating why single large diameter pipelines are most optimal is given in appendix A. Combining the large pipeline diameter with great water depths results in a challenging engineering task. Finally, adding a budget which is considerably lower than equivalent oil pipeline projects limits the possible materials and installation options. A feasibility study performed by Brewer, back in 1979, suggests that for land-based OTEC, commercial electric power generation in the range of 10 to 40 MW is possible. Brewer estimated that this would translate to pipe diameters of 4.6 to 9.1 m [15]. According to Bluerise, the scale currently of interest for the large scale commercialization of land-based OTEC plants on small (sub-)tropical islands is 10 MW. A CWP with a minimum diameter of 2.5 m would currently be required for this type of plant. Cold water pipelines this size have yet to be installed.

2.1 History

The first land-based large diameter cold water pipeline was installed in 1930 by French inventor Georges Claude, to supply the first true OTEC installation. After three failed attempts he finally succeeded to install a deep water pipeline at Matanzas bay, Cuba. This corrugated steel pipeline had a diameter of 1.6 m and was installed in three sections. The planned 700 m of water depth for the cold water pipeline was sadly not achieved after all. As a results the cold water supply was not cold enough and the resulting power production of the OTEC installation was not very impressive [14]. His eventual success in installing such a large diameter pipeline in deep water with very limited means can be seen as an exceptional achievement. Especially since the oil and gas industry, now

known for its great offshore engineering achievements, had at the time barely started with offshore pipelines. The offshore industry and ocean engineering expertise had yet to be established.

After his land-based OTEC efforts, Claude started to work on the first floating OTEC plant. This OTEC plant was planned to create ice for the city of Rio de Janeiro. A vertical pipeline had to be installed below the floating OTEC vessel, which up to this day remains a very challenging engineering job. Claude's attempts failed and he gave up on OTEC [14]. This report will solely focus on the technical challenges encountered with the deployment of a land-based CWP, as those for a floating OTEC CWP are fundamentally different.

OTEC and eventually SWAC research was only truly restarted during the 1970s, as high oil prices were driving interests for alternative energy sources. A small land-based demonstration OTEC plant rated at 100 kW was successfully installed by Japan on the island of Nauru and became operational in 1981. This was the first working land-based OTEC installation after Claude [10]. Japan has since then installed several relatively small diameter pipelines, in example for use in deep sea water research, aquaculture, deep sea water cooled agriculture and OTEC [16].

Aside from Japan, Hawaii has also functioned as an incubator for OTEC research. Around the same time as in Japan the US started financing OTEC research and this resulted in a current total of four installed cold water pipelines on Hawaii [17][18]. These pipelines were installed by Makai Ocean Engineering, which can be considered the world leading expert on this specific subject [5]. The NELHA institute was the primary driving factor behind OTEC research on Hawaii. Aside from a couple of small OTEC pilots, NELHA is known for using the cold seawater for a range of applications in the Hawaii Ocean Science and Technology (HOST) park. Examples of these are SWAC, commercial water sales, aquaculture, general deep sea water research, deep sea water cooled agriculture and so on.

All these more recent cold water pipelines are fabricated out of high density polyethylene or HDPE. HDPE is an excellent material for cold water pipes due to its low thermal conductivity and ease of installation, as it is very flexible and buoyant.

Other applications where large diameter pipelines are used are for instance marine outfalls, water desalinations plants and intakes for industrial cooling water. These can exceed the current records for cold water pipes for OTEC and SWAC by diameter, however these are installed in much shallower waters. The unique challenge of installing very large diameter pipes in very deep water, which is required for large scale OTEC, has never been met before.

A collection of some land-based cold water pipelines of historic or characteristic value is given in table 2.1.

Year	Location	Initiator	Purpose	Pipe Material	Waterdepth [m]	Pipe Length [m]	Pipe Diameter [mm]	Vol. Flow Rate [m^3/s]
1930	Matanzas bay, Cuba	Georges Claude	22 kW OTEC	Corrugated Steel	<700	2000	1600	0.2
1981	Republic of Nauru	Japanese Consortium	100 kW OTEC	HDPE	580	945	700	0.382
1981	Ke-ahole Point, Hawaii	NELHA	OTEC, SWAC, Aquaculture	HDPE	610	1676	305	0.0694
1984	Ke-ahole Point, Hawaii	U.S. DOE / NOAA	OTEC CWP Test Program	FRP	Shallow	24.4	2438	-
1987	Ke-ahole Point, Hawaii	NELHA	OTEC, SWAC, Aquaculture	HDPE	640	1829	475	0.189
1987	Ke-ahole Point, Hawaii	HOST / NELHA	OTEC, SWAC, Aquaculture	HDPE	670	1838	1016	0.845
1999	Cayuga Lake, NY	Cornell University	20 kton lake district cooling	HDPE	76	3219	1600	2.02
2001	Ke-ahole Point, Hawaii	HOST / NELHA	OTEC, SWAC, Aquaculture	HDPE	914	3048	1397	1.70
2003	Lake Ontario	City of Toronto	75 kton lake district cooling	HDPE	115	5000	3x1600	4.38
2006	French Polynesia	Intercont. Bora Bora Resort	450 ton SWAC	HDPE	915	2350	400	0.075

Table 2.1: Previous Land-based OTEC/SWAC CWP Installations [5][10][13][17][19][20][21]

2.2 Materials

When zooming in on the materials which can be used for cold water pipelines, one can see that the majority of recent cold water pipelines is made out of the thermoplastic HDPE. Other well-known materials which have been used or proposed in the past for large diameter cold water pipelines are steel, concrete and GRP/FRP composites [13][15]. A lot wider range of materials has been used in the past for other piping appliances. These materials could also be considered for large diameter cold water pipelines. Examples of such materials are: all sorts of metals, steel reinforced HDPE, PP, PVC, PB and ABS.

Several aspects should be considered when picking a material for a deep sea cold water pipeline for the use in OTEC/SWAC;

- Ease of installation
  - Material weight in water
  - Material flexibility (and minimum allowed bending radius)
  - Allowed Tensile strength
- Resistance to corrosion due to the marine environment
- Thermal Conductivity
- Sensitivity to biofouling
- Surface roughness
- Availability in large diameters
- Material Price
- Sensitivity to fatigue (i.e. during installation or if installed buoyant)

HDPE performs very good on almost all of these aspects, with its high flexibility, negative weight in water, long life-time both fatigue and corrosion wise and cheap to average material price. Furthermore, a lot of experience has been gathered over the past years with deep sea HDPE CWP installations. This experience shows that biofouling is no issue for HDPE and that the pipes have a long life-time [5]. Furthermore, a proven installation methodology for land-based HDPE CWPs is established for diameters up to 1.6 m [22].

Material properties according to one of the biggest and best known long-length large diameter HDPE pipe manufacturers; Pipelife, are given in table 2.2. In this table the design stress represents a limiting stress which can be used to determine the required pipe wall thickness for a load case. These design stress values are lowered with safety factors of 1.6 and 1.25. Without safety factor the design stress after 50 years and at time zero are respectively 10 MPa and 15 MPa. This difference in stress over time is due to the viscoelasticity of HDPE. Strains encountered in relatively short periods of time result in higher stresses than the same strains encountered in longer periods of time. Therefore, the modulus of elasticity for HDPE is also higher for quick deformations than for long-term loads.

Material Property	Unit	Value
Density	kg/m^3	960
Design stress after 50 years	MPa	6.3 / 8.0 *
Design stress at time zero	MPa	9.4 / 12.0 *
Modulus of elasticity at time zero	MPa	1050
Modulus of elasticity after 50 years	MPa	200
Poisson's ratio	-	0.4 – 0.5
Average coefficient of thermal expansion	$°C^{-1}$	$0.2 \cdot 10^{-3}$
Min. Radius of curvature for PE-pipe during sinking (SDR<26)	m	$20 - 30 \cdot D$

* Safety Factors are 1.6 and 1.25 respectively

Table 2.2: HDPE (PE100) Material Properties at T = 20°C [23]

Other sources show higher numbers for the yield stress and tensile strength of polyethylene than pipelife gives as design stress. In example, the Cambridge Materials Data Book provides a yield stress of 17.9 – 29 MPa and tensile strength of 20.7 – 44.8 MPa for polyethylene [24]. Furthermore, the region in which HDPE is linear-elastic is up to about 2% strain [25]. If this fact is combined with the modulus of elasticity of 1050 MPa given by Pipelife, this would result in a stress of 21 MPa at 2% strain. While non-linearity occurs before yielding and far before ultimate failure and thus, higher stresses do not pose a direct threat. Therefore it is assumed that 15 MPa as design stress limit, combined with a Young's modulus of 1050 MPa provides a safe, conservative framework for designing with HDPE.

HDPE is currently fabricated in pipes up to a maximum diameter of 4 m. Manufacturers providing these large diameters are for instance Enviropipes and manufacturers using the largest available KRAH pipe production line equipment. Pipelife produces HDPE pipe with a maximum diameter of 2.5 m.

Most other proposed plastics have properties similar to HDPE, each with its own advantages and disadvantages. Some are more brittle while others are extremely flexible. Care should be taken with plastics, for instance some sorts are degrading quickly when exposed to UV light or have other peculiar characteristics.

The pipeline industry has extensive experience with concrete and steel pipes. However, these materials both have very high densities and might therefore not be very suitable for large diameter, deep water installations. Most common pipeline installation methods would require very large and expensive installation vessels or an enormous amount of added buoyancy to install such a heavy pipeline.

Finally, fibre reinforced composites are a promising, relatively new material. A benefit of composites would be that the material can be engineered to specially suit the demands of large diameter, deep sea water pipelines. A downside is the limited use in past offshore large diameter pipelines and therefore little available experience and high costs.

2.3 Environment

The environment in which a cold water pipe is installed will have a great influence on its design and installation. Several environmental factors can be considered:

- Waves in shallow water
- Current in all water depths
- Seabed morphology (steepness and roughness/irregularities)
- Temperature differences

Waves can induce large forces on structures. The influence of waves is the largest at the water surface and decreases quickly with depth. Therefore the influence of waves on the cold water pipeline is most distinct during the installation, when the pipeline is at the water surface, and in the shallow-water area where the pipeline enters the sea. Breaking waves can especially induce large impact loads. Therefore pipelines are often protected from these in the surf zone, by for instance trenching or by covering the pipeline with rocks.

Ocean currents also induce forces on sub-sea structures. Unlike waves, currents can still be significant near the seabed in greater water depths, as the current induced water velocities decrease much slower with depth. In general, the water velocities due to currents are most distinct at the sea surface. Currents have much more stable velocities than waves, but without doubt have to be considered for the pipeline stability on the seabed. Currents also impact the pipeline installation, increasing installation loads. Furthermore, currents and waves can induce scour, a phenomenon in which the soil (sand) around a structure is washed away. This can potentially destabilize the pipeline.

Seabed shelves and slopes suitable for land-based OTEC are generally quite steep. This steepness increases the pipeline installation difficulty. Sudden changes in steepness can also be problematic as these can induce permanent bends or suspends in the installed pipeline. Furthermore the seabed can also be quite rough with lots of irregularities and sharp edges. An example of such a seabed is one consisting of volcanic rock with many outcroppings and irregularities, as can be found on Hawaii [26]. It is considered best to avoid such sections of seabed, as they can damage the pipeline. A manner to do so is by installing the pipeline buoyant, floating above the seabed [26]. It is thus very important to carefully study the seabed morphology of an intended OTEC site, as it will strongly influence the pipeline design and installation method.

Temperature differences in the water in which the pipeline is installed can cause internal stress in the pipeline and will increase or decrease its total length. The sensitivity to temperature depends on the material chosen for the pipeline. The cold water pipeline will experience both warm water near the surface and quite cold water near the bottom at the same time.

An additional type of load which can be encountered by the cold water pipe are incidental loads. This are loads which are hard to predict and thus hard to anticipate on. Examples of such loads are dragging anchors or dropped objects, human error or equipment failure during installation and earthquakes [27].

2.4 Installation

Several methods have been used in the past to install pipelines. Regular steel (oil & gas) pipelines are most often installed using S-lay, J-lay or reel-lay pipe-laying vessels [28]. Pipe-laying vessels use tensioners to control the pipeline tension and a stinger to support its overbend. The principle of S-lay is illustrated in figure 2.1. A benefit of these vessels is that they offer great control over the installation parameters and are thus a low risk option. However, large diameter, deep water pipe-laying vessels have very high day rates and thus far are not able to install as large diameter pipelines as required for large scale OTEC. An illustrative example of this is the fact the world's largest offshore construction vessel, the Allseas Pioneering Spirit, is only able to lay pipe up to a diameter of 68 inches (about 1.73 m) [29]. Therefore, these conventional installation methods are not considered as feasible for OTEC.

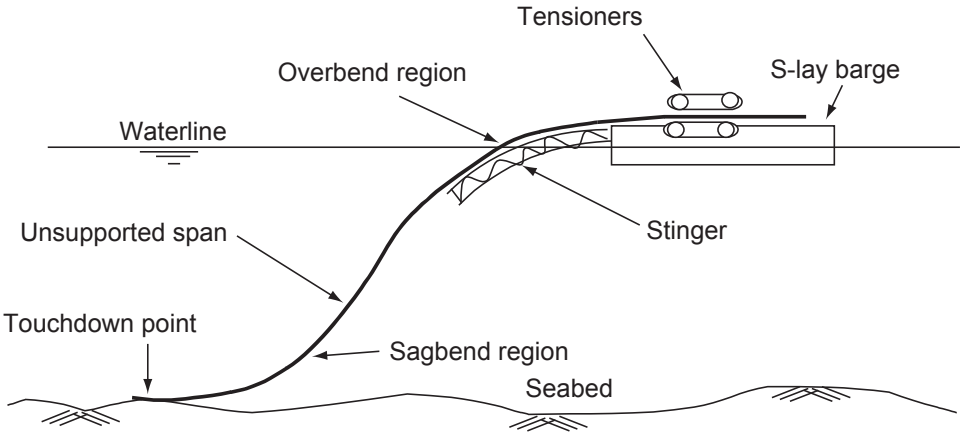

Figure 2.1: Conventional S-lay Method [28]

Other methods established for offshore pipeline installations are tow-methods. These can be separated into four categories [28]:

- Bottom tow
- Off-bottom tow
- Mid-depth tow
- Surface tow

Bottom tow is performed by pulling the pipeline to it is projected position by letting it slide over the seabed. This requires a smooth seabed surface and added protection to the pipeline to ensure the pipeline is not damaged during the bottom tow installation.

With off-bottom tow the pipeline is being towed whilst floating just off the seabed. This is done by first ensuring the pipeline itself is slightly buoyant. Then, free hanging chains are attached to the pipeline to ensure it does not float up to the surface but remains at a controlled distance above the seabed. Extensive seabed mapping is also required for this method, to be able to avoid irregularities in the seabed. Furthermore careful engineering of the balance between the pipeline weight / buoyancy, chain weight and potential buoyancy tanks is required.

The configuration for mid-depth tow is slightly similar to off-bottom tow. Two tug boats are now pulling the pipeline in opposite direction, one on the front and one at the end of the pipeline. In this way the exact depth and shape of the pipeline can be controlled quite accurately. Once the pipeline arrives at its final destination, the tension can be decreased and the pipeline is gradually lowered to the seabed.

The last tow installation method is surface tow. The pipeline is now buoyant, filled with air or equipped with buoyancy tanks, and positioned at the sea surface during transportation and positioning. For this method no chains for added weight are used. The pipeline can be lowered to the seabed by controlled flooding of the pipeline or buoyancy tanks. This is a delicate operation where the tension in the pipeline is very important to prevent buckling. The installation curvature of the pipeline looks similar to the s-lay installation method.

Figure 2.2: Pipelife long length HDPE Pipe Bundle Surface Tow [30]

Most previous OTEC cold water pipes have been installed using the surface tow method. This is due to the fact that it is quite a simple method and that no expensive equipment is required, which makes this method very cheap and practical. Surface tow is mainly performed with HDPE pipe, which due to its slight natural buoyancy in seawater floats by itself. Figure 2.2 shows the manner in which large diameter, long length HDPE pipe is transported overseas. The surface tow installation method, combined with HDPE pipes, is also commonly used for other marine outfalls and seawater intakes. Furthermore it is an established method for pipeline diameters of atleast up to 1.6 m and in depths suitable for OTEC [22]. A more detailed description of this promising method and how it is applied for CWPs is given;

2.4.1 Float and Sink Installation Method

The installation part of the surface tow method, from here on called the float and sink method, has been the method of choice for past OTEC/SWAC HDPE cold water pipe installations. This method has been used by a range of OTEC pioneers. Georges Claude first used a float and sink method using steel pipe and buoyancy tanks to install his land-based OTEC cold water pipe [14]. Furthermore all four cold water pipelines on Hawaii and several SWAC pipelines have been installed partly or wholly using this method [18].

The pipeline sections are first transported to the installation site, floating on the sea surface. At or near the installation site, these pipeline sections are then joined (predominantly using butt fusion joining/welding) to form the complete pipe string. Connecting the pipe sections can be performed on land as well as at sea. Weights are connected to the pipeline to ensure that the naturally buoyant HDPE pipe has sufficient weight to sink once flooded and will remain stable on the seabed. In some previous projects, sections of the cold water pipeline where not directly weighted. Weights were connected to the pipe, but suspended a predetermined distance below the pipeline using a collar and cable. In this way the pipeline would remain floating a certain distance above the seabed, instead of lying directly on it. This approach is mainly used to avoid seabed irregularities.

Finally, the pipeline is pulled into position using a tug boat on the offshore end and secured in place on the onshore end. By flooding the pipeline from the onshore end and controlling the amount of air which leaves the pipe on the offshore end, the pipeline can be sunk in a controlled way. Tension is still applied to control the catenary shape of the pipeline during sinking. The float and sink procedure is shown in figure 2.3.

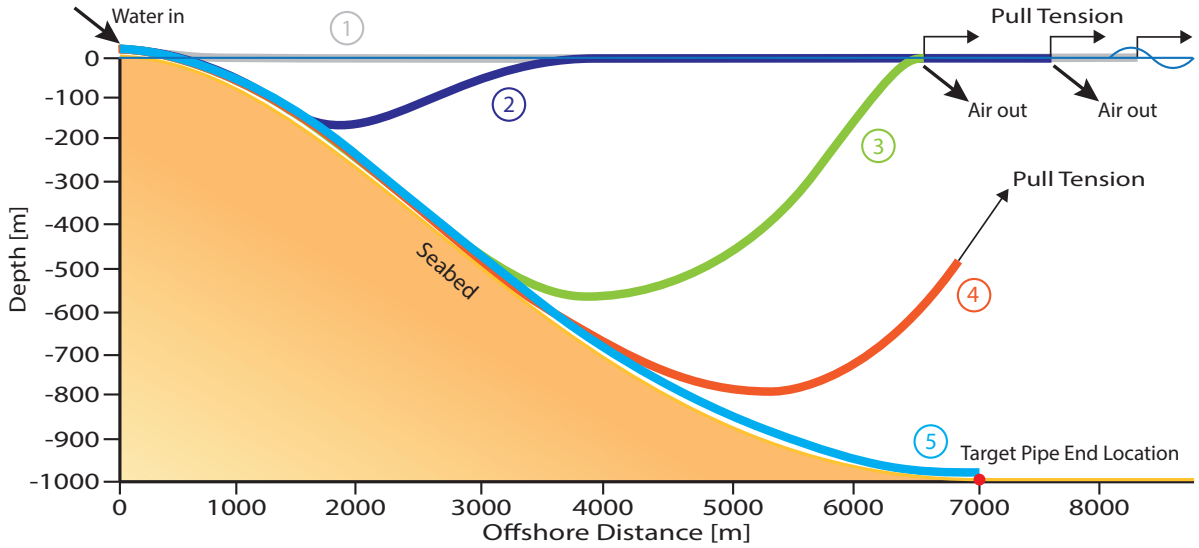

Figure 2.3: Float and Sink Procedure

The pipeline can be retrieved to the sea surface again by pumping air back into offshore end of the pipeline. This reverses the sinking process. The ability to retrieve the pipeline can be very useful to abort the installation if some unforeseen events occur. The technical principle of sinking the pipeline by flooding is further illustrated in figure 2.4.

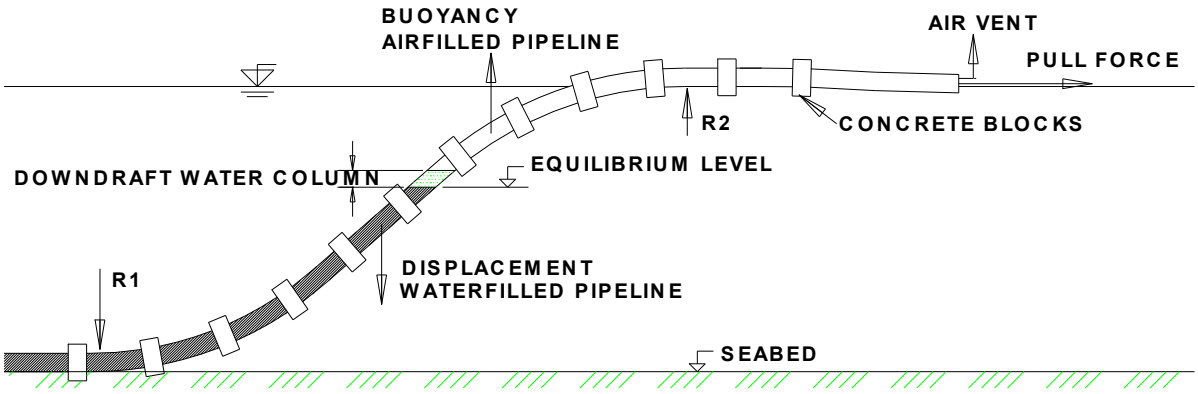

Figure 2.4: Flexible Pipeline Sinking by Flooding Technique [30]

Considering the fact that this method currently is the industry standard for installing HDPE pipelines of considerable diameter in deep water, this thesis will initially focus on this method. The method will be modelled to see whether it is technically feasible for the installation of very large diameter pipelines, the size of which is suitable for large scale OTEC. If it is not, both with HDPE and other pipe materials, alternative methods will be proposed to look for an installation method which can provide a satisfying result.

"For land-based plants, there is a validated design for high-density polyethylene pipes of diameter less than 1.6 m."

L.A. Vega [22]

3

Static Analysis of the Conventional CWP Installation Method

The method currently used for most deep water, medium to large diameter cold water pipelines is the float and sink method. In this method the pipeline is initially floating on the sea surface, above its target location. The pipeline is then flooded from the shore in offshore direction, which will sink it to the seabed. As a result, the pipeline will have an S-like shape during the installation. In this situation the bottom-left part of the S is resting on the seabed and the top-right part is positioned at the sea surface. This is shown in figures 2.3 and 2.4. Eventually when the pipeline offshore end is reached it will be lowered to the seabed in a controlled way. The installation curvature will now look like a J, until the offshore end touches down on the seabed.

To understand the scale up to which this installation method can be used, the installation procedure will be modelled. Using this model the pipeline curvature and stress in the pipeline can be determined during all phases of the installation. In this way, using the known limits of the material, the limits of the installation method can be found. It is expected that either the minimum curvature allowed is first exceeded or the maximum allowed stress.

The final moment where the pipeline still has an S-shape, just before transitioning into J-lay, is considered to be the most critical situation. At this point the longest length of pipe is suspended, which likely results in the most severe loads. Therefore, this is the situation which will be taken as governing for the pipeline installation limits.

For the initial model, the material properties of HDPE PE100 (Pipelife) will be used. HDPE appears to be the most optimal material which has a good combination of the desired aspects as discussed in section 2.2. Furthermore, it has been used in multiple similar projects and is therefore part of the current practice or conventional method. In this study, the installation limits of HDPE CWPs are therefore first examined. If HDPE turns out to be unsuitable for very large diameter CWPs another material can

Target Input Waterdepth	1000 m
Seabed Slope Steepness	1:7
Pipe External Diameter	1.4 m
Pipe diameter/wall thickness ratio SDR	18
Pipe Material Properties	HDPE PE100, see table 2.2
Air Fill Ratio (determining pipeline weight)	0.2
Installation Pull Force	50 t
Design Wave Height / Current Speeds	Not included in static analysis

Table 3.1: Base Case Parameters; Curaçao

be selected. This material should compensate the specific shortcomings of the HDPE whilst not failing at other aspects.

A range of variables can be identified for the installation of a cold water pipeline:

- Waterdepth
- Seabed Slope Steepness
- Pipe Diameter
- Pipe Wall Thickness
- Pipe Material Properties
- Pipeline Weight
- Installation Pull Force / Top Tension
- (Environmental Conditions (Waves, Current))

The sensitivity of the pipeline installation method to all of these variables will be checked to see the influence of changing one of these. In this way the design of the pipeline can be optimized and configured for the installation parameters.

For the base case model, parameters approximately corresponding to the planned Curaçao CWP installation will be used. These can be found in table 3.1.

3.1 Model Theory

Pipelines can be modelled using a range of theoretical models, both analytical and numerical. Some examples of commonly used theoretical models are [28]:

- Natural Catenary Theory
- Stiffened Catenary Theory
- Elastic Beam Theory
- Non-linear Beam Theory

- Elastic Rod Theory
- Finite Element Method

These methods each have their restrictions. For instance the natural catenary theory assumes negligible bending stiffness and no axial deformation. The elastic beam theory does consider bending stiffness but is limited to small deflections. Improved and more complex versions of the natural catenary theory and elastic beam theory; the stiffened catenary theory and the non-linear beam theory do allow for a wider range of use. The finite element method can generally be used and is often implemented as Finite Element Analysis (FEA) in engineering software packages.

The natural catenary theory will be used for creating a first analytical model of the float and sink installation procedure in section 3.2. As the pipeline is installed in very deep water and made out of relatively flexible HDPE it is expected that the influence of stiffness will be almost negligible, thus making this theory suitable for a first quick model. Furthermore, the effect of stiffness would decrease critical bends, which renders the natural catenary theory conservative.

A situation similar to the one encountered in this thesis are deep water marine risers. Comparative modelling using the natural catenary theory and stiffened catenary theory shows very little influence of stiffness in deep water steel catenary risers [31].Furthermore, the fact that the natural catenary theory allows for analytical modelling instead of numerical modelling makes it easy to use. Analytical modelling also provides a deeper understanding of the fundamental behaviour of a system, compared to more abstract numerical models.

Furthermore, a range of industrial software packages is available for calculating loads in marine pipelines during installation. Examples of these are:

- Orcina Orcaflex
- Ansys Aqwa
- Simulia Abaqus FEA (ABAQUS)
- Flexcom-3D

A comparative, second study will be performed in section 3.3 and 3.4 using engineering software, to verify the results of the first analytical natural catenary model. Using multiple approaches to solve the same problem may additionally lead to a better understanding of the problem.

Orcina Orcaflex is chosen for this verification as it uses sufficiently different modelling theory, is specifically designed for marine statics and dynamics problems, is easy to use and available at the Delft University of Technology. Orcaflex is widely used in the marine pipeline, offshore mooring, marine power cable and riser industry and is specialized for modelling these kinds of offshore applications. It provides static as well as dynamic analysis of complete offshore systems, using finite element and lumped mass element methods to do so. Furthermore it can deal with large deflections, which is required for the float and sink installation method [32]. A simplified illustration of how finite element model theory is used inside Orcaflex is shown in figure 3.1.

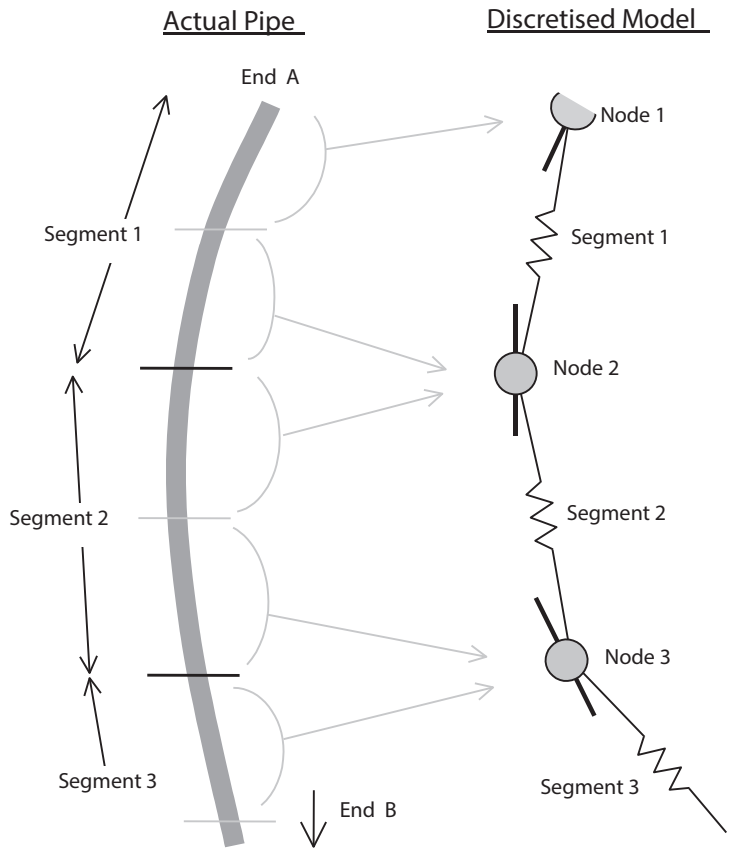

Figure 3.1: Orcaflex Finite Element Method Theory Implementation for Lines [32]

3.2 Analytical Model

The natural catenary theory can be used to describe the curvature of a chain or chord with a specific weight and under a certain tension. In this theory it is assumed that the catenary line has no bending stiffness and is inelastic. This theory has a long history of usage in the offshore industry, primarily for modelling catenary line moorings. An overview of the catenary curve as modelled with natural catenary theory is given in figure 3.2.

The equation which describes the catenary curve is given in formula 3.1 [33].

$$z = c\cosh(\frac{x}{c}) \tag{3.1}$$

where;

$$c = \frac{H_0}{w} \tag{3.2}$$

and;

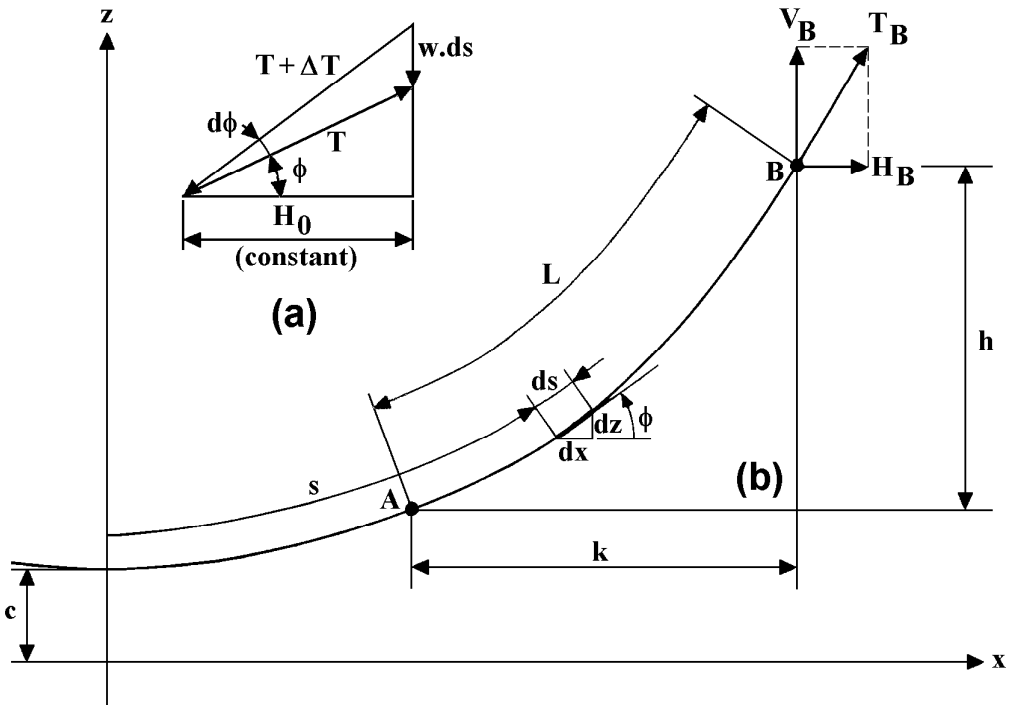

Figure 3.2: Catenary Line Model Sketch and Parameters [33]

z = vertical coordinate of catenary curve
x = horizontal coordinate of catenary curve
c = Uniform scaling parameter
H_0 = Horizontal tension at the horizontal base of the catenary
w = Catenary line weight per unit length in water

In this model horizontal forces on the pipeline, other than the horizontal pull tension, are not included. Examples of such forces would be caused by waves and current. Therefore by static equilibrium, the horizontal tension in the pipeline at the horizontal base of the catenary (H_0) and the rest of catenary is equal to the horizontal top tension applied by the tug boat to control the catenary.

The catenary line weight in water w is determined by the pipeline dimensions, pipe material and the chosen air fill ratio a_a. The air fill ratio represents the ratio between the vertical height of the overbend section and the vertical height of the sagbend section of the pipeline, where the upwards and downwards forces are in equilibrium. The overbend section is filled with air while the sagbend is filled with water. This principle is sketched in figure 2.4. If the depth down to which the pipeline is filled with air is equal to the air fill ratio multiplied with the total vertical height of the pipeline string, the pipeline is in static equilibrium and will remain in position. The air fill depth can be increased or decreased by increasing or decreasing the air pressure in the pipeline. As a result the pipeline will start raising or sinking.

The air fill ratio itself is determined during the design of the pipeline and can be controlled by adding weight or buoyancy to the pipeline. This is generally done by securing concrete collars to the pipeline. More added weight and thus a higher w will result in a bigger air fill ratio. Furthermore, heavier pipe due to added weight has greater stability on the

seabed once installed. Figure 3.3 shows weighted HDPE pipe at the sea surface, before it is flooded and sunk.

Figure 3.3: HDPE pipe with concrete weights before installation [30]

The air fill ratio can be determined using formula 3.3, which is derived from vertical static equilibrium of forces (weight and buoyancy) of the pipe [23].

$$a_a = \frac{w_{cw} + w_{pipew}}{\pi \frac{d^2}{4} \gamma_w} 100\% \tag{3.3}$$

where;

a_a = air fill ratio
w_{cw} = weight of concrete weights in water distributed per meter pipe
w_{pipew} = weight of pipeline in water filled with water per meter pipe (negative for HDPE)
d = pipeline internal diameter
γ_w = Specific gravity of surrounding water

Rewriting formula 3.3 provides the ability to calculate the required weight of concrete weights per meter pipe, given the desired air fill ratio:

$$w_{cw} = \frac{a_a \pi \frac{d^2}{4} \gamma_w}{100\%} - w_{pipew} \tag{3.4}$$

where;

$$w_{pipew} = \frac{\pi g}{4}((D^2 - d^2)\rho_{pipe} + (d^2 - D^2)\rho_w) \tag{3.5}$$

and;

g = gravitational acceleration
D = pipeline external diameter
ρ_{pipe} = Pipeline material (HDPE) density
ρ_w = Seawater density

By summing the weight of the concrete weights and the weight of the pipeline, the net pipeline weight in water per meter of pipe; w can be found. This is done for both the water-filled sagbend section and the air-filled overbend section of the pipeline in formula 3.6 and 3.7.

$$w_1 = w_{cw} + w_{pipew} \tag{3.6}$$

$$w_2 = w_{cw} + w_{pipea} \tag{3.7}$$

where;

$$w_{pipea} = \frac{\pi g}{4}((D^2 - d^2)\rho_{pipe} + d^2\rho_a - D^2\rho_w) \tag{3.8}$$

and;

w_1 = Water-filled sagbend section pipeline weight per meter
w_2 = Air-filled overbend section pipeline weight per meter
w_{pipea} = Weight of pipeline in water filled with air per meter pipe
ρ_a = Air density

Continuing with the catenary theory, these calculated pipeline parameters can be used to further determine the catenary characteristics. For instance the parameter s, which represents an axis along the catenary curve. This parameter thus measures the length of the pipeline from the horizontal base of the catenary, where $s = 0$, dependent of the horizontal distance. The relation for finding s is given in formula 3.9 [33].

$$s = c\sinh\frac{x}{c} \tag{3.9}$$

Furthermore, the horizontal and vertical force components and resulting tension can be determined using formula 3.10, 3.11 and 3.12 [33].

$$H = wc = \text{Top Horizontal Pull Tension} \tag{3.10}$$

$$V = ws = wc\sinh\frac{x}{c} \tag{3.11}$$

$$T = \sqrt{H^2 + V^2} \tag{3.12}$$

where;

H = horizontal force in pipeline
V = Vertical force in pipeline
T = Tension in pipeline

Other useful parameters for assessing a pipeline installation configuration are the angle of the section of pipeline relative to the horizontal and the bending radius. These can also be directly derived from the normal catenary theory. The angle of the catenary relative to the horizontal is given in formula 3.13 [33]. The bending radius can be derived by differentiating the slope of the catenary with respect to s. The slope of the catenary is given in formula 3.14 and is differentiated in formula 3.15. The resulting formula for the bending radius of the catenary is given in formula 3.16 [34].

$$\phi = \arctan \sinh \frac{x}{c} \tag{3.13}$$

$$\frac{dz}{dx} = \tan \phi = \frac{ws}{H_0} \tag{3.14}$$

$$\frac{1}{\cos^2 \phi} \frac{d\phi}{ds} = \frac{\kappa}{\cos^2 \phi} = \frac{w}{H_0} = \frac{1}{c} \tag{3.15}$$

$$R = \frac{1}{\kappa} = \frac{c}{\cos^2 \phi} \tag{3.16}$$

where;

ϕ = Pipeline section angle relative to horizontal
R = Radius of Curvature or Bending Radius
κ = Curvature

3.2.1 Float and Sink Natural Catenary Model

For this model two catenaries have been connected to each other. The first catenary represents the sagbend of the pipeline. The second catenary is flipped horizontally and vertically and represents the overbend. This is illustrated in figure 3.4.

The boundary conditions of the catenaries are such that the axial tension and pipeline section angle should be the same at the intersection point between the sagbend and overbend. Furthermore, the sagbend catenary is connected to the seabed where its slope is the same as the seabed slope at the touch down point (TD). The overbend catenary

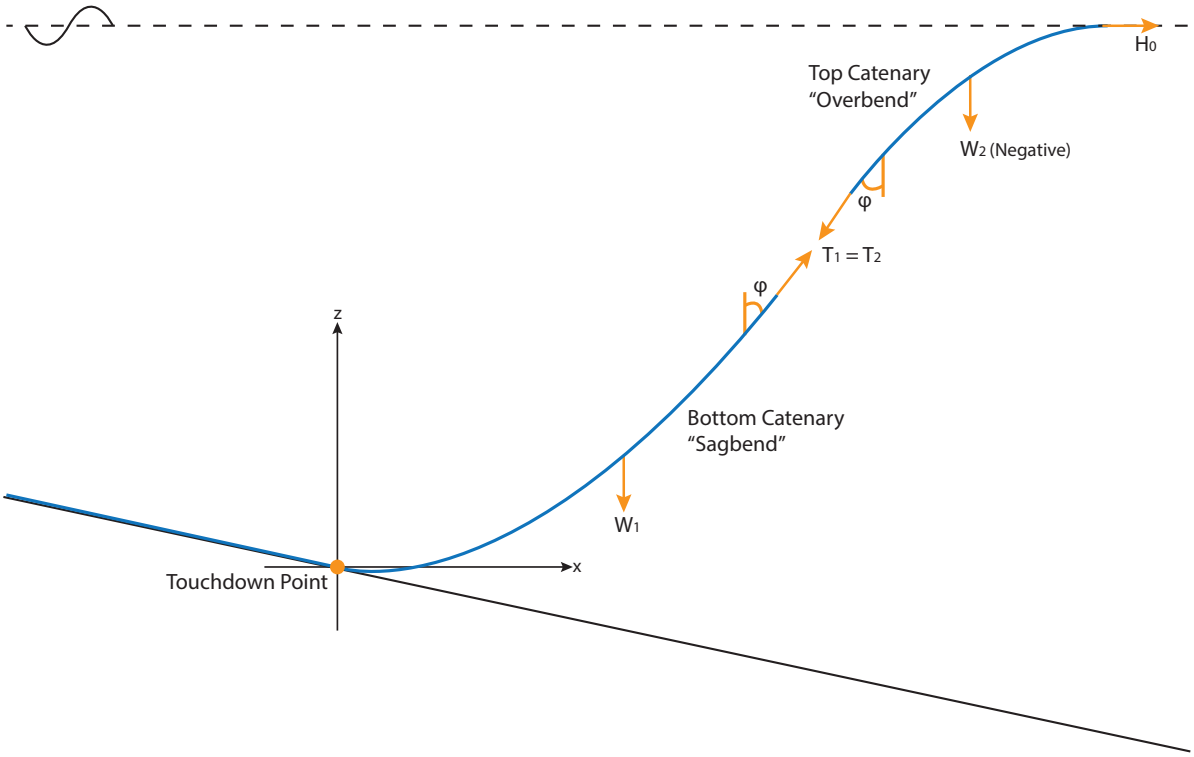

Figure 3.4: Float and Sink Combined Catenary Model

executes when it is completely horizontal, at the sea water surface. The top tension / pull force on the overbend catenary is assumed in line with the pipeline end and thus completely horizontal.

The model is created using Matlab, which is also directly used to generate the corresponding figures used in this report.

Although the natural catenary theory is an analytical theory, some numerical loops have been included in the Matlab model. This was for instance required to find the exact ratio between the heights of the two catenaries. Another numerical step was included to find the depth at which the pipeline would leave the seabed in the most critical s-lay configuration, for a certain target installation depth. This was required as the pipeline touch down depth, where the pipeline transitions from lying on the seabed to the suspended catenary, depends on the length of pipeline suspended in the catenary. This suspended length, from TD to horizontal at sea level, should be exactly sufficient to reach the target installation depth.

Furthermore, it shall be noted that this model is purely static and no dynamic factors are included. Also environmental disturbances such as waves and current are not included. Therefore a significant safety factor will have to be implemented in the design of a cold water pipe using this model.

3.2.2 Results

To test the Matlab model, the base case parameters from table 3.1 are used as input. An overview of the resulting installation catenary configuration in the most critical configuration can be found in figure 3.5. The plotted scenario shows the pipeline at the point where it is about to transition from s-lay to j-lay and thus where the pipeline end is about to submerge below the sea surface. Therefore, the suspended length of both catenaries combined should be sufficient to precisely reach the target pipeline end position depth, shown as a red dot in figure 3.5.

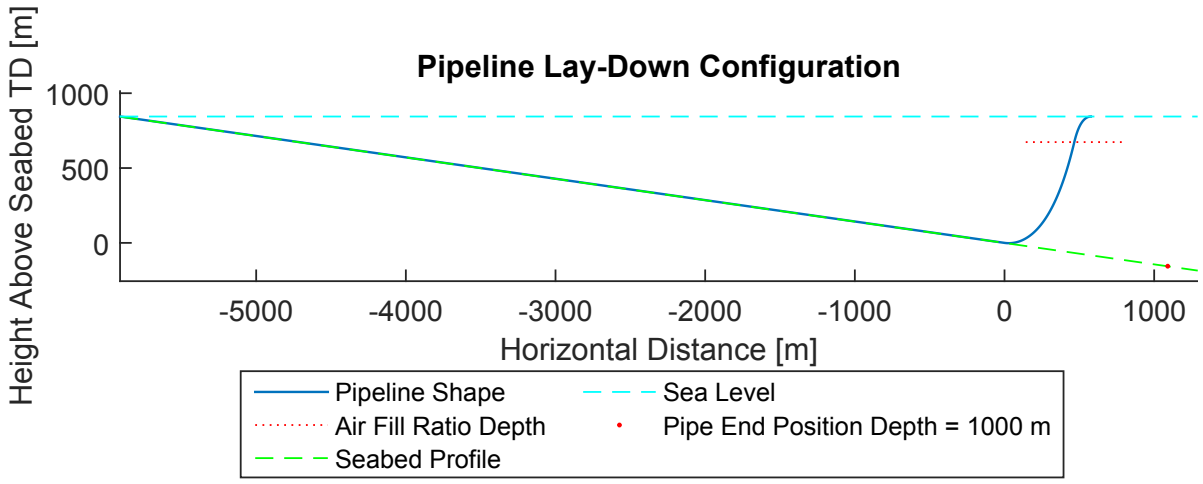

Figure 3.5: Pipeline Installation Catenary Configuration

At first glance, the model seems to produce plausible results in terms of what the installation configuration looks like.

More interesting are the effects of the actual loads on the pipeline during the installation, such as the axial tension in the pipeline and the curvatures encountered by the pipeline. These are given in figure 3.6 and 3.7. Here, the minimum bending radius limit of $20 * D$, as recommended by Pipelife (see table 2.2), is indicated.

These results are corresponding with expectations and appear very reasonable. No data from comparative cases is known and thus direct comparison cannot be made.

HDPE pipe manufacturer Pipelife has developed a set of simple equations which can be used to check important parameters. These equations have also been derived from the natural catenary equations and are given below [23]:

$$R_{1,min} = \frac{P}{w_1} \tag{3.17}$$

$$R_{2,min} = \frac{P}{w_2} \tag{3.18}$$

$$T = P + w_1 h \tag{3.19}$$

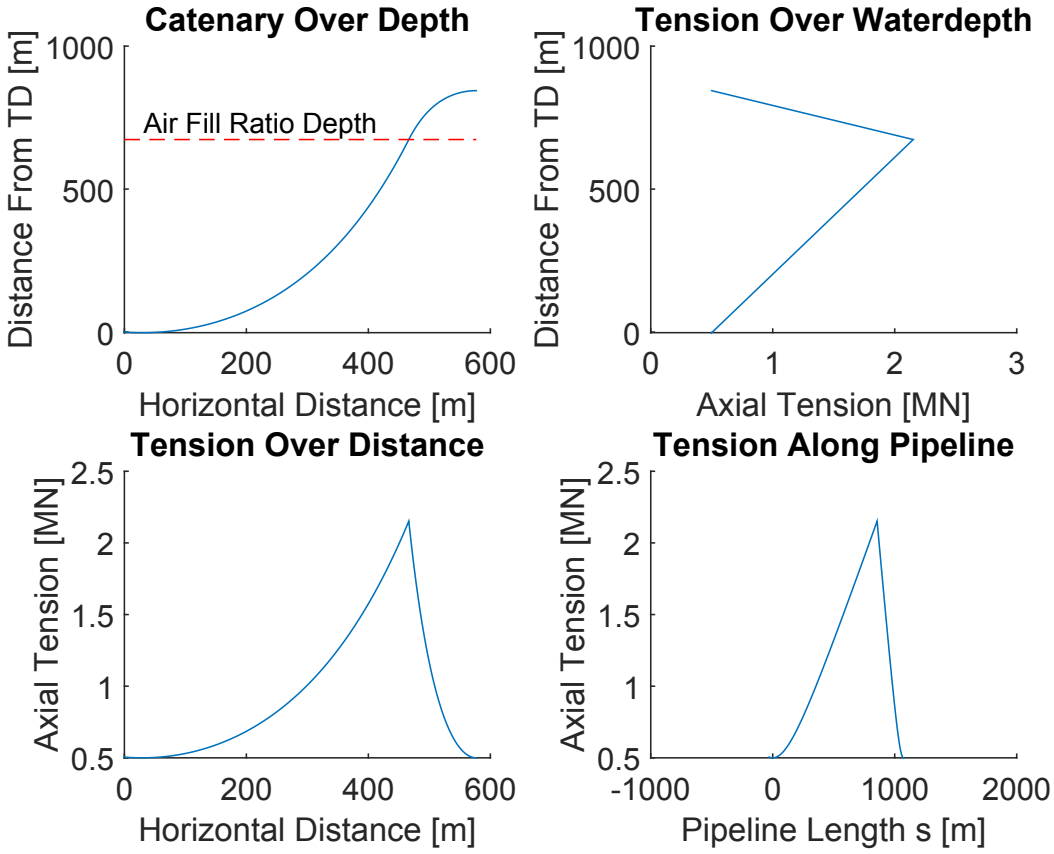

Figure 3.6: Tension in the Pipeline

where;

$R_{1,min}$ = Minimum bending radius (MBR), water filled section in [m]
$R_{2,min}$ = Minimum bending radius (MBR), air filled section in [m]
w_1 = Net weight of water filled section in [N/m]
w_2 = Net buoyancy in air filled section in [N/m]
P = Pulling force in [N]
T = Tension force in intersection/turning point in [N]
h = Internal water height in pipeline in [m]

If the values used in the Matlab model are put in to these three equations, it is found that both the equations and the Matlab model result in the exact same numbers for the two minimum bending radii and maximum tension encountered by the catenary, see table 3.2. Therefore, it can be concluded that the Matlab model represents a correct implementation of the natural catenary theory.

Additionally to the simple Pipelife equations, engineering software will be used in section 3.3 to further verify these results.

Aside from the axial tension and bending radii encountered, stress in the pipeline is also an interesting aspect to consider. Stress in the pipe will be caused by internal pressure in the pipe, external pressure from the seawater, axial tension and bending. A summary

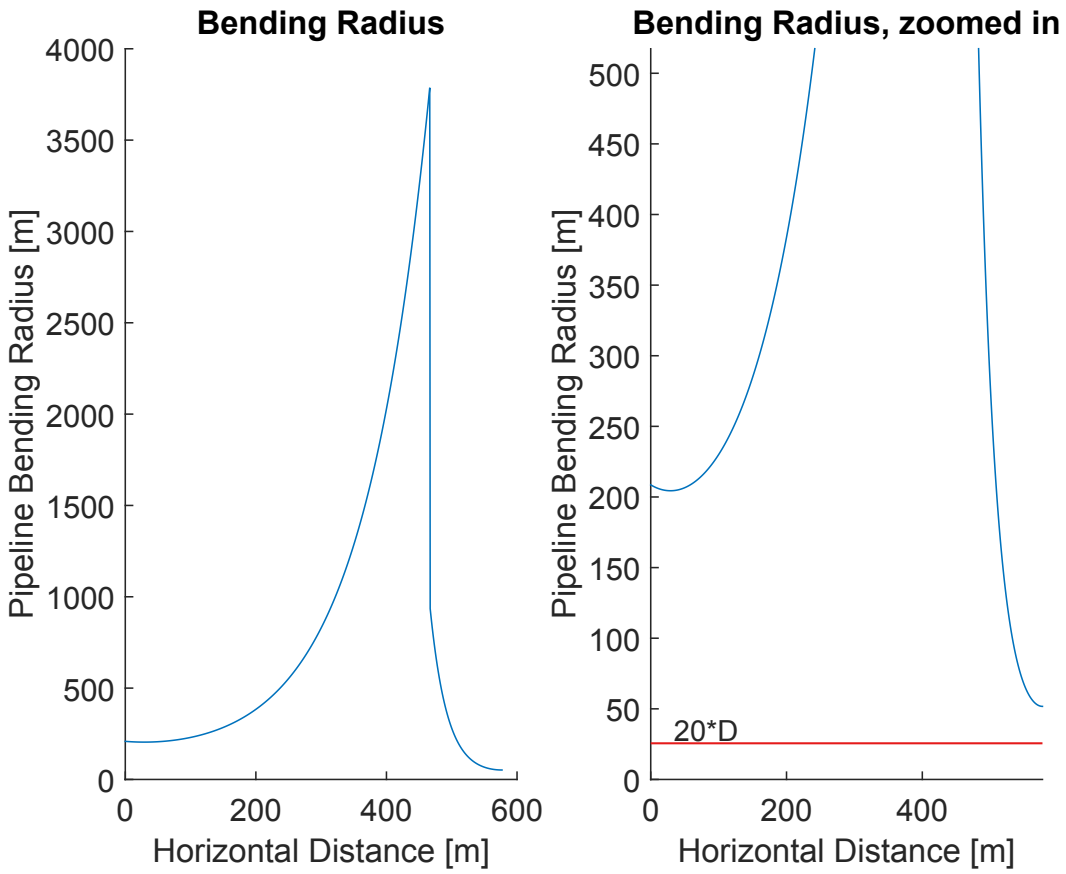

Figure 3.7: Pipeline Bending Radius along horizontal distance

of the loads encountered by the pipe is given in figure 3.8. For a more detailed analysis, additional loads such as thermal gradients and environmental influences should also be included.

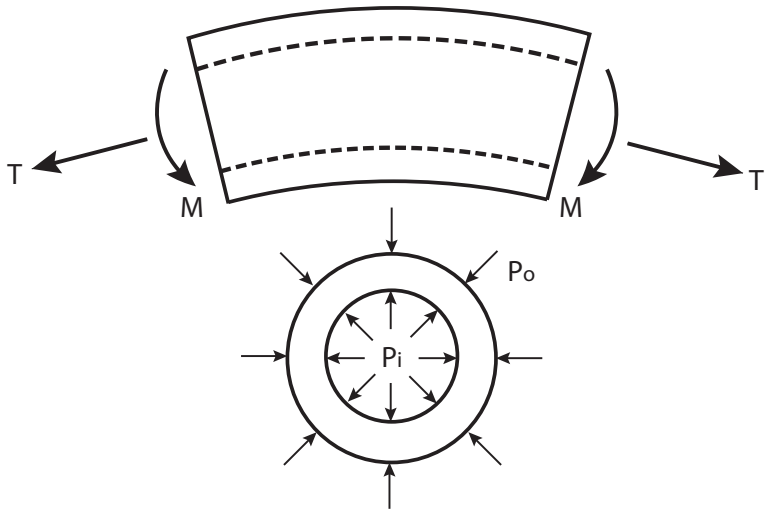

Figure 3.8: Loads on pipe

Internal pressure in the pipeline varies. From the sea level down to the air fill point the

		Matlab	Equations
w_1	[N/m]	2446.041	2446.041
w_2	[N/m]	9664.846	9664.846
P	[N]	500000	500000
h	[m]	675.372	675.372
$\mathbf{R_{1,min}}$	**[m]**	**204.412**	**204.412**
$\mathbf{R_{2,min}}$	**[m]**	**51.734**	**51.734**
T	**[MN]**	**2.152**	**2.152**

Table 3.2: Base Case Natural Catenary Model Results

pipe is filled with air at a constant pressure. From the air fill point down the pipe is filled with water at the same pressure as the surrounding sea water. This surrounding sea water, especially at greater depths, generates a high external pressure on the pipe wall material. Stress is caused in the pipe material due to the external and internal pressure.

Considering the fact that the used base case HDPE pipe has an SDR of 18, the thin walled pressure vessel assumption can not be used to calculate stress in the pipe due to pressure. The criteria for using the thin walled pressure vessel equations is that the ratio between the diameter and the wall thickness should be equal to or more than 20 [35]. Therefore the general thick walled pressure vessel equations will be used, also known as Lamé's equations. Furthermore, as a very long cylinder is used, the pipeline is modelled as an open cylinder and therefore the pressure will not generate axial stress. Hoop stress and radial stress according to the thick walled pressure vessel assumption can be calculated using formula 3.20 and 3.21. The hoop stress and radial stress are not uniform through the wall thickness of the pipe, as can be seen in the equations [36] and figure 3.9.

$$\sigma_h = \frac{p_i r_i^2 - p_o r_o^2}{r_o^2 - r_i^2} - \frac{r_i^2 r_o^2 (p_o - p_i)}{r^2 (r_o^2 - r_i^2)} \tag{3.20}$$

$$\sigma_r = \frac{p_i r_i^2 - p_o r_o^2}{r_o^2 - r_i^2} + \frac{r_i^2 r_o^2 (p_o - p_i)}{r^2 (r_o^2 - r_i^2)} \tag{3.21}$$

where;

σ_h = Hoop/tangential stress in the pipe
σ_r = Radial stress in the pipe
p_i = Internal pressure
p_o = External pressure
r_i = Internal pipe radius
r_o = External pipe radius
r = Stress calculation radius, point in the pipe wall in which the stress is calculated

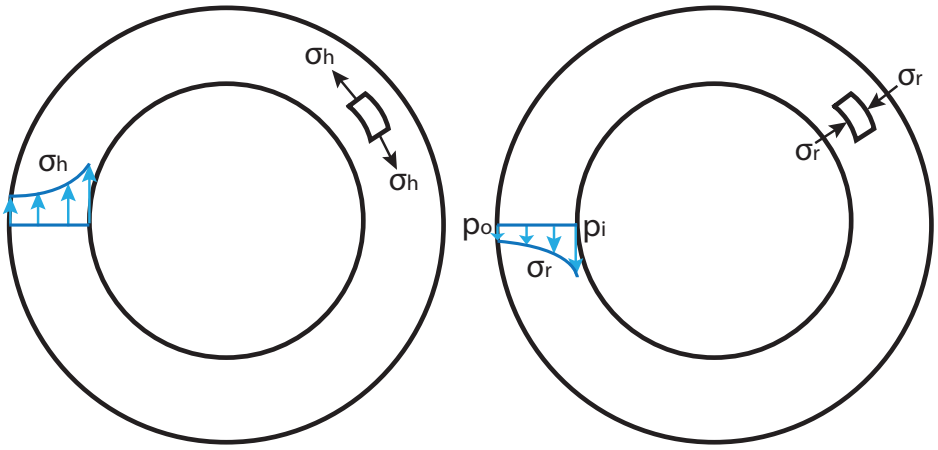

Figure 3.9: Hoop Stress and Radial Stress in pipe wall

Axial tension, generated by the top pull and the weight of the pipe, is used to control the shape of the catenary and thus generates axial stress in the pipe material. The axial tension varies along the pipeline catenary as can be seen in figure 3.6. The resulting axial stress can be calculated using formula 3.22. The axial stress due to tension is uniform through the wall thickness of the pipe.

$$\sigma_{at} = \frac{T}{A} \tag{3.22}$$

where;

σ_{at} = Axial stress in the pipe due to tension
T = Axial tension in the pipe
A = Pipe material surface over which the load is distributed

Finally, the bending of the pipeline also induces stress in the pipe wall material. This is predominantly an axial stress and the magnitude of this stress depends strongly on the location in the pipe wall. For instance, the material on the outside of a bend will experience tension as the pipe wall is stretched, while the material on the inside of a bend will experience compression as the pipe wall is compressed. To find the amount of stress in the pipeline due to bending, the curvature as a function of moment is first given in formula 3.23. This relation can then be combined with the classic formula for simple beam bending, which is given in formula 3.24, to eliminate some variables.

$$\frac{1}{R} = \kappa = \frac{d\phi}{ds} = \frac{M}{EI} \tag{3.23}$$

$$\sigma_{ab} = \frac{Mr}{I} \tag{3.24}$$

where;

M = Bending moment
E = Pipe wall material Young's Modulus
I = Area moment of inertia
r = Stress calculation radius, distance from neutral line where the stress is calculated

After this, the bending stress can now be found using the bending radius as shown in formula 3.25.

$$\sigma_{ab} = \frac{EIr}{IR} = E\frac{r}{R} \tag{3.25}$$

where;

σ_{ab} = Axial stress in the pipe due to bending
R = Pipeline Bending Radius

Both axial stress components can be summed to find the net axial stress. To find the combined stress in the pipe material due to all stresses the Von Mises theorem is used [36]. This theorem is shown in formula 3.26. The Von Mises stress is used as the critical stress and thus should stay below 15 MPa for HDPE.

$$\sigma_v = \sqrt{\frac{(\sigma_h - \sigma_r)^2 + (\sigma_r - \sigma_a)^2 + (\sigma_a - \sigma_h)^2}{2}} \tag{3.26}$$

where;

σ_v = Von Mises stress
σ_h = Total hoop stress
σ_r = Total radial stress
σ_a = Total axial stress

To find the most critical location where stress occurs, all stresses are calculated at four locations in the pipe cross-section and along the complete length of the pipeline, see figure 3.10;

1. At the outside diameter of the pipe, at the outside of the bend
2. At the inside diameter of the pipe, at the outside of a bend
3. At the inside diameter of the pipe, at the inside of a bend
4. At the outside diameter of the pipe, at the inside of a bend

All stresses which occur in the base case pipeline installation along the pipeline at the four critical locations are given in figure 3.11.

In figure 3.11 it can be noted that the combined Von Mises stresses in case 2, 3 and 4 exceed the limit of 15 MPa, which is the maximum allowed stress in HDPE without safety factors. Therefore, the base case pipeline installation using this configuration will

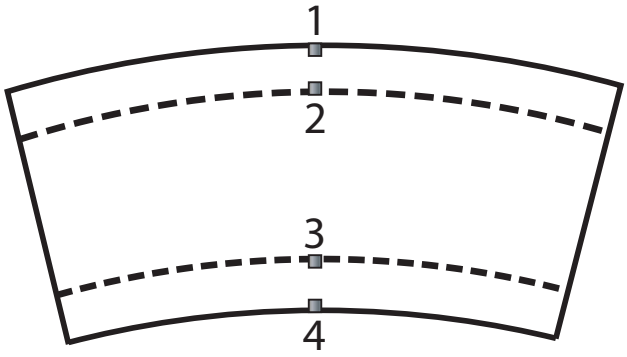

Figure 3.10: Critical Stress Locations in the Pipe

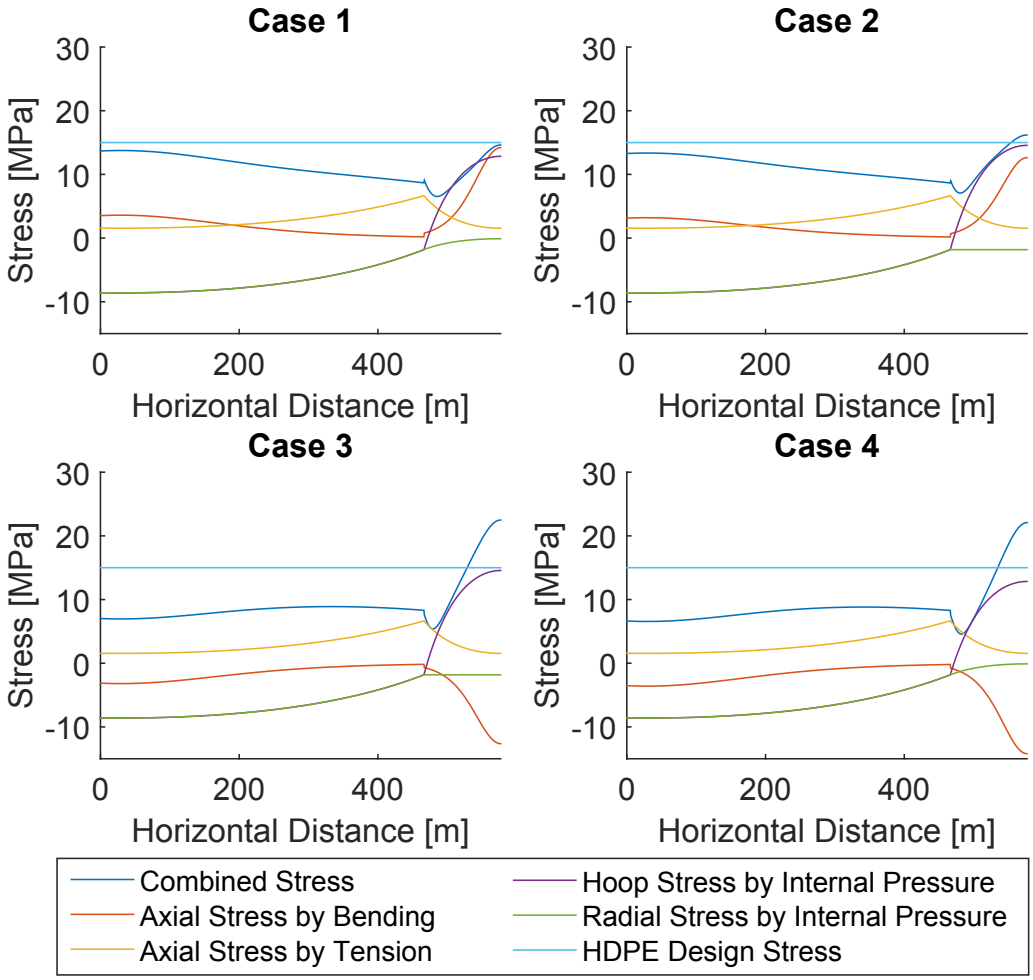

Figure 3.11: Stress in the Pipe along Horizontal Distance in the Base Case Situation

likely fail, although the bending radii encountered initially did not exceed the set MBR limit. In this configuration, the axial stress due to bending and the hoop stress due to internal pressure are the most significant. Therefore, the most critical location is at the sea surface, where the smallest bending radius and the largest internal pressure relative to external pressure are encountered. Furthermore, the highest stress is encountered in case 3, at the internal diameter of the pipe on the compressive side of the bend. The

radial stress becomes significant especially in greater depths, due to the high external water pressure. Luckily the other stresses in this area are relatively low. However, when the pipeline catenary transitions from s-lay to j-lay the pipe encounters even larger water depths and thus larger compressive radial and hoop stress at the seabed. In some situations the currently chosen most critical situation, the transition point from s-lay to j-lay, might therefore not be the most critical in terms of stress.

To check whether j-lay can be more critical in the base case, the j-lay part of the installation is modelled. The pipeline end is assumed to follow the path of the s-lay catenary from the sea surface down to the target location at the seabed, as illustrated in figure 3.12.

The maximum stress along the pipeline catenary is taken at every point of the descent of the pipeline end, this results in figure 3.13. In this figure the pipeline end is at the sea surface on the left of the plots, where the pipe end depth is 0 m. The pipeline end is at the seabed on the right of the plots, at its target depth of 1000 m, where the pipe end depth is 1000 m. From figure 3.13 it can be concluded that the highest stresses are encountered when the pipeline end is still at the sea surface as initially assumed. In this base case situation, j-lay is therefore not more critical. However, different conditions might result in a different result.

As a final check the pipeline is analysed for buckling. Buckling is a phenomena where the pipeline rapidly loses its shape and fails due to a certain load profile. Buckling during the installation can occur in two situations; pipe under-pressure (external pressure > internal pressure) and excessive bending.

Significant under-pressure should in principle not occur during the pipe installation. The compressor ensures that sufficient air pressure is available to create an over-pressure in the air filled section of the catenary and an internal pressure equal to external pressure in the water filled section. If the compressor fails and somehow air enters the pipeline through the onshore end, the pressure inside the pipeline will drop and under-pressure will occur. This situation should be prevented as this under-pressure will very likely cause buckling.

Buckling due to excessive bending is an effect which is already accounted for by the minimum radius of curvature, or minimum bending radius limit (MBR) of $20 * D$. The true minimum bending radius for a specific HDPE pipe to prevent radial buckling can be calculated using formula 3.27 [23].

$$a_{crit} = 0.89(SDR - 1) \tag{3.27}$$

where;

a_{crit} = Critical pipe bending ratio R/D
SDR = Pipe diameter / wall-thickness ratio D/t

For the base case, using an SDR of 18, the critical bending radius limit will thus be $15.13 * D$ without any safety factor. The true critical minimum bending limit is thus a bit lower than the initially used, slightly conservative minimum bending limit of $20 * D$.

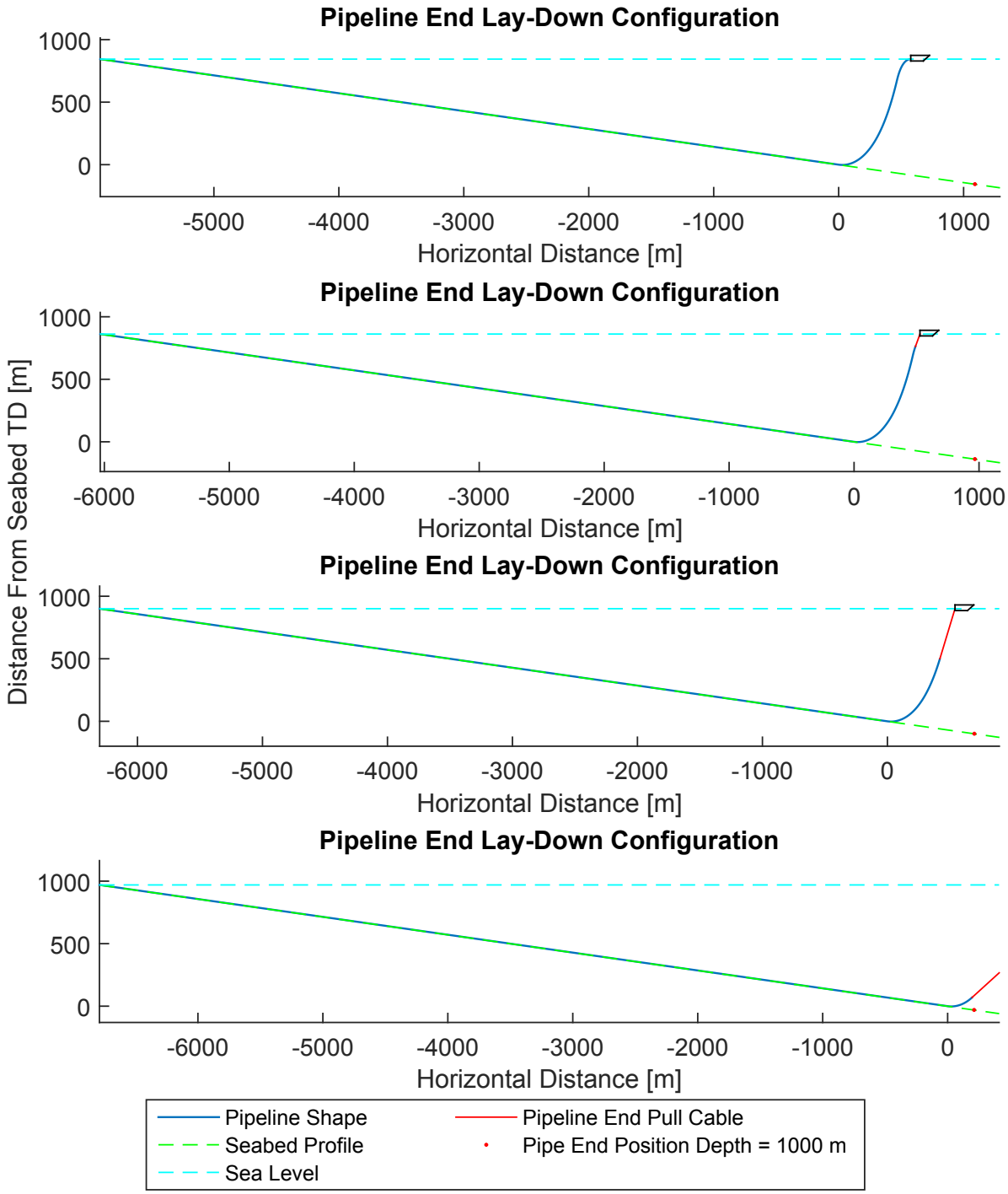

Figure 3.12: J-lay Pipeline End Installation, pipeline end respectively 0m, 100m, 400m and 900m below the water surface

Therefore, it can be concluded that in the base case buckling is not a problem as long as the installation is performed as prescribed and the already set minimum bending radius limit is honoured. When a higher SDR pipe is used the limit of $20 * D$ might become too low, thus care should be taken when using different configurations.

Furthermore, in the overbend, where the bending is most significant, a high internal pressure is encountered. This internal pressure will decrease both the amount of oval-

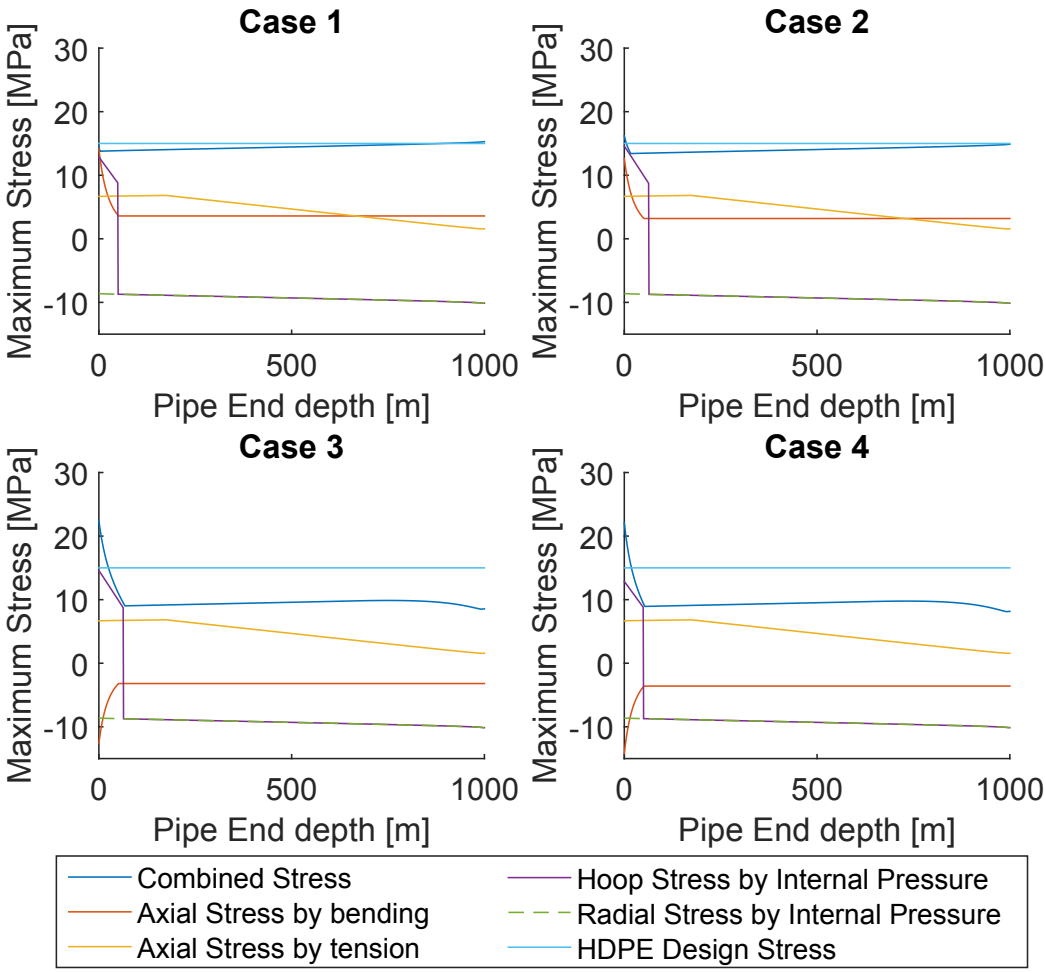

Figure 3.13: Maximum Stress in the Pipe along J-lay Pipe End Depth below Sea Surface during pipe end lay-down in the Base Case Situation

ization due to bending and stiffness of the pipe. Thereby, the internal pressure increases the amount of bending moment which can be handled by the pipe before buckling occurs [37]. This is complex phenomena, dependent of many pipe specific factors. Therefore, this effect is not included in any further analysis in this report.

3.2.3 Parameter Sensitivity

To be able to find the maximum possible pipeline dimension, which can be installed using the float and sink method a parameter sensitivity study is done. By piecewise varying the input parameters within a range of interest while keeping all other parameters constant at the base case values, the influence of that single parameter can be found. This is done for the air fill ratio, target installation depth, pipeline outer diameter, SDR, seabed slope and horizontal top pull force as shown in table 3.3. All foreseen OTEC installations are well within these ranges.

It should be noted that some extends of the ranges used for the sensitivity studies will not provide strictly correct results, when using the natural catenary theory. For instance,

Parameter	Range of Interest
Air Fill Ratio a_a	0.05 – 0.95
Target Installation Depth	35 – 1500 m
Pipeline Outer Diameter	0.5 – 10 m
SDR	4 – 50
Seabed Slope	0.1 – 30°
Horizontal Top Pull Force	1 – 1000 t

Table 3.3: Sensitivity Study Input Parameters

very small installation depths or very large pipe diameters combined with a small SDR will not comply with the boundary condition of negligible bending stiffness. Using such large ranges will however be useful in providing a rough trend estimate at the ends of the sensitivity plots.

Furthermore, some ranges are beyond the current industry capabilities. For instance, HDPE pipe is currently not produced in diameters even close to 10 m. Also one of the strongest marine installation vessels in the world can only deliver 390 tons of bollard pull, which is way below the maximum of the range proposed here for top pull force [38]. Such high ranges are included for the sake of theoretical technical feasibility, as an indication of what would be required.

The maximum axial tension and the minimum bending radius encountered in the pipeline catenary during installation are considered as a good indication of the positive or negative influence of a parameter. Combined stress is a more absolute measure of the influence of a parameter. A parameter can for instance have a negative influence on the maximum axial tension, but a positive influence on the minimum bending radius encountered. The combined stress allows to distinguish the actual influence on the pipeline integrity, when all positive and negative influences of a certain parameter are weighed and summed.

The results of the sensitivity analysis are shown in table 3.4. An increase in maximum axial tension and/or an increase in maximum combined stress is considered disadvantageous, while an increase in minimum bending radius is considered advantageous. For detailed sensitivity study plots for every parameter, reference is made to appendix B.

Table 3.4 also includes an influence rating, which gives an idea of how strongly the parameters influences the output values. This rating of weak, moderate and strong influence is determined by observing the output of the axial tension, minimum bending radius and combined stress and comparing these in a reasonably practicable range with the output of other input parameters.

If the minimum bending radius and maximum combined stress are assumed as governing, an optimum can be found. Both the minimum allowed bending radius and the maximum allowed combined stress shall not be exceeded. Decreasing the pipeline outer diameter and SDR results in a better outcome for both bending radius and combined stress when decreased. However decreasing the pipe diameter or increasing the wall thickness decreases the volume flow capacity of the pipeline. The other variables do either not influence both the bending radius and the stress, or increasing the variables

Parameter	If increased, max. Axial Tension:	If increased, min. Bending Radius:	If increased, max. Combined Stress:
Air Fill Ratio a_a	Below 0.5: Increases, moderate Above 0.5: Decreases, moderate	Below 0.5: Increases, weak – moderate Above 0.5: Decreases, weak – moderate	Increases, weak – moderate
Target Installation Depth	Increases, moderate	Remains Constant	Increases, weak
Pipeline Outer Diameter	Increases, strong	Decreases, strong	Increases, strong
SDR	Increases, weak	Decreases, weak	Increases, weak
Seabed Slope	Decreases, weak	Remains Constant	Decreases, weak
Horizontal Top Pull Force	Increases, moderate	Increases, strong	Before Optimum: Decreases, moderate After Optimum: Increases, weak

Table 3.4: Parameter Sensitivity Study Results

will cause one to get better and the other worse. Such variables should be optimized as far as practicably possible. For instance, the maximum encountered stress can be decreases as much as possible by varying a certain parameter, while still staying above the minimum bending radius limit when doing so.

3.2.4 Installation Method Limits

The minimum bending radius and the maximum stress allowed determine the maximum possible pipeline dimensions. Therefore both the stress and bending radius have been calculated for a wide range of configurations to find the maximum pipeline diameter which can be installed using the float and sink method. The minimum bending radius allowed is set at 20 times the outer diameter of the pipe and the maximum allowed stress is set at 15 MPa. These values are according the HDPE pipe material characteristics as given in section 2.2. No safety factors are included in these two limits. Furthermore, the model used does not include dynamic behaviour. Therefore, extreme care should be taken when trying to translate these theoretical limits to real life installation limits.

Starting out with the base case parameters as stated in table 3.1 and varying both the pipe outside diameter and the top pull will provide a better understanding of the limits of installing a large diameter deep water pipeline. The pipe outside diameter and top pull are first chosen, as these have the strongest influence on the minimum bending radius and maximum combined stress, see table 3.4. The results of this analysis are shown in three dimensional figures 3.14 and 3.15. In these figures, the coloured planes are the minimum bending radius and maximum stress encountered for the combinations

of pipe diameter and pulling force. The red planes represent the limits as stated before; Minimum Bending Radius $= 20 * D$ and Maximum Combined Stress $= 15$ MPa.

In the minimum bending radius plot the area above the red plane is of interest, for this is the range of possible combinations with respect to bending radius. In the maximum combined stress plot the area below the red plane is of interest, for this is the range of possible combinations with respect to stress. It can be noted that the range of combinations possible, with respect to stress, is much more limited.

To further clarify the maximum pipe diameter which can be installed, given the limits of bending radius and stress, the limit lines have been plotted in figure 3.16 and 3.17. Here it is reconfirmed that the maximum combined stress in this configuration is most limiting, as it can be seen that much larger pipeline diameters can be installed when looking at the minimum bending radius compared to the maximum combined stress.

From figure 3.17 it can be concluded that the largest pipeline diameter which can theoretically be installed in the base case scenario is around 2.25 m. This would require a top tension of around 440 t, which is quite a challenge and would require multiple very strong marine installation vessels.

To further optimize the pipeline design and installation procedure, the pipeline SDR and air fill ratio are now varied. The target installation depth and seabed slope are kept at the base case values as these can't be varied much in a real life situation either.

Lowering the SDR and thus increasing the pipe wall thickness will greatly increase the range of pipe diameters which can be installed and decrease the top tension required to do so. Decreasing the SDR by too much will however not make sense, as it will decrease the possible volume flow rate of the pipe and strongly increase the material costs of the pipeline. Furthermore, increasing the wall thickness will also decrease the likelihood that HDPE pipe suppliers are available which are able to manufacture the pipe, especially for very large diameters. For instance, the production capacity of Pipelife currently is limited to a maximum diameter of 2.5 m combined with an SDR of at least 23 [39].

To comply with current production capabilities the SDR should be increased to 23 for large diameter pipe. Using this as input for the model does however not result in a feasible installation; the stress does not remain below 15 MPa, even for relatively small diameter pipelines.

Increasing the air fill ratio up from 0.2 will only decrease the installation capabilities, as the combined stress encountered increases quickly. Lowering the air fill ratio slightly decreases the minimum bending radius encountered but also decreases the maximum stress, which is more critical. Therefore, when optimizing for the air fill ratio, it is lowered below 0.2 to find an optimum air fill ratio. This optimum air fill ratio might differ for changing input parameters.

The optimum air fill ratio is determined using the base case input parameters from table 3.1. For these parameters the results are shown in figure 3.18. From this figure it can be seen that for the largest diameter pipelines an air fill ratio of 0.14 is most optimal, as this air fill ratio allows for the largest pipeline diameters to be installed when using top pull tensions of about 600 to 1000 t. An air fill ratio of 0.12 is more optimal for installing pipelines with a slightly smaller outside diameter. This can be concluded as

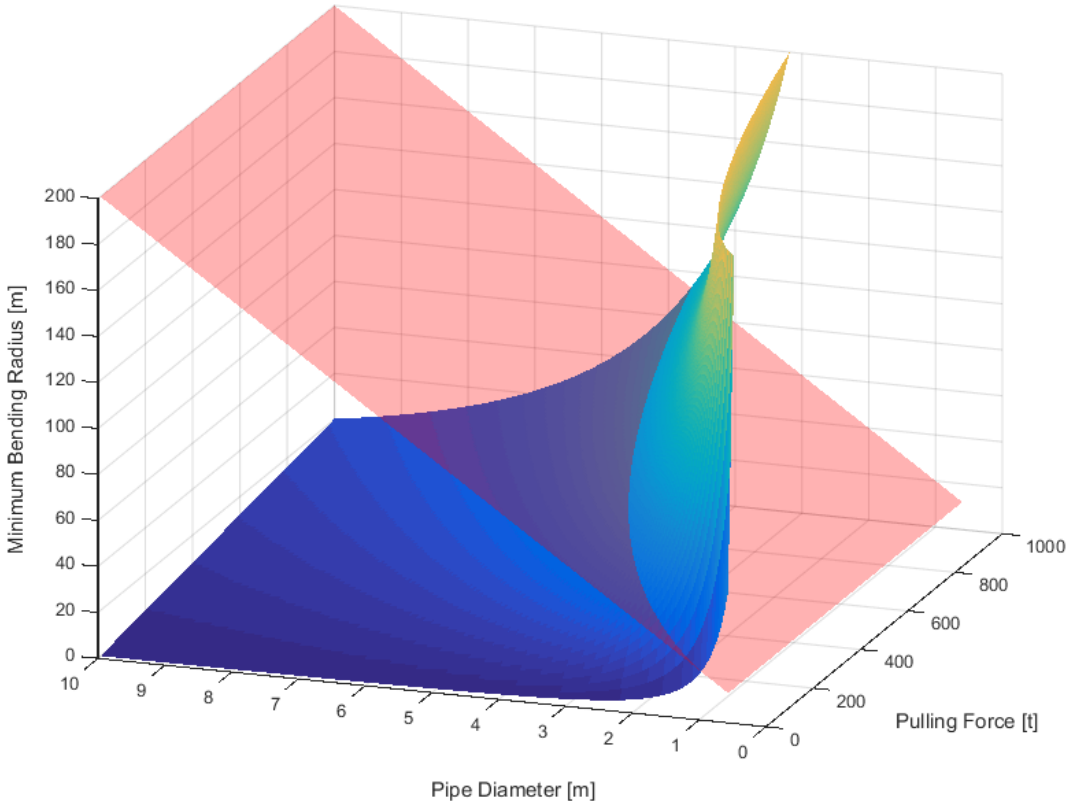

Figure 3.14: Minimum Bending Radius for Pipe Diameter and Pulling Force Combinations, where the red plane indicates the $20 * D$ limit

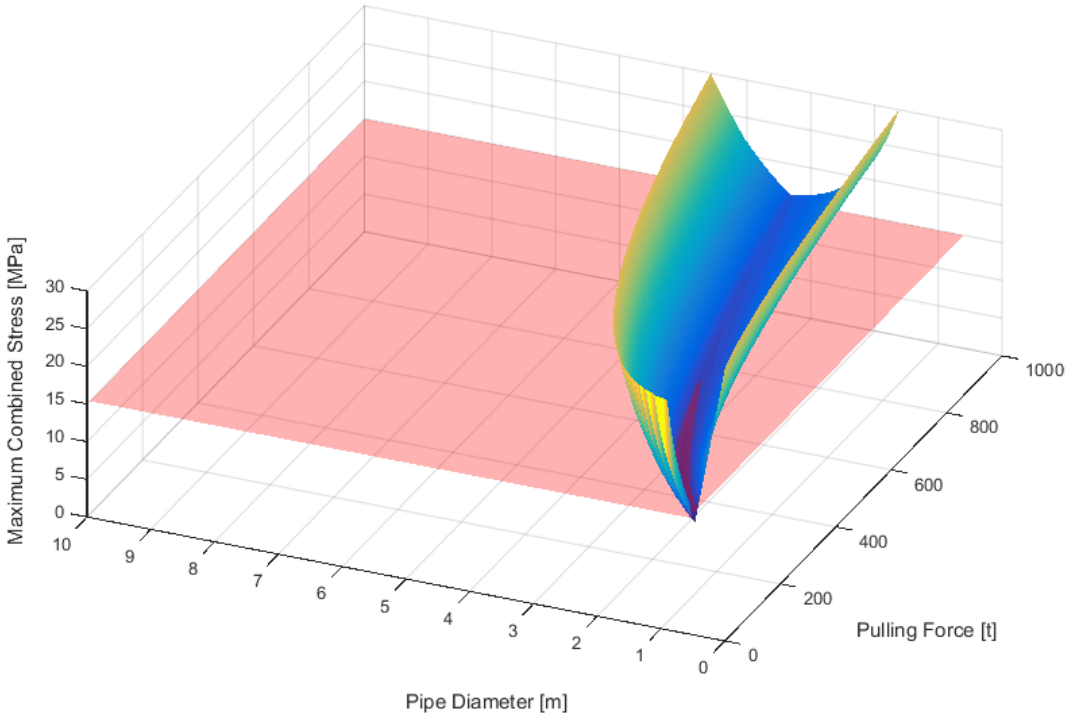

Figure 3.15: Maximum Combined Stress for Pipe Diameter and Pulling Force Combinations, where the red plane indicates the 15 MPa limit

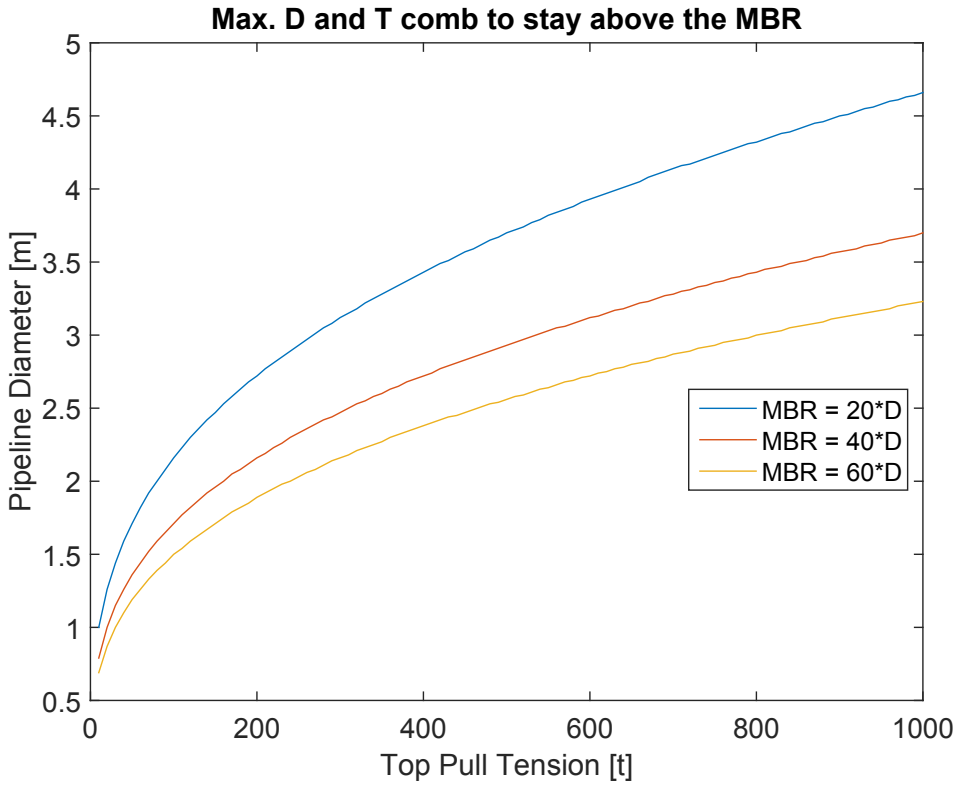

Figure 3.16: Maximum Pipeline Diameter and Pull Tension Combinations with respect to Minimum Bending Radius (MBR) Limits

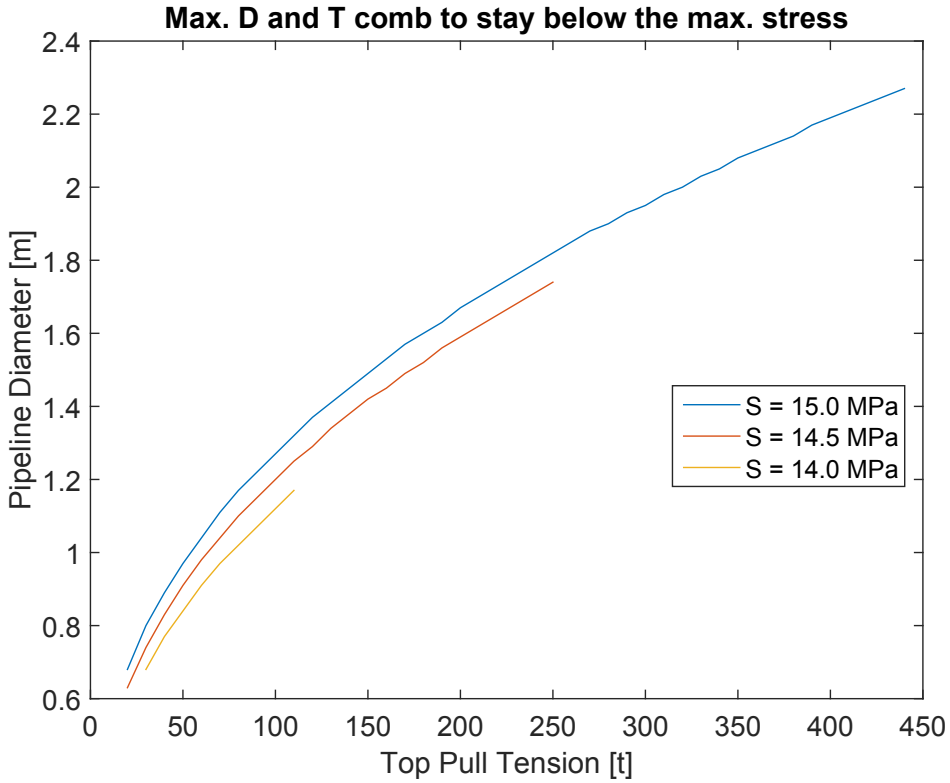

Figure 3.17: Maximum Pipeline Diameter and Pull Tension Combinations with respect to Maximum Combined Stress Limits

the same amount of tension allows to install larger pipeline diameters at this air fill ratio, compared with other air fill ratios, in the range from 350 to 600 t. Reducing installation top tension below 350 t results in an air fill ratio of 0.1 to be the most optimal, until it is again outperformed by an even lower air fill ratio at a lower installation top tension.

Figure 3.19, shows the influence of the air fill ratio on the minimum bending radius encountered. Here it can be concluded that a higher air fill ratio is more optimal when considering the minimum bending radius (up to an air fill ratio of 0.5), as the sensitivity study pointed out. Comparing figure 3.18 and 3.19 however points out that the combined maximum stress is more limiting as it does not allow for diameters to be installed as large as the minimum bending radius allows for. As has been concluded before. Therefore the air fill ratio should be lowered to the optimum rate for the used pipeline diameter and top tension combination, with respect to the maximum allowed combined stress.

When using the base case parameters, whilst changing the air fill ratio, it can be concluded that the largest pipe diameter which can be installed is about 3.5 m in diameter. This would require 1000 t of horizontal top tensions and an air fill ratio of 0.14. A more practical horizontal top tension of 350 t results in a maximum pipe diameter of about 2.5 m at an air fill ratio of 0.12. Lowering the air fill ratio has thus resulted in a significant improvement, compared to the previous 2.25 m maximum diameter which can be installed at an air fill ratio of 0.2 with a top pull tension of 440 t. No safety factors are included in these findings.

For purely theoretical insights an optimum is created by lowering the SDR to 12 and match it to the optimum air fill ratio for this SDR, which is 0.16 for the largest diameters. Decreasing the SDR further than 12 will cause the wall thickness to be more than twice the current industry capability. This is assumed to be unrealistic and expensive. The remaining parameters used for this optimum are corresponding with the base case.

As can be seen in figures 3.20 and 3.21, the maximum pipeline diameter which can be installed has been increased significantly. In this scenario, which features a pipe of dimensions which can currently not be supplied, a maximum diameter of about 3.85 m can be installed using a tension of 1000 t. Furthermore, stresses decrease much quicker compared to the base case when using a slightly smaller diameter and the same tension. This can be seen in figure 3.21 where a limit of 13.5 MPa instead of 15 MPa still provides the possibility to install a pipe of about 3.7 m diameter. Whereas, in the base case a limit of 14 MPa already poses a problem for a 1.2 m diameter pipe (figure 3.17).

3.3 Engineering Software Model

In this section the Orcina Orcaflex marine dynamics finite element software package is used to verify the results of the natural catenary model.

The float and sink installation is modelled using the standard Orcaflex vessel as tow boat, a constant tension winch to model the horizontal pull tension, a homogeneous pipeline as the HDPE pipe to be installed and a flat seabed with a slope of 1/7. The pipeline is anchored to the seabed and given a length such that the touchdown point is at the same

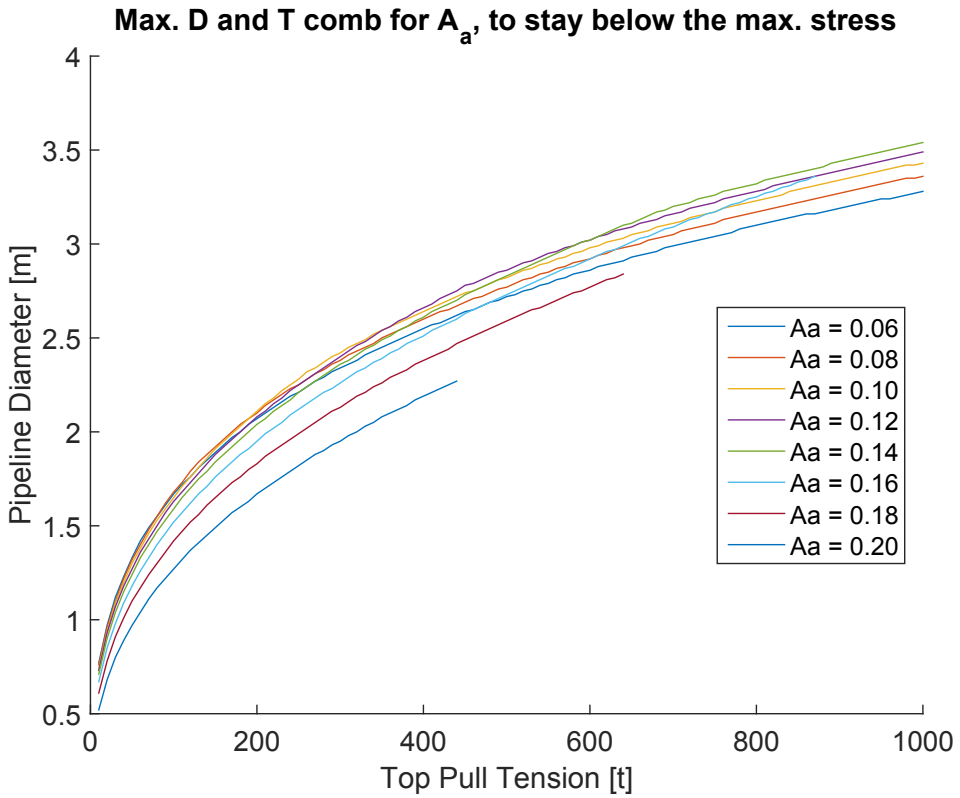

Figure 3.18: Maximum pipeline diameter which can be installed with respect to the maximum allowed stress of 15 MPa when varying the pull tension and air fill ratio

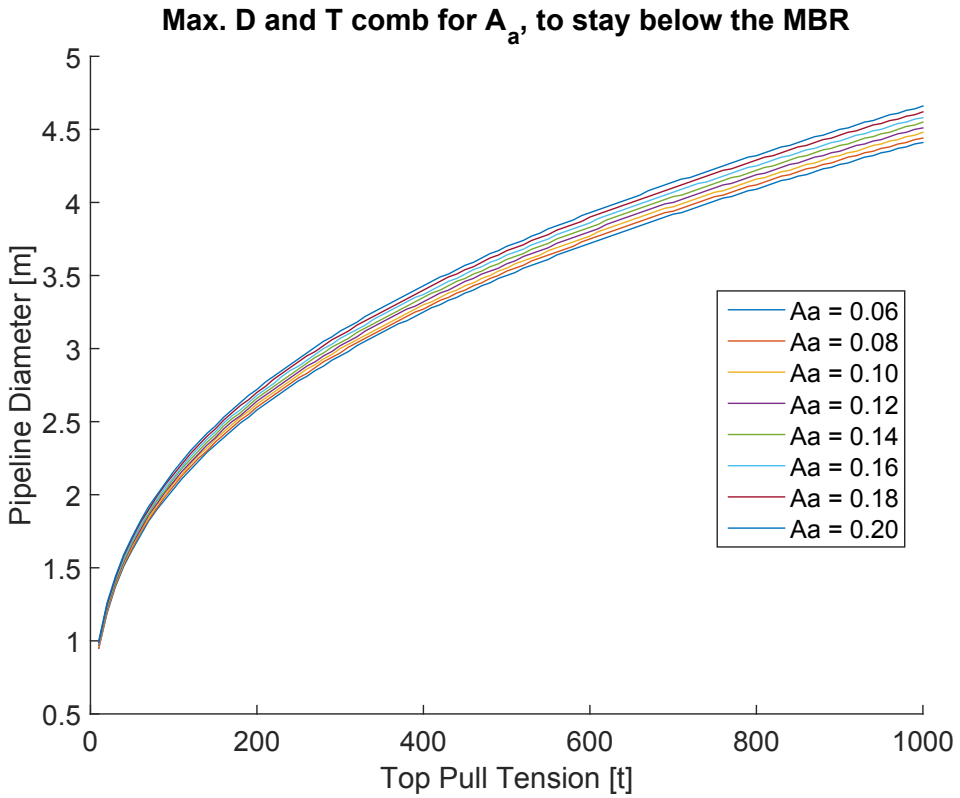

Figure 3.19: Maximum pipeline diameter which can be installed with respect to the minimum bending radius (MBR) of $20 * D$ when varying the pull tension and air fill ratio

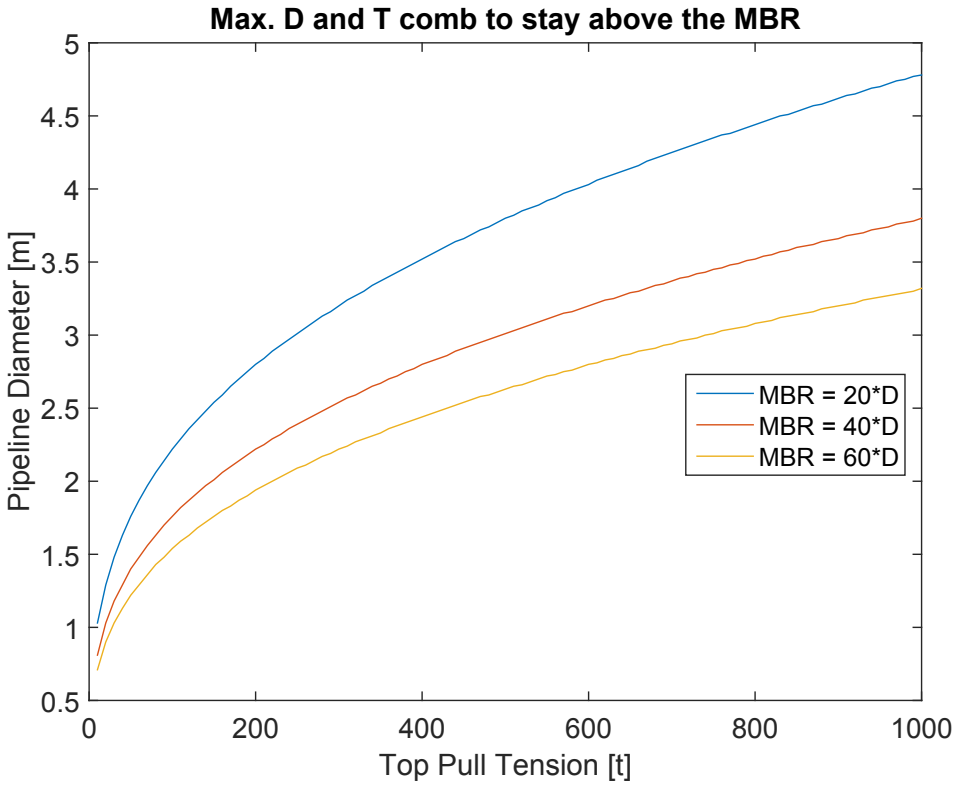

Figure 3.20: Maximum pipeline diameter which can be installed for $A_a = 0.16$ and $SDR = 12$, with respect to Minimum Bending Radius (MBR) Limits

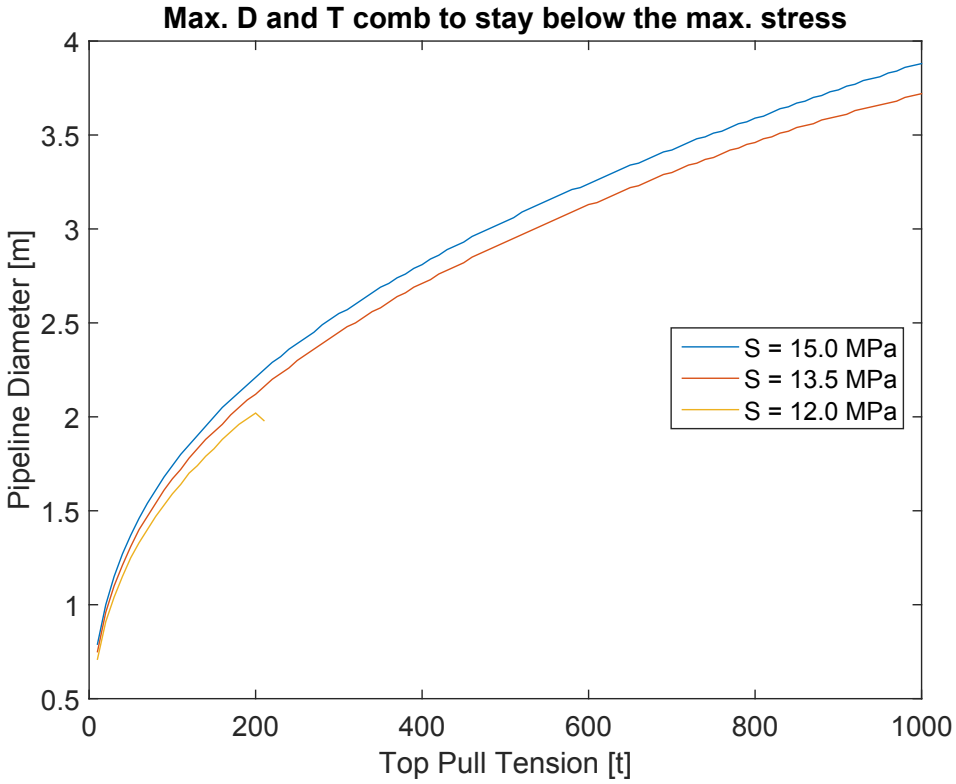

Figure 3.21: Maximum pipeline diameter which can be installed for $A_a = 0.16$ and $SDR = 12$, with respect to Maximum Combined Stress Limits

depth as it was using the Matlab model and just hits the sea water surface on the other end.

To model the different contents in the pipeline, it is split into two separate lines with a 6D buoy connecting the two. The lower line is modelled as flooded with sea water and the upper line is modelled as filled with air, at the pressure which would be required to keep the seawater from rising. Furthermore, the 6D buoy has been given negligible properties of its own to prevent it from interfering with the actual results. The buoy is only used to rigidly connect the two lines with infinite stiffness, such that their orientation angles at the buoy are the same. This method is performed as instructed by Orcina, for use of the connection of two lines.

The added ballast weight is modelled by increasing the density of the pipeline material, so the external and internal diameter of the pipeline are not altered compared to the first model. The resulting model in the Orcaflex environment is shown in figure 3.22.

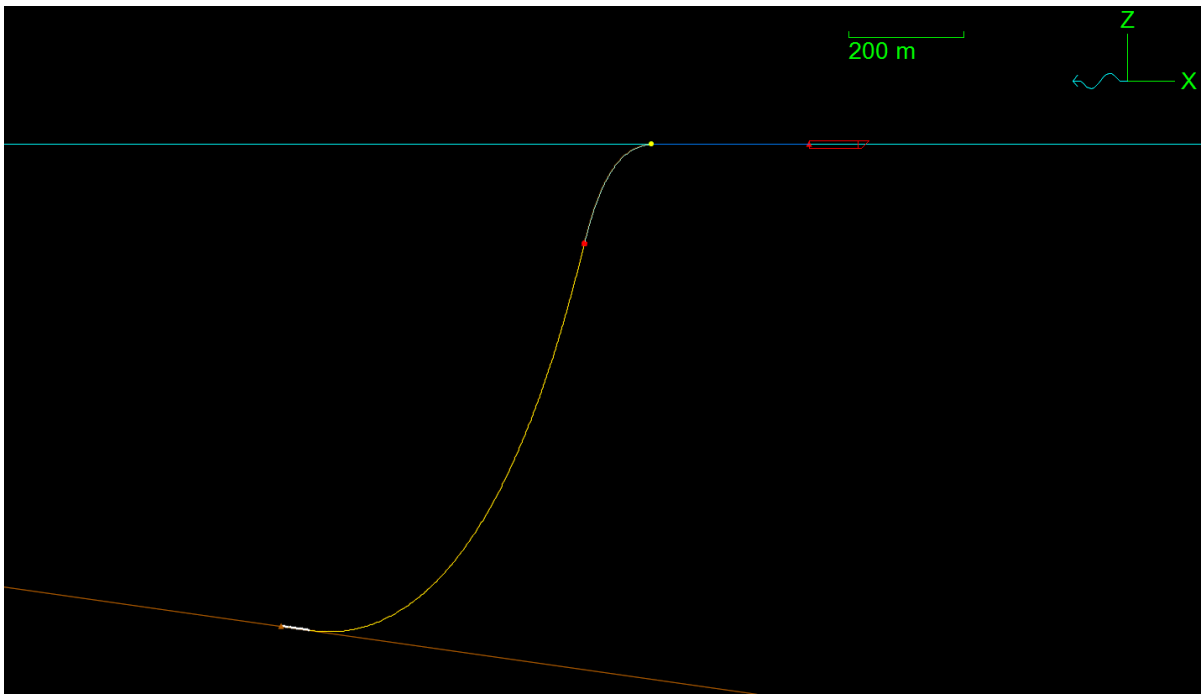

Figure 3.22: Base Case Orcaflex Model of the Float and Sink Installation Method

In figure 3.22 the brown line represents the sloped seabed, the light blue horizontal line represents the sea water level, the red ship shape represents the standard orcaflex vessel used as tug boat, the dark blue line represents the winch and wire, the grey line represent the air-filled piece of the pipeline, the small red square represents the 6D buoy used to connect the two lines and the yellow line represents the sea water filled piece of the pipeline.

Orcaflex performs a two-step static analysis. The first step is set-up to perform a natural catenary analysis, which is mainly used to roughly determine line shape/location input for step two. The second step is set-up to perform full statics analysis. This analysis includes the effects of bending stiffness and interactions with other shapes [32].

Comparing figure 3.5 and figure 3.22, it can be concluded that both the results from the

natural catenary Matlab model and the Orcaflex model appear very similar. The exact difference in results from both methods is investigated in section 3.4.

Results from the Orcaflex model are exported and post-processed using Microsoft Excel. Furthermore, results from the Orcaflex model are achieved only through static analysis. Dynamic analysis possibilities in Orcaflex are not used at this point as this would result in a wrong comparison.

3.4 Comparison of Methods

To investigate the difference between the analytical natural catenary Matlab model and the numerical full statics Orcaflex model, the base case is first modelled in Orcaflex as well, using the same parameters from table 3.1.

The effective tension from Orcaflex, which is the same as the axial tension from Matlab in figure 3.6, is shown along the arc length, which is the same as the pipeline length s in Matlab, in figure 3.23. Comparing these two figures, it can be concluded that the tension from both models is very similar. As the shape looks the same and the same maximum of about 2,2 MN is reached.

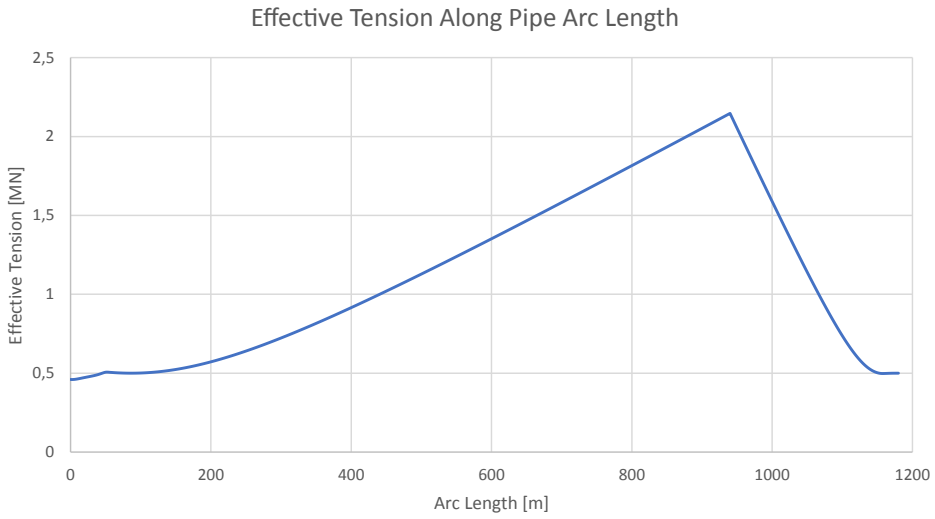

Figure 3.23: Base Case Orcaflex Effective Tension along Arc Length

In the Orcaflex model, arc length 0 m is not exactly the touchdown point, as it is in the Matlab model. The Orcaflex model uses a bit longer total pipeline length, to ensure correct shape and thus the first section of arc length is lying on the seabed. Therefore, Orcaflex results are shifted somewhat to the right, to higher arc lengths compared with the Matlab model.

The same comparison as for tension is now done for the bending radius. For this purpose, figure 3.7 can be compared with figure 3.24. The Orcaflex results again shows great similarities with the Matlab model. In general the shape of the results looks the same, except for the ends of the pipeline which are a bit longer in the Orcaflex model and thus straightened out, showing a very high bending radius as they continue a bit further then

the Matlab results. However, the minimum bending radius encountered in the Orcaflex model is significantly higher than the one in Matlab. In Matlab a minimum of about 50 m is found, while Orcaflex shows a minimum of about 70 m. The Orcaflex model hereby shows that bending at the top of the catenary is less significant when bending stiffness is included.

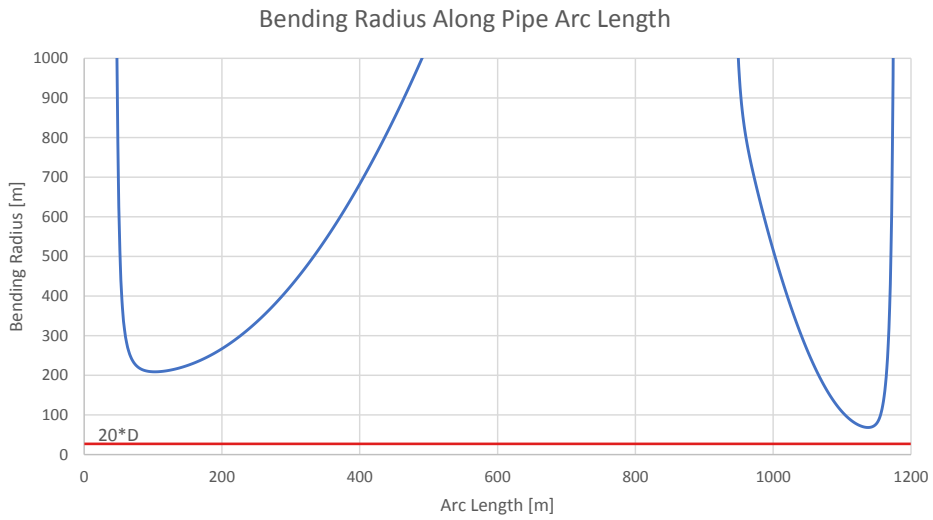

Figure 3.24: Base Case Orcaflex Bending Radius along Arc Length

Finally, the encountered stress is compared for both models. For this purpose figure 3.11 and figure 3.25 can be compared. The Orcaflex results in figure 3.25 show the maximum Von Mises stresses, calculated at the most critical location in the pipe wall, which is automatically found by Orcaflex. From the comparison it can be concluded again that the results from Orcaflex show great resemblance with the results from Matlab. The major difference is the maximum Von Mises stress encountered at the top of the catenary. Where the Matlab model shows a worst case maximum of about 23 MPa, the Orcaflex model only returns a worst case maximum of about 18 Mpa. This difference is likely predominantly caused by the lesser amount of bending due to stiffness in the Orcaflex model.

For a more general impression of the difference between the natural catenary model and Orcaflex, results from a number of cases are compared where the pipeline diameter, SDR, top tension and air fill rate are altered. The remaining parameters are kept constant at the base case parameters from table 3.1. The cases considered are given in table 3.5. The resulting value's for comparison from Matlab and Orcaflex are given in table 3.6

When looking at table 3.6, an inconsistency can be noted. While the minimum bending radius encountered is higher using Orcaflex, as expected due to included stiffness, the Von Mises stress encountered in the Orcaflex model is higher for most cases. Only when the minimum bending radius encountered is a lot lower than the Matlab model, as in the base case, the Von Mises stress in Orcaflex is lower. When considering the fact that the axial/effective tension and internal and external pressure are roughly equal in both models and bending is less significant in the Orcaflex model, one would expect the resulting stress in the Orcaflex model to be lower. As this is not the case, the theory behind the Matlab and Orcaflex models is now investigated and compared.

	D_{out} [m]	SDR	T_{top} [t]	A_a
Base Case	1.4	18	50	0.2
Case 1	2.25	18	440	0.2
Case 2	2.5	18	350	0.12
Case 3	3.5	18	1000	0.14
Case 4	3.7	12	1000	0.16

Table 3.5: Matlab vs Orcaflex Comparison Cases

	Min. Bending Radius [m] % of $20 * D$ Limit			Max. Von Mises Stress [MPa] % of 15 MPa Limit		
	Matlab	Orcaflex	Difference	Matlab	Orcaflex	Difference
Base Case	51.734 184.76 %	68.414 244.34 %	+32.24 %	22.489 149.93 %	17.725 118.17 %	-21.18 %
Case 1	176.258 391.68 %	189.644 421.43 %	+7.59 %	15.037 100.25 %	16.861 112.41 %	+12.13 %
Case 2	103.126 206.25 %	123.494 246.99 %	+19.75 %	14.331 95.54 %	15.355 102.37 %	+7.15 %
Case 3	153.866 219.81 %	177.394 253.42 %	+15.29 %	14.826 98.84 %	16.885 112.57 %	+13.89 %
Case 4	160.425 216.79 %	190.620 257.59 %	+18.82 %	13.354 89.03 %	14.152 94.35 %	+5.98 %

Table 3.6: Matlab vs Orcaflex Comparison

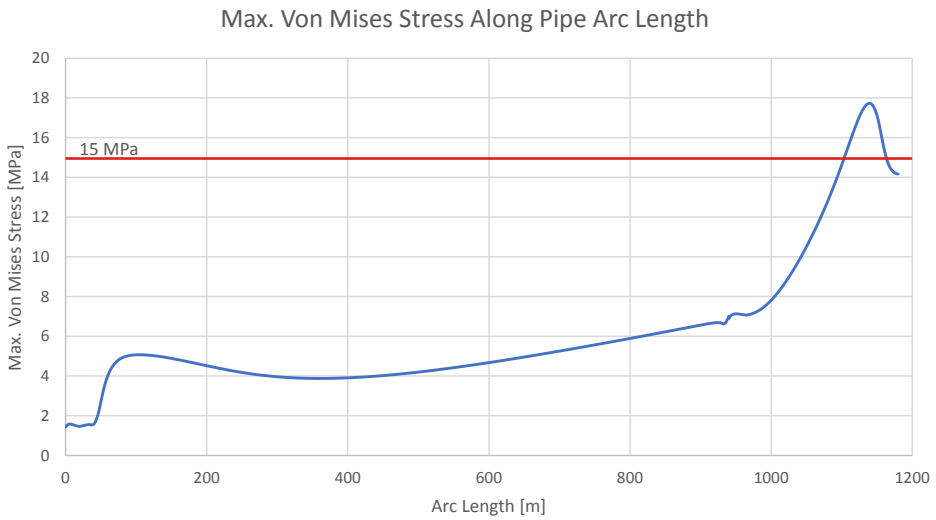

Figure 3.25: Base Case Orcaflex Maximum Von Mises Stress along Arc Length

In the Matlab model some assumptions have been made while calculating stress. First of all, the pipe was assumed to be an open-ended pipe for considering the stress due to internal pressure and external pressure. Orcaflex assumes a closed-ended pipe to calculate resulting stresses. Second, shear stresses were neglected in the Matlab model. To investigate which of these assumptions is invalid and results in the difference of the Matlab and Orcaflex model, the effect of each of these assumptions is investigated independently.

The Matlab model has been adjusted for a closed-ended pipe to visualize the influence of a closed-ended pipe on the combined stresses encountered. This has been done according to formula 3.28, which calculates the axial wall tension in the pipe with the closed-ended pipe assumption. Here, the first part of the equation represents the initial tension as used with the open-ended pipe assumption. The second part of the equation represent the additional longitudinal tension in the pipe due to the difference in internal and external pressure and pipe cross-section surface area.

$$T_{closed-ended} = T + (P_i A_i - P_o A_o) \tag{3.28}$$

where;

$T_{closed-ended}$ = Axial Wall Tension with closed-ended pipe
T = Initial Axial Tension in pipe, see formula 3.12
P_i = Internal Pressure
P_o = External Pressure
A_i = Cross-Sectional Surface Area of the internal diameter of the pipe
A_o = Cross-Sectional Surface Area of the external diameter of the pipe

After adjusting the analytical Matlab model to the closed-ended pipe assumption, stresses increase in most situations. Stresses are now higher than the stresses in Orcaflex, as expected when more severe bending is encountered. This is illustrated in table 3.7, where

	Min. Bending Radius [m] % of $20 * D$ Limit			Max. Von Mises Stress [MPa] % of 15 MPa Limit		
	Matlab	Orcaflex	Difference	Matlab	Orcaflex	Difference
Base Case	51.734 184.76 %	68.414 244.34 %	+32.24 %	20.054 133.69 %	17.725 118.17 %	-11.61 %
Case 1	176.258 391.68 %	189.644 421.43 %	+7.59 %	17.393 115.95 %	16.861 112.41 %	-3.06 %
Case 2	103.126 206.25 %	123.494 246.99 %	+19.75 %	17.313 115.42 %	15.355 102.37 %	-11.31 %
Case 3	153.866 219.81 %	177.394 253.42 %	+15.29 %	18.364 122.43 %	16.885 112.57 %	-8.22 %
Case 4	160.425 216.79 %	190.620 257.59 %	+18.82 %	15.959 106.39 %	14.152 94.35 %	-11.32 %

Table 3.7: Matlab Improved with Closed-Ended Pipe vs Orcaflex Comparison

the Matlab columns now shows the results with the closed-ended pipe assumption instead of with the open-ended pipe assumption as in table 3.6. The assumption that longitudinal stresses in HDPE due to internal pressure could be neglected was thus untrue.

Orcaflex is used to investigate whether shear stresses can be neglected in the Matlab model, as this computer program provides a good insight in the shear stresses occurring. The results used to assess the shear stresses are the Max x-y Shear Stresses, which provide a good indication of the highest shear stresses in the pipe.

Results for all 5 cases show relatively low maximum shear stresses. The max x-y shear stress for the base case is shown in figure 3.26. The other 4 cases show similar numbers, the maximum shear stress is close to 300 kPa, either a bit higher or lower, and thus only about 1–2 % of the maximum Von Mises stress encountered. Therefore, the assumption that the shear stresses are negligible is justified.

Concluding, the results from the numerical Orcaflex and analytical Matlab model are very similar. The analytical model is a bit more conservative as expected, due to the exclusion of bending stiffness, and therefore includes a small safety factor. This safety factor differs, corresponding to the significance of the influence of the bending stiffness in the installation configuration. When a pipe with large bending stiffness is installed using relatively low top tension, the effect of bending stiffness will be more significant compared to the opposite type of installation.

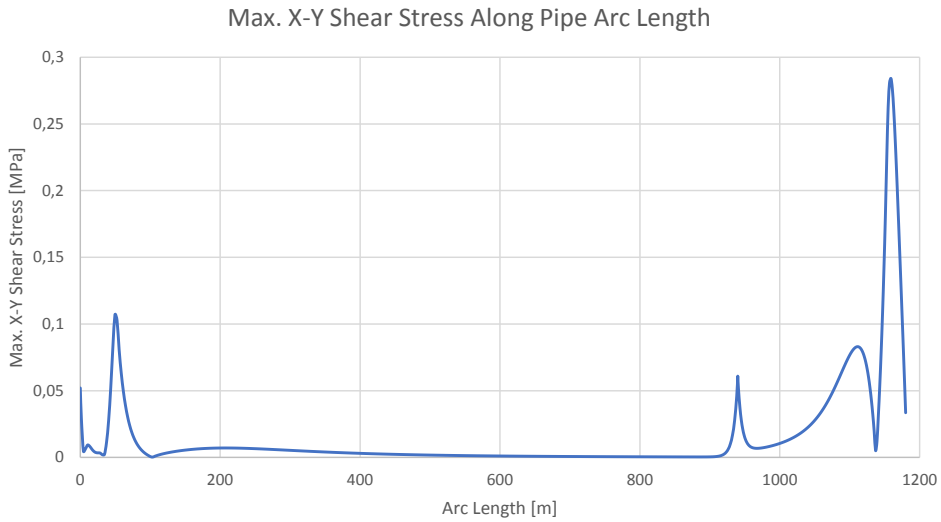

Figure 3.26: Base Case Orcaflex Maximum X-Y Shear Stress along Arc Length

3.5 Improved Analytical Model

With the new assumption of a closed-ended pipe, the stresses generated by the analytical Matlab model have changed significantly. Therefore the results from section 3.2 are no longer valid. A clear example of this is the new stress distribution in the pipeline in the base case with closed-ended pipe assumption, as can be seen in figure 3.27. As the stresses in the large diameter cases have gotten higher, as can be seen in table 3.7, the pipe diameter limits will now probably be lower than those which have been found before. Furthermore, optimums found before, such as the air fill ratio, might also have shifted. Therefore, sensitivity and optimization studies to find the limits of the installation method with respect to stress are redone using the improved model;

The sensitivity study has been redone for stress in appendix C.1. If this new sensitivity study is compared with the previous sensitivity study from appendix B, it can be concluded that the general trends remain the same. Therefore, the findings established from the first sensitivity study are still valid.

In figure 3.28 the optimal air fill ratios have been redetermined for the improved analytical model in base case configuration. When this figure is compared with figure 3.18 it can be concluded that the closed-ended pipe assumption has significantly changed the outcome of the optimization. The smallest air fill ratio used in the model; 0.06, is now the most optimal for the installation of large diameter pipelines. An air fill ratio of 0.10 and especially 0.08 result in pipe diameters which can be installed which are almost as large as for 0.06. Therefore, it is assumed that lowering the air fill ratio further will not result in a significant increase in the maximum pipe diameter which can be installed. Additionally, such a low air fill ratio might cause the pipeline stability after installation to be too low. This is due to the fact that the air fill is a function of the total pipeline weight in water and the internal diameter of the pipe, as shown in 3.3. Therefore, when a pipeline has a low air fill ratio it either has a low line weight overall or a relatively large internal diameter (as a result of small wall thickness and high density material). In the case of low line weight this would thus result in a demand for additional weighting

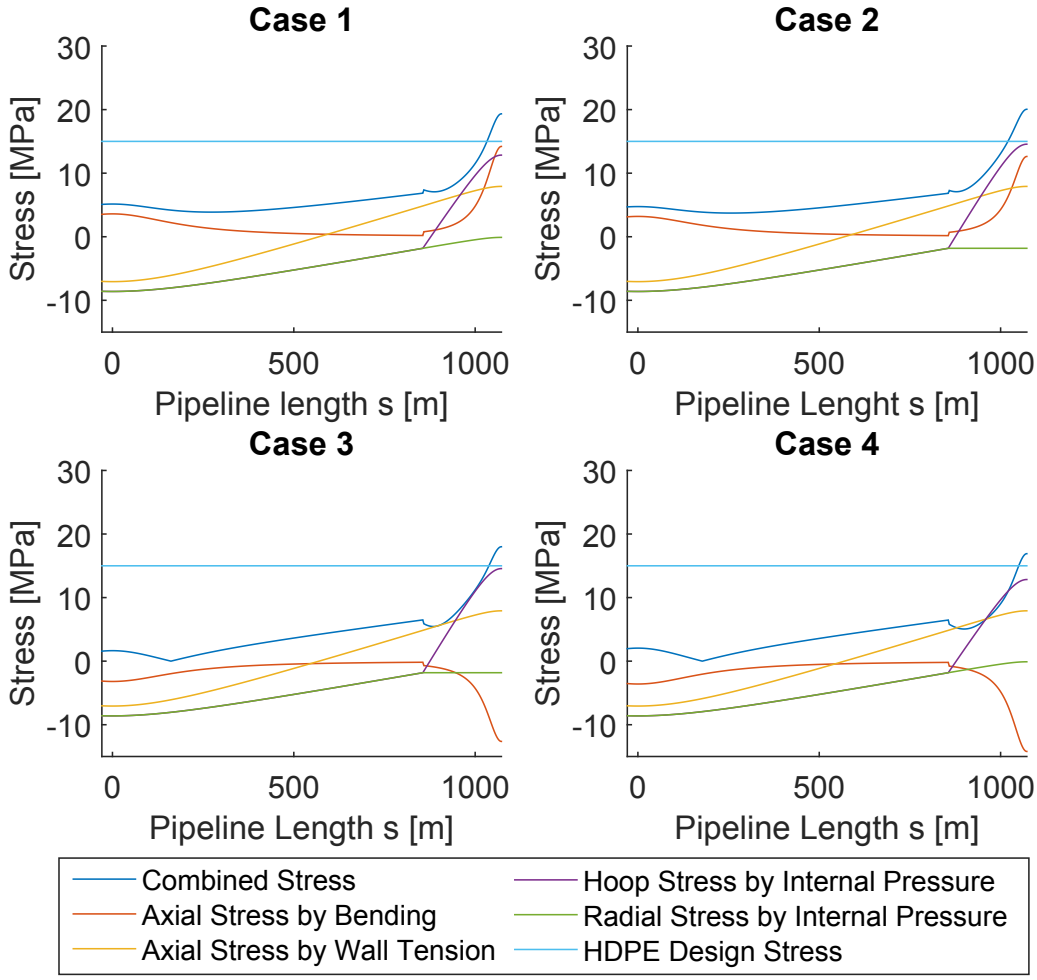

Figure 3.27: Stress in the pipe along horizontal distance in the base case situation, with closed-ended pipe

or securing of the pipeline after installation. If this is not done and the pipe remains to light after installation, it might be displaced by currents or waves as a result of too low pipeline stability.

This decrease in stress with a lower air fill ratio is caused by the coupled decrease in internal air pressure in the pipe. A lower internal pressure decreases the hoop, radial and longitudinal stresses due to internal pressure in the overbend.

From figure 3.28 it can be concluded that the largest pipe which can be installed now in the base case scenario with an SDR of 18, an air fill ratio of 0.06, a maximum combined stress of 15 MPa and a top tension of 1000 t has an outside diameter of about 2.9 m. If the top tension is limited at 350 t again, the maximum outside diameter which can be installed is about 2.3 m.

It should again be noted that these limits are purely static theoretical limits, without any safety factor but the conservativeness of the natural catenary model.

For more detailed stress level information in optimized cases, including lower SDRs, reference is made to appendix C.2.

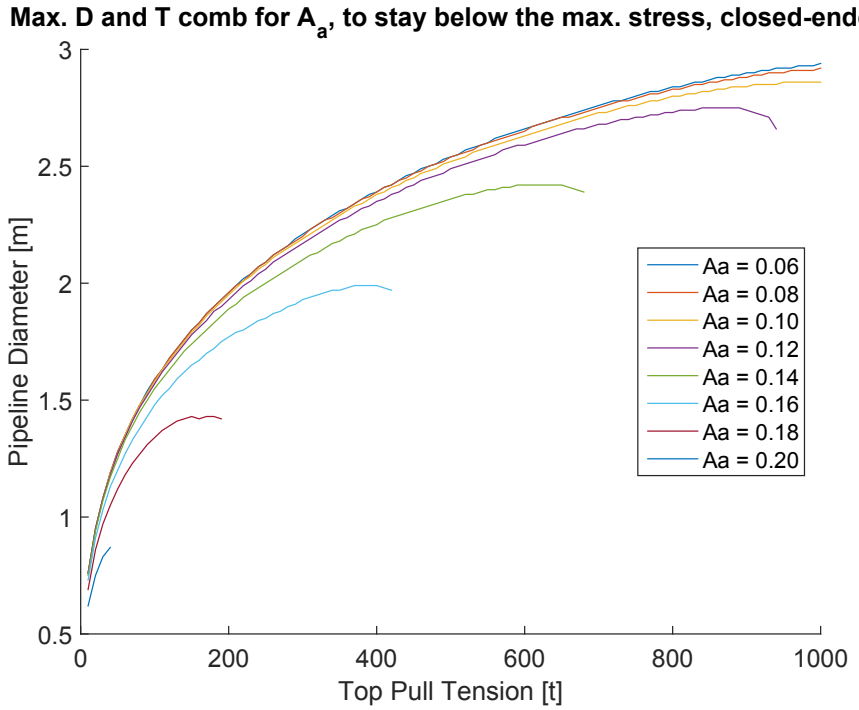

Figure 3.28: Maximum pipeline diameter which can be installed with respect to stress when varying the pull tension and air fill ratio, including closed-ended pipe

3.6 Conventional Installation Method Conclusion & Discussion

The conventional CWP installation method, the float and sink method, does not provide sufficient installation capability to install HDPE pipe diameters as large as required for large scale land-based OTEC plants. As the ultimate limit of what can practically be installed using this method is about 2.3 m, even without taking dynamics into account. The effect of dynamics due to environmental influences such as waves and current will further decrease this limit. Therefore, alternatives are required for the float and sink installation method with HDPE pipe.

Firstly, some adjustments to the current float and sink installation method with HDPE pipe can be imagined. For instance, the weight of the pipeline catenary can be decreased by introducing some vertical upward force. A lower catenary weight will allow for a wider catenary and thus less bending with less horizontal pull tension. This vertical upward force can be achieved by for instance adding removable buoyancy modules to the pipeline. Another possibility would be to have a number of lifting vessels slightly lift the catenary at certain intervals, relieving some tension in the catenary due to the weight of the pipeline. Introducing local vertical loads on the pipe catenary will alter the stress in the pipe. Therefore further analysis would be required to assess whether techniques such as these would actually be beneficial overall.

Another method to prevent excessive bending of the pipeline during installation would be by using bend restrictors at the most critical pipe bending locations. These bend

restrictors will prevent the pipe from bending beyond a certain limit. Bend restrictors have a long history of use. They are for instance often used during the installation of submarine power cables. A difficulty with using bend restrictors with the float and sink method is that the worst bend locations constantly shift. Therefore, a way should be found to move the bend restrictors along with the critical bends.

Furthermore, one can also imagine that installing multiple smaller diameter pipelines instead of one large diameter pipeline might be a viable solution. In this case the conventional proven and relatively cheap float and sink installation method can be used without taking great risks. The economical impact of this will however have to be assessed for the specific projects. Additionally, multiple smaller pipes will result in more hydraulic losses due to an increase in pipe wall friction.

The following chapters provide a more detailed analysis of possibilities to further stretch the limit of CWP diameters which can be installed. Chapter 4 does this by analysing alternative pipe materials for use with the float and sink installation method. Completely different installation methods which might increase the installation capabilities are introduced in chapter 5.

"The number of materials available to engineers is vast: 160,000 or more."

M. F. Ashby [40]

4

Alternative Pipeline Materials

In this chapter an effort is made to extend the range of diameters which can practically be installed using the float and sink installation method. This is done by considering alternative pipe materials. Alternative materials will be selected by desired material characteristics. Material characteristics which are assumed to be of significant importance for the installation capabilities are:

- Density
- Flexibility (modulus of elasticity)
- Maximum allowed stress during installation

For the float and sink pipeline installation method to be viable, the density of the pipeline material should not differ too much from the density of sea water (preferably a bit higher), which is around 1025 kg/m^3. HDPE, with a density of 960 kg/m^3 as can be found in table 2.2, is very close. When a material has a lower density, more ballast weight will have to be added to guarantee similar seabed stability and air fill ratio. This results in extra expenses. Similarly, higher density requires less ballast weight, resulting in lower expenses for ballast. This is valid until the point at which extra buoyancy might be required. This extra buoyancy ensures that the pipeline weight w does not become too large, which would cause a very high top tension to be required to maintain a sufficient wide catenary shape. Furthermore, very high density material pipelines may even no longer be buoyant when filled with air, which enforces large amounts of added buoyancy to be required. Added buoyancy adds extra costs and complexity to the float and sink installation method, especially when considering the large depth which the buoyancy tanks will have to be able to endure. An example of an HDPE pipe installation equipped with extra buoyancy, suitable for shallow water, is given in figure 4.1

High flexibility or elasticity, and thus a low modulus of elasticity results in a pipeline which can deform significantly when only experiencing limited amounts of stress. This is illustrated by formula 3.25 and by the definition of the modulus of elasticity, which is

Figure 4.1: HDPE pipe installation with added shallow water buoyancy bags [41]

given in formula 4.1 and which is roughly valid in most materials when elastic deformation occurs (in the linear-elastic regime) [40].

$$\text{Elastic Modulus E} = \frac{\text{Stress } \sigma}{\text{Strain } \epsilon} \tag{4.1}$$

The float and sink installation method enforces large deformations on the pipeline. A lower elastic modulus will result in lower stress with respect to the amount of strain that occurs. The elastic modulus will however also influence the shape of the pipeline catenary. The significance of this influence can be indicated using the bending stiffness, which resembles the resistance against bending. The bending stiffness of a pipeline can be determined using formula 4.2.

$$\text{Bending Stiffness K} = \frac{\text{Load p}}{\text{Deflection w}} = EI \tag{4.2}$$

where;

$$\text{Area Moment of Inertia I} = \frac{\pi}{4}(r_o^4 - r_i^4) \tag{4.3}$$

When a relatively flexible material with a low modulus of elasticity is used, the pipeline catenary will be relatively accurately represented by the natural catenary theory. The shape of the pipeline catenary when a stiff material with high modulus of elasticity, i.e. steel, combined with a large diameter is used will deviate from the natural catenary theory. This has been shown to a lesser extent in section 3.4. The higher pipeline bending stiffness will prevent the pipeline from bending as much as a natural catenary. Therefore, for high bending stiffness, the natural catenary model is no longer valid. Nevertheless, the natural catenary theory provides a conservative approximation.

A higher modulus of elasticity is in most materials accompanied by a higher allowed maximum stress. This, combined with the fact that higher bending stiffness decreases bending curvatures and thus encountered stresses, causes a higher modulus of elasticity not always directly to be a bad thing for this installation method. Careful analysis of pipe designs with high bending stiffness should be performed using sophisticated models to determine the exact influence of a higher modulus of elasticity.

It is easier to determine the positive effect of the last material property; maximum allowed stress. A higher maximum allowed stress is always positive as this enables for larger pipeline deformations when other material properties are kept constant, or provides larger safety margins when the deformations and material properties are kept constant. Therefore, in general a higher maximum allowed stress will facilitate larger diameter pipelines to be safely installed. The value used as maximum allowed stress is chosen as the yield stress. The yield stress represents the point at which a material transitions from purely elastic deformation to plastic deformation. In general plastic deformation during installation is undesired. Although plastic deformation is not as much of a problem in some materials as it is in others, here it is chosen as a conservative and safe limit.

Additionally, to provide a more absolute way to measure the installation capabilities using a certain material, the maximum allowed strain is introduced. This maximum allowed strain can be derived from formula 4.1 and is a function of the modulus of elasticity and the maximum allowed stress. The maximum allowed strain is given in formula 4.4.

$$\text{Max. Allowed Strain } \epsilon_{max} = \frac{\text{Max. Allowed Stress } \sigma_{max}}{\text{Elastic Modulus E}} \tag{4.4}$$

A higher maximum allowed strain is assumed positive, as this allows for larger pipeline deformations and thus a larger range of pipeline diameters which can be installed using less top tension. Furthermore, a maximum allowed strain similar to or slightly lower than that of HDPE, combined with a significantly higher modulus of elasticity is also assumed positive. As this indicates a much higher maximum allowed stress, while the amount of bending that is allowed is not significantly decreased. This larger allowed stress provides room for the stresses caused by tension and internal pressure, which are not influenced by the modulus of elasticity. As a result, other parameters such as the air fill ratio and top tension can then be further optimized. An additional benefit of a higher modulus of elasticity is the higher stiffness which results in less bending altogether. The maximum allowed strain for HDPE is 0.0143 if the Pipelife material characteristics are used. Materials which have the potential to replace HDPE as pipeline material should have a maximum allowed strain equal or higher to that of HDPE and a density preferably slightly higher than the density of water, combined with other beneficial properties, and are discussed hereinafter;

4.1 Selecting Alternative Pipeline Materials

Alternative materials for a pipeline design which can be used with the float and sink pipeline installation method are initially selected according to the most important material characteristics, as discussed at the start of this chapter. Material characteristics charts are used to do so and find optimal materials which combine a range of good properties. A first chart like this can be found in figure 4.2.

Figure 4.2 illustrates the relation of material density and its Young's modulus for a wide range of materials. HDPE, enclosed in the envelope of PE, which is again enclosed in the envelope for polymers can be found in the almost pure center of the chart. Charts like

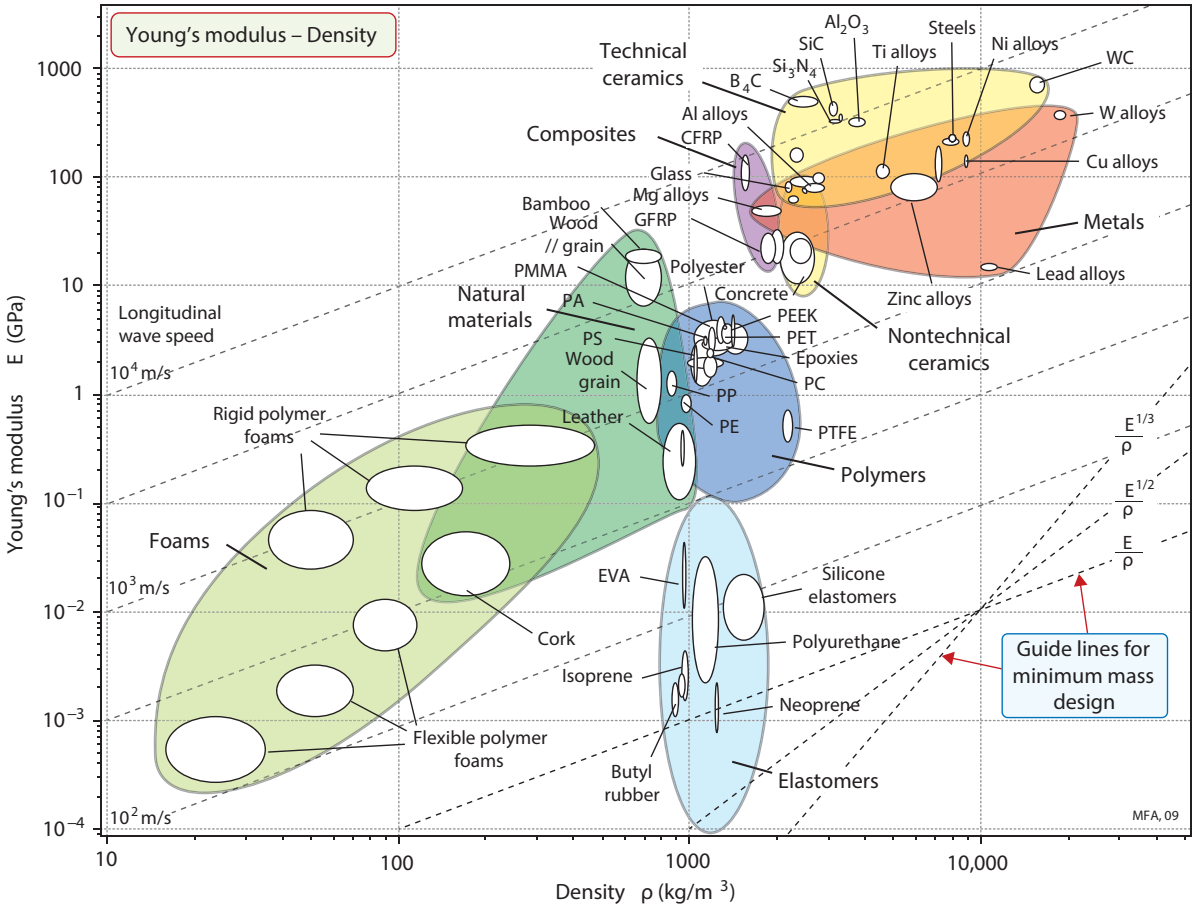

Figure 4.2: Young's modulus plotted against material density, with material classes enclosed in coloured envelopes [40]

this will from now on be filtered for a range of desired material properties as discussed hereafter;

The maximum density a pipe material is allowed to have in this study is set at 2000 kg/m^3. Higher densities would cause the pipe to become too heavy. At 2000 kg/m^3 reasonably low air fill ratios without added buoyancy are still possible, which ensures that the internal pressure in the pipe during installation can be kept at an acceptable level. For example, a 3 m outer diameter pipe with a wall thickness of 0.15 m and a density of 2000 kg/m^3 would result in a minimum air fill ratio (thus without additional weighting) achievable without adding buoyancy of 0.223.

A lower limit for density is not set in this study, as the amount of weighting required for HDPE is already quite high and increases only slowly when the density is decreased. For instance, the same 3 m outer diameter pipe as before now with the density of HDPE of 960 kg/m^3 requires about 1260 kg/m of additional weighting for an air fill ratio of 0.2. A pipe with the same dimensions, but with a density close to zero, only requires about twice as much additional weighting to achieve an air fill ratio of 0.2.

Continuing the material selection, the maximum allowed strain is now plotted against the yield stress of all materials within the allowed density range. This is done in figure

4.3. This chart and others following are created using the CES Edupack 2014 materials database software package.

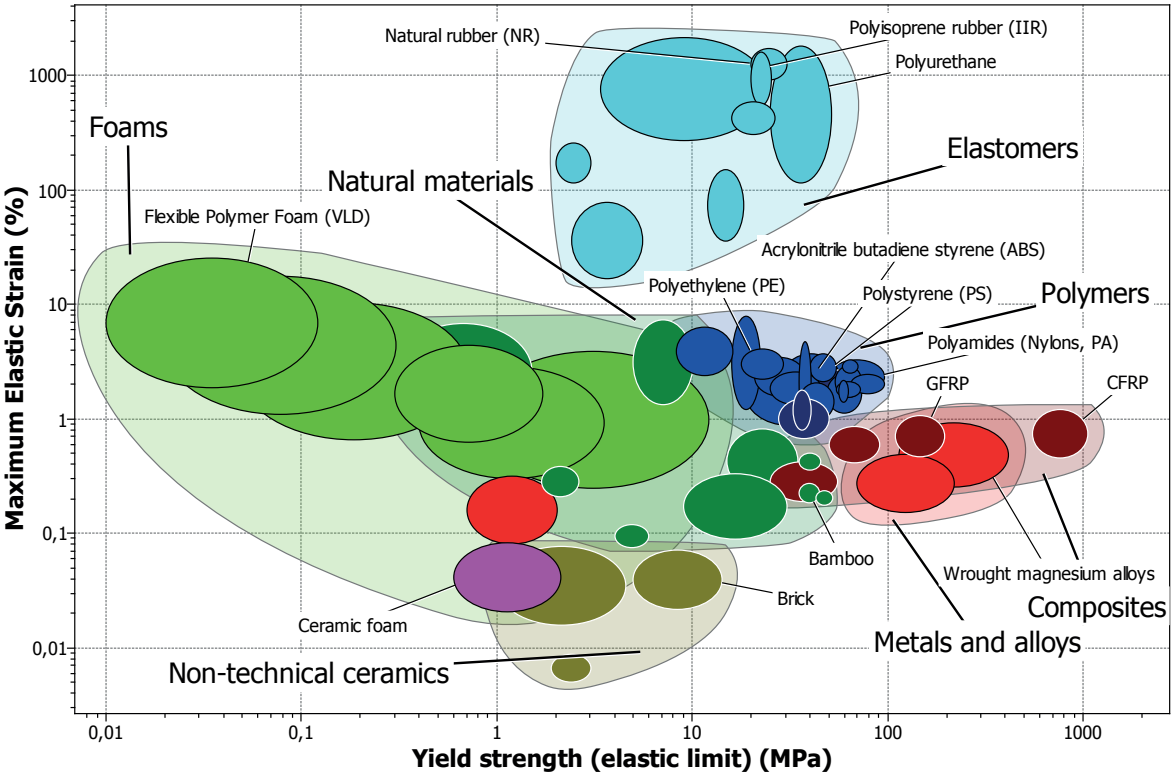

Figure 4.3: Maximum allowed strain plotted against the yield stress, with material classes enclosed in coloured envelopes [42]

It can be noted in figure 4.3 that some material classes have been thinned quite significantly due to the density limit. For instance, metals and alloys currently only features 2 types of magnesium alloys. Materials located in the quadrant to the right and up from PE are supposed to be able to bear larger deflections and stresses than PE and are thus more optimal in this respect.

To further filter the results, the minimum yield stress limit is now set at 10 MPa. This limit is chosen as it is believed that when doing an installation in a 1000 m waterdepth, or 10 MPa of pressure, somewhere during the lifetime of the pipe (either during installation or after) combined stresses of this magnitude can be expected. Even though radial, hoop and axial stress due to external pressure cancel each other when combined into Von Mises stress, when the pipe is installed and at rest. The minimum maximum allowed strain limit is set at 1% and thus slightly below the maximum allowed strain in HDPE according to Pipelife.

Additionally, materials used for a pipe should not shrink too much due to the high water pressure at 1000 m depth. 10 MPa of compressive stress in all three principal directions in the pipe material, caused by this hydrostatic pressure should not result in strain of more than 10%. More shortening of the pipe and decrease in diameter is expected to become troublesome during installation, and will result in extra large pipe diameters and extra length to be required to guarantee similar performance after installation. To

assess for this criteria the principal strain at 10 MPa of principal stress (both the same in all three directions for a pure water pressure load) is plotted against the yield stress in figure 4.4. The principle strains can be calculated using formula 4.5.

$$\begin{aligned} \epsilon_h &= \frac{1}{E}(+\sigma_h - \nu\sigma_r - \nu\sigma_a) \\ \epsilon_r &= \frac{1}{E}(-\nu\sigma_h + \sigma_r - \nu\sigma_a) \\ \epsilon_a &= \frac{1}{E}(-\nu\sigma_h - \nu\sigma_r + \sigma_a) \end{aligned} \tag{4.5}$$

where;

ϵ_h = Strain in hoop direction
ϵ_r = Strain in radial direction
ϵ_a = Strain in axial direction
ν = Poisson's ratio

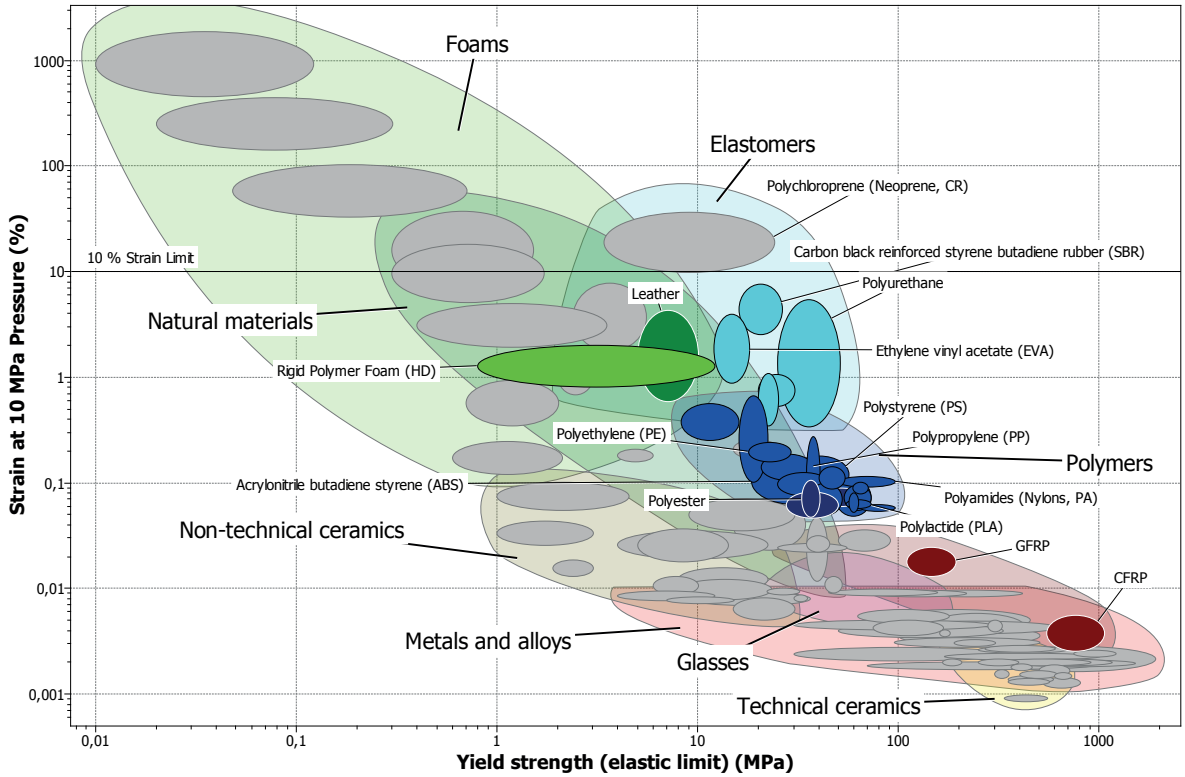

Figure 4.4: Principal strain due to 10 MPa of hydrostatic pressure plotted against the yield stress, with material classes enclosed in coloured envelopes [42]

The grey-coloured envelopes in figure 4.4 indicate materials which have failed one or more of the criteria. In other graphs these have been excluded.

Economics of a pipeline are also very important for OTEC projects, as high CAPEX can render the project economically infeasible. The pipeline, especially in a land-based

OTEC plant, accounts for a very large portion of the CAPEX [43]. Therefore it is of importance to select a material which both provides good performance and is affordable. The typical costs of the materials which remain at this stage is given in figure 4.5.

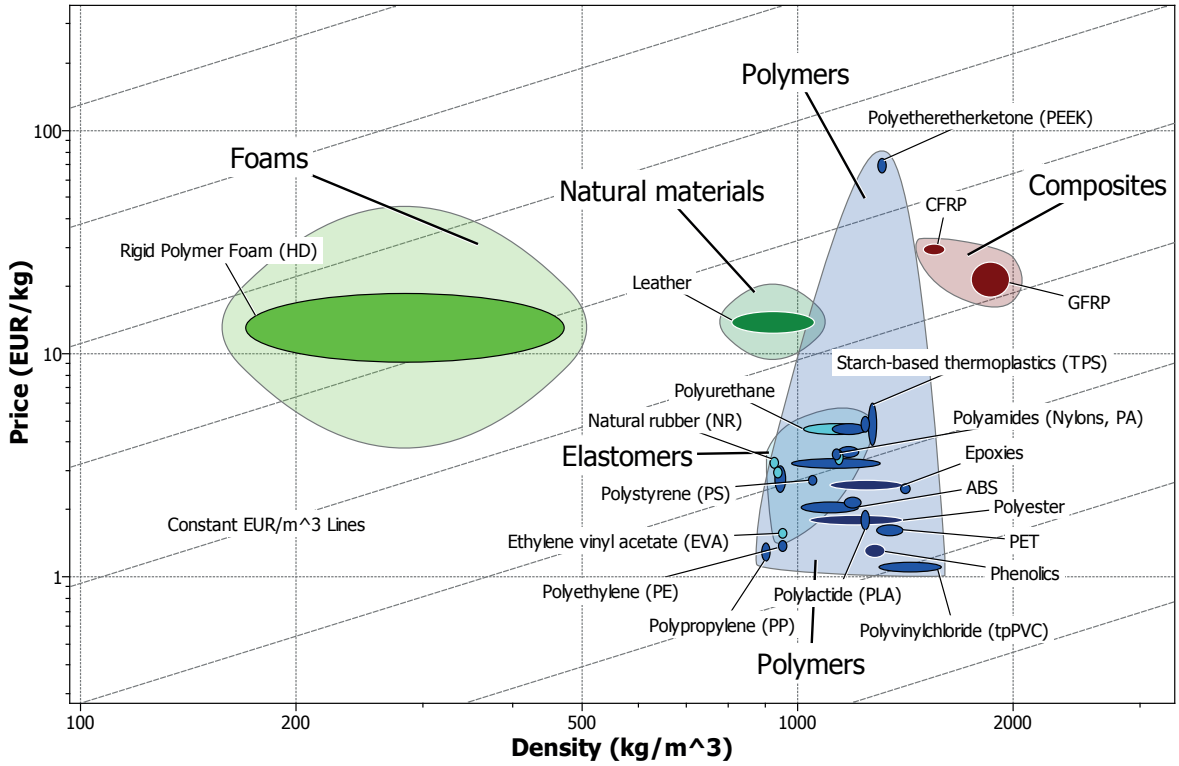

Figure 4.5: Materials price in Euro per kg plotted against the material density, with material classes enclosed in coloured envelopes [42]

Combining figure 4.3, 4.4 and 4.5 results in a solid base to assess the remaining materials performance- and price-wise. However this is not the complete package of criteria which a good material for a pipe has to fulfil. Additional criteria are discussed below;

Starting off, it is desired that the pipe material is a good thermal insulator, so that the cold seawater does not heat up significantly during transportation to the OTEC installation. This is especially important when considering the long length of the cold water pipe for onshore OTEC or SWAC.

Furthermore, the material should be resistant to salt-water and UV-radiation so it will last for the lifetime of the OTEC installation.

Finally, producibility, joinability and availability are also key. The material has to be able to be made into a pipe at manageable costs by i.e. extrusion or less favourable; moulding. After production the pipe sections then have to be joined on location. Joining with the use of for instance butt fusion welding, like with HDPE, is preferred over less optimal solutions such as bolted flanges. Whether pipe sections of a specific material are already available for sale and whether there is some history of usage of the material in similar applications is also considered important. Picking a widely available material is key to saving time and money and minimizing risk.

Based on expected performance according to the plots, the following materials are chosen for further analysis:

- Glass-Fiber-Reinforced Polymer (GFRP)
- Polyurethane (PU)
- Acrylonitrile Butadiene Styrene (ABS)
- Polyamides (Nylons, PA)

Furthermore, these materials are sufficiently different for comparison. As there is one stiff composite, one very flexible elastomer and two polymers with significantly different price and performance. From the plots it can be seen that there are much other materials left which are promising as well. Especially a lot of polymers are concentrated around PE, ABS and PA in terms of similar material characteristics and price and thus the choice for these materials was not an absolute one. If for instance ABS performs very well at all aspects but one, it might be possible to find a very similar polymer which also satisfies at that last aspect.

4.2 Detailed Comparison of Alternative Pipeline Materials

In this section the four chosen materials and HDPE will be compared in more detail. As a start, the material characteristics of interest according to the CES Edupack Level 2 database are given in table 4.1. In this table the availability of a material represents whether it is currently being made in large size pipes. This is established by an internet enquiry for available suppliers, instead of the CES Edupack.

From this table it can be seen that for some materials the range of certain material characteristics is very wide. This is due to the fact that the Level 2 CES Edupack data is used, which includes in the envelope of a certain material a lot of possible configurations of the material. In Level 3 these materials have been further separated into more detailed materials. For instance PU can be made into thermosetting and thermoelastic elastomers and can have a lot of different fillers. For further analysis it is important to choose a more detailed material configuration than the main material.

Therefore, for all four materials it is now further discussed which exact material configuration results in the desired material characteristics for the float and sink pipe installation method for a CWP. It should be noted that specific details about these materials, as discussed in the coming sections, are acquired from the CES Edupack software package, which has proven to be a very helpful source. This does not include details about the availability of a material as a pipe, which are acquired through an internet industry enquiry.

	PE	GFRP	PU	ABS	PA
Density [kg/m^3]	939 – 960 avg. 949	1750 – 1970 avg. 1860	1020 – 1250 avg. 1130	1010 – 1210 avg. 1110	1120 – 1140 avg. 1130
Young's Modulus [GPa]	.621 – .896 avg. .746	15 – 28 avg. 20.5	.002 – .03 avg. .00775	1.1 – 2.9 avg. 1.79	2.62 – 3.2 avg. 2.9
Yield Strength [MPa]	17.9 – 29 avg. 22.8	110 – 192 avg. 145	25 – 51 avg. 35.7	18.5 – 51 avg. 30.7	50 – 94.8 avg. 68.8
Max. Elastic Strain [%]	2.28 – 4.09 avg. 3.05	.477 – 1.05 avg. .709	118 – 1800 avg. 461	.901 – 3.28 avg. 1.72	1.71 – 3.31 avg. 2.38
Price [EUR/kg]	1.32 – 1.45 avg. 1.38	18.2 – 25.8 avg. 21.7	4.39 – 4.82 avg. 4.6	1.96 – 2.16 avg. 2.06	3.4 – 3.74 avg. 3.56
Thermal Conductivity [W/m.°C]	.403 – .405 avg. .419	.4 – .55 avg. .469	.28 – .3 avg. .29	.188 – .335 avg. .251	.233 – .253 avg. .243
Salt Water Durability	Excellent	Excellent	Excellent	Excellent	Acceptable
Manufacturability	Excellent	Average	Good	Excellent	Good
Joinability	Excellent	Poor	Good	Excellent	Excellent
Availability	Excellent	Good	Poor	Good	Average

Table 4.1: Detailed Alternative Material Characteristics [42]

4.2.1 Glass-Fiber-Reinforced Plastic

GFRPs are composites made of glass fibers embedded in a thermosetting resin such as polyester or epoxy. The embedded glass fibers result in a much stiffer and tougher material than what the plastic would be like without fibers.

When the range of available GFRPs available in CES Edupack is scanned on level 3 it can be noted that there are more optimal material characteristics available for our purpose than the general GFRP characteristics. An example of this is the epoxy matrix based E-glass fiber; Epoxy SMC (glass fiber). The material characteristics of Epoxy SMC (glass fiber) are given in table 4.2.

GFRP pipe is currently made all over the world and so it has good availability. Past experience is also available with large diameter GFRP pipes, however not as long lengths as are produced for HDPE. Joining GFRP pipe sections cannot be done by (thermal) welding, as is possible for most plastics. Instead, GFRP will have to be glued and cured or bolted. Furthermore, GFRP can not be extruded like most plastics. More time-consuming techniques such as moulding and filament winding are used.

Epoxy SMC (Glass Fiber) is about 3 times as expensive as HDPE. It is however much stronger and stiffer, which can lead to less wall thickness required and thus less material. Furthermore, it has a significantly higher density, reducing the amount of ballast weighting required.

To assess the true performance of Epoxy SMC (Glass Fiber) in the float and sink installation method, the optimization script used for HDPE is ran. This optimization script

	Epoxy SMC (Glass Fiber)
Density [kg/m^3]	1500 – 1800 avg. 1640
Young's Modulus [GPa]	13.8 – 27.6 avg. 19.5
Yield Strength [MPa]	110 – 193 avg. 146
Poisson's Ratio	.313 – .342 avg. .327
Max. Elastic Strain [%]	.491 – 1.14 avg. .748
Price [EUR/kg]	3.86 – 4.87 avg. 4.34
Thermal Conductivity [W/m.°C]	.6 – .7 avg. .648
Salt Water Durability	Excellent
Manufacturability	Average
Joinability	Poor
Availability	Good

Table 4.2: Detailed Material Characteristics Epoxy SMC (Glass Fiber) [42]

finds the largest pipe diameter which can be installed for a certain configuration. It should be noted that GFRP has a much higher stiffness than HDPE and therefore, the results of the natural catenary Matlab script will have an even greater error than for HDPE.

For the optimization, the average material characteristics of Epoxy SMC (Glass Fiber) are used, as given in table 4.2. The maximum allowed stress will be assumed as the average yield strength divided by a safety factor of 1.5. This results in a maximum allowed stress of 97 MPa (When the average yield strength of PE according to the CES Edupack is divided by 1.5, this results in approximately 15 MPa). Furthermore, the same target installation depth, slope steepness and SDR are used as before (table 3.1).

The results of the Matlab optimization study for Epoxy SMC (Glass Fiber) are given in figure 4.6. From this figure it can be seen that the pipe diameters which can be installed when using GFRP and the float and sink installation method are smaller according to natural catenary theory. The maximum diameter which can now be installed is about 2.15 m with 350t of top tension and an optimum air fill ratio of 0.5. The optimum air fill ratio is a lot higher for GFRP than for HDPE. This is caused by the significantly higher yield strength, which now causes stress due to internal air pressure to be less significant.

To verify the results, the Epoxy SMC pipe is modelled in Orcaflex which does include the effect of the high stiffness. The parameters used are a 2.15 m outer diameter pipe with 350 t top tension. All other parameters are the same as for the Matlab optimization. Furthermore the base case configuration is also modelled using GFRP. Finally, an extra case is added indicating the limit of the pipe material as calculated by Orcaflex. In this extra case the same parameters as for the optimized Epoxy SMC case are used; an air fill ratio of 0.5, top tension of 350 t, pipe outer diameter as indicated and the base case parameters for the remaining variables. The results of this are given in table 4.3.

As can be concluded from table 4.3 and table 3.7, similar pipe diameters can be installed

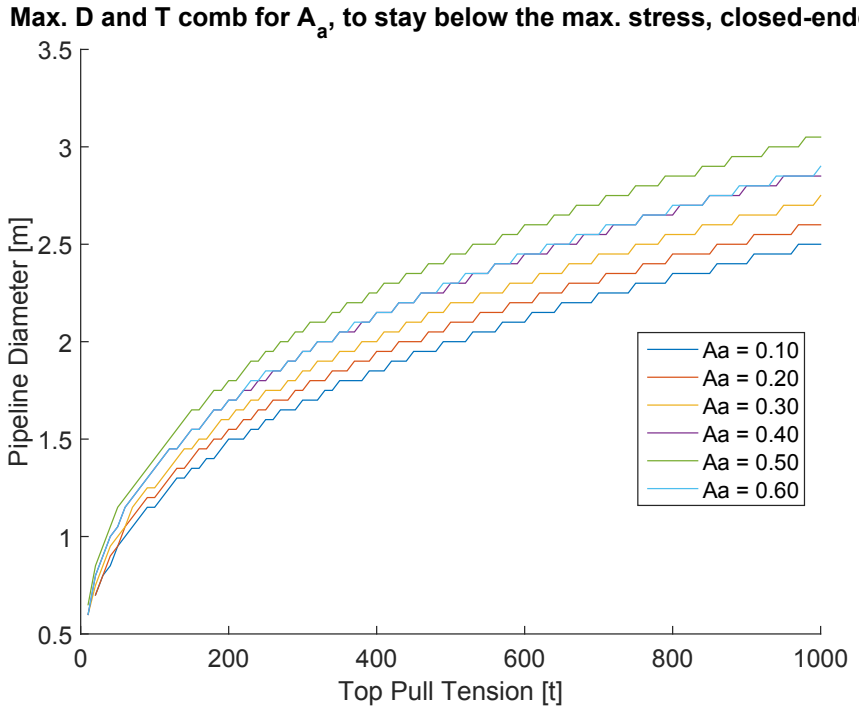

Figure 4.6: Maximum pipeline diameter which can be installed with respect to stress when varying the pull tension and air fill ratio, GFRP

when using GFRP as with HDPE when using the same SDR. Epoxy SMC (Glass Filled) is slightly more optimal than HDPE as relatively slightly less stress is encountered for similar configurations.

4.2.2 PolyUrethane

Polyurethane is a versatile polymer and can, aside from the elastomeric grade, also be produced in thermoplastic and thermosetting grades.

When the range of all possible configurations of PU is analysed on level 3 in CES Edupack, the grades most suitable for the float and sink installation method are the ther-

	Max. Von Mises Stress [MPa]			% of Max. Stress	
	Matlab	Orcaflex	Difference	Matlab	Orcaflex
Base Case	265.634	77.849	-70.69 %	273.85 %	80.26 %
D = 2.15 m, T = 350 t	93.369	79.272	-15.10 %	96.26 %	81.72 %
D = 2.5 m, T = 350 t	139.329	105.541	-24.25 %	143.64 %	108.81 %

Table 4.3: Matlab, Closed-Ended Pipe vs Orcaflex Comparison for GFRP

	TPU Shore A85/D35	
Density [kg/m^3]	1180 – 1210	avg. 1200
Young's Modulus [GPa]	.0285 – .0398	avg. .0337
Yield Strength [MPa]	38 – 49.4	avg. 43.3
Poisson's Ratio	.48 – .495	avg. .487
Max. Elastic Strain [%]	105 – 158	avg. 129
Price [EUR/kg]	3.82 – 4.94	avg. 4.34
Thermal Conductivity [W/m.°C]	.151 – .172	avg. .161
Salt Water Durability	Excellent	
Manufacturability	Excellent	
Joinability	Excellent	
Availability	Poor	

Table 4.4: Detailed Material Characteristics TPU polyester Shore A85/D35 [42]

moplastic polyurethanes. These are very suitable as they can be extruded and welded, just like HDPE, yet still have the flexible and though elastomeric mechanical properties. A typical thermoplastic polyurethane grade, selected for further analysis, is TPU (Thermoplastic Polyurethane elastomer), Polyester, aromatic type, Shore A85/D35. The materials characteristics for TPU polyester Shore A85/D35 are given in table 4.4.

TPU is widely available, yet not made into large diameter pipes. It is used for all sorts of flexible hoses/tubes, such as in consumer products and fire-hoses. TPU is also about 3 times as expensive as HDPE. The density of TPU is slightly higher than HDPE, which reduces the amount of ballast weighting required and thus saves costs.

To assess the true performance of TPU in the float and sink installation method, the Matlab optimization script used for HDPE is ran again. This script should return quite accurate results as PU barely has any stiffness. The large strain which might occur in TPU during the installation, due to the low Young's modulus might however result in some inaccuracy. This is due to the fact that the natural catenary model assumes infinite axial stiffness and thus no axial strain. According to the CES Edupack, the chosen TPU grade can have a strain of more than 500 % at yield.

For the optimization, the average material characteristics of the chosen TPU are used, as given in table 4.4. The maximum allowed stress is again assumed as the average yield strength divided by a safety factor of 1.5. This results in a maximum allowed stress of about 29 MPa. Furthermore, the same target installation depth, slope steepness and SDR are used again.

The results of the Matlab optimization study for TPU are given in figure 4.7. From this figure it can be seen that when using TPU, much larger pipe diameters can be installed even when using low top tensions. The maximum pipe diameter which can now be installed is about 10 m (possibly larger, but the optimization is limited to a maximum

	Max. Von Mises Stress [MPa]			% of Max. Stress	
	Matlab	Orcaflex	Difference	Matlab	Orcaflex
Base Case	17.919	17.812	-0.597 %	61.79 %	61.42 %
D = 10 m, T = 350 t	27.08	18.542	-31.53 %	93.38 %	63.94 %
D = 25 m, T = 350 t	347.796	19.162	-94.49 %	1199.3 %	66.08 %

Table 4.5: Matlab, Closed-Ended Pipe vs Orcaflex Comparison for TPU

outer diameter of 10 m), when a top tension of 350 t is used and an optimum air fill ratio of 0.25.

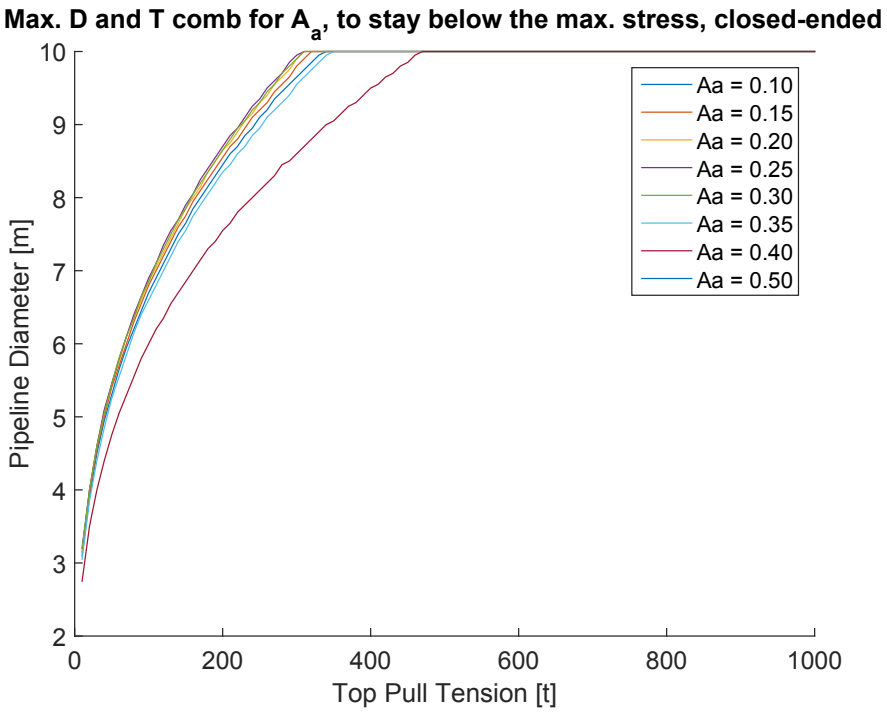

Figure 4.7: Maximum pipeline diameter which can be installed with respect to stress when varying the pull tension and air fill ratio, TPU

To check in which way the strain effects the installation capabilities, some pipe configurations are again modelled in Orcaflex. The base case is modelled, the Matlab optimum at 350 t top tension and 10 m outer diameter is modelled and an extra case is again modelled, indicating the limit of what can be installed according to Orcaflex. This extra case also uses 350 t top tension, an air fill rate of 0.25 and furthermore the same parameters as in the base case. The results of these three cases are given in table 4.5.

As can be concluded from table 4.5 and 3.7 much larger pipe diameters can be installed when using TPU than when using HDPE, using the same SDR. The maximum pipe diameter which can be installed when using TPU actually seems practically unlimited

	ABS unfilled, extrusion	
Density [kg/m^3]	1020 – 1080	avg. 1050
Young's Modulus [GPa]	2 – 2.9	avg. 2.41
Yield Strength [MPa]	29.6 – 44.1	avg. 36.1
Poisson's Ratio	.394 – .422	avg. .408
Max. Elastic Strain [%]	1.15 – 1.95	avg. 1.5
Price [EUR/kg]	2.01 – 2.22	avg. 2.11
Thermal Conductivity [W/m.°C]	.226 – .235	avg. .23
Salt Water Durability	Excellent	
Manufacturability	Excellent	
Joinability	Excellent	
Availability	Good	

Table 4.6: Detailed Material Characteristics ABS unfilled, extrusion [42]

when looking at the Orcaflex results. This is probably due to the fact that the stress due to bending does not increase significantly, due to the low Young's modulus. The bending in Orcaflex is also coupled to the bending stiffness, which increases due to the larger diameters and therefore the increase in bending of the pipe will relatively be less, compared to the natural catenary model. This effect appears significant enough to almost cancel the increase in stress.

As the maximum allowed stress is not reached by quite a large margin, the wall thicknesses can probably be decreased significantly when using TPU. This will result in lower material costs.

A drawback of the low modulus of elasticity of TPU is that a pure TPU pipe of reasonable wall thickness will very likely buckle due to the external pressure caused by sucking cold deep seawater through the pipe during operation. To solve this problem, the ring stiffness of a TPU pipe would have to be increased. This can for instance be done by including spiralling steel wire or strip in the pipe wall material. Such solutions to increase the ring stiffness should not influence the bending stiffness of the TPU pipe by too much, as this will decrease the installation capacity.

4.2.3 Acrylonitrile Butadiene Styrene

ABS is a widely produced engineering thermoplastic with a great balance of properties and price.

ABS is also available in a range of configurations, with all sorts of fillers and special purpose added properties, like flame retarded or high-impact. Regular unfilled ABS for extrusion is chosen as most suitable for the CWP. The material characteristic for unfilled ABS extrusion grade according to the CES Edupack level 3 database are given in table 4.6.

	Max. Von Mises Stress [MPa]			% of Max. Stress	
	Matlab	Orcaflex	Difference	Matlab	Orcaflex
Base Case	35.948	26.214	-27.08 %	149.78 %	109.23 %
D = 2.2 m, T = 350 t	24.858	22.628	-8.97 %	103.58 %	94.28 %
D = 2.4 m, T = 350 t	29.213	25.230	-13.63 %	121.72 %	105.13 %

Table 4.7: Matlab, Closed-Ended Pipe vs Orcaflex Comparison for ABS

ABS can be extruded and welded (hot plate / butt fusion), just like HDPE. ABS is also available as pipe and in quite large diameters, yet is not as common as HDPE.

ABS is slightly more expensive than HDPE, by about 1.5 times. It is however stronger so less material might be required. Furthermore, ABS also has a slightly larger density. This results in less costs for ballasting.

One negative aspect of ABS, which has to be considered, is that it has poor resistance against UV radiation. This decreases the lifetime of the pipe when exposed to UV radiation. Therefore, especially at the landfall and in shallow water, the use of ABS should be considered with care. This problem can be overcome by stabilizing the ABS or for instance, by using a coating. Low UV resistance can also be a problem for the other materials and should thus also be carefully examined. The other chosen materials are not as bad as ABS, yet are still sensitive to UV radiation.

To assess the true performance of ABS in the float and sink installation method, the Matlab optimization script is ran again. This script should return quite accurate results as the material properties of ABS, mainly in terms of the Young's modulus, are within the same order of magnitude as for HDPE.

For the optimization, the average material characteristics of the chosen grade of ABS are used again, as given in table 4.6. The maximum allowed stress is again assumed as the average yield strength divided by a safety factor of 1.5. This results in a maximum allowed stress of about 24 MPa. Furthermore, the same installation parameters are used as in the base case aside from the ABS material characteristics.

The results of the Matlab optimization study for ABS are given in figure 4.8. From this figure it can be seen that when using ABS, similar pipe diameters can be installed as when using HDPE. The maximum pipe diameter which can now be installed is about 2.2 m, when a top tension of 350 t is used and an optimum air fill ratio of 0.2.

To again check these results, three pipe configurations are modelled in Orcaflex. The base case is modelled, the Matlab optimum at 350 t top tension and 2.2 m outer diameter is modelled and an extra case is again modelled indicating the limit of what can be installed according to Orcaflex. This extra case again uses 350 t top tension, an optimal air fill ratio of 0.2 and furthermore the same parameters as in the base case. The results of these three cases are given in table 4.7.

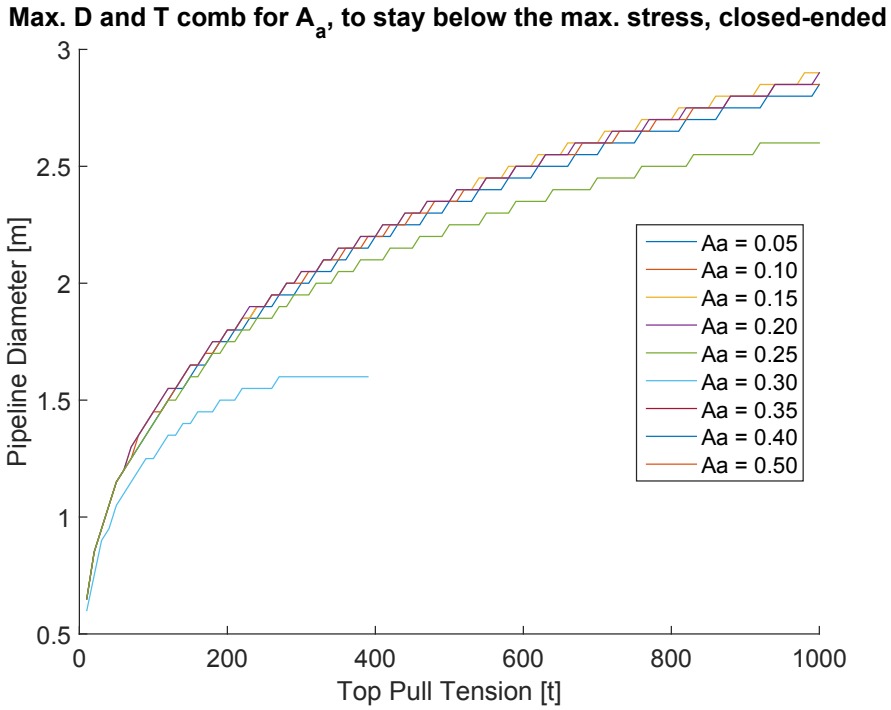

Figure 4.8: Maximum pipeline diameter which can be installed with respect to stress when varying the pull tension and air fill ratio, ABS

As can be concluded from table 4.7 and 3.7, similar pipe diameters can be installed when using ABS as with HDPE when using the same SDR.

4.2.4 PolyAmide

Polyamides/Nylons are lightweight, strong and durable thermoplastics and are also found in natural forms, such as silk. One well-known application is Kevlar, the fiber used in bullet proof vests.

Polyamides are widely used and also available in a wide range of configurations; for instance filled with glass, minerals, carbon and stainless steel or unfilled. Special grades of PA enable extrusion, these special grades are required due to the very low viscosity of PA. The PA chosen here as most suitable for the float and sink CWP installation is PA Type 6, unfilled, Moulding and extrusion. The material characteristics of PA Type 6 for moulding and extrusion according to the CES Edupack level 3 database are given in table 4.8.

Furthermore, PA can be welded like HDPE and is available in pipe. Large diameter PA pipe producers where however not found.

PA type 6 is slightly more expensive than HDPE, by about 2 times. It is however significantly stronger with similar modulus of elasticity and has a slightly higher density. Therefore, less pipe material and added ballasting might be required, resulting in a reduction in costs.

	PA Type 6, unfilled	
Density [kg/m^3]	1130 – 1150	avg. 1140
Young's Modulus [GPa]	.944 – 1.18	avg. 1.06
Yield Strength [MPa]	38.6 – 48.2	avg. 43.1
Poisson's Ratio	.34 – .36	avg. .35
Max. Elastic Strain [%]	3.5 – 4.77	avg. 4.09
Price [EUR/kg]	3.4 – 3.74	avg. 3.56
Thermal Conductivity [W/m.°C]	.233 – .253	avg. .243
Salt Water Durability	Excellent	
Manufacturability	Good	
Joinability	Excellent	
Availability	Average	

Table 4.8: Detailed Material Characteristics PA Type 6, Unfilled, Moulding and Extrusion [42]

One negative aspect of PAs are that they are very moisture sensitive, absorbing a lot of water. This can lead to dimensional instability and will alter material properties. Absorption of water reduces the tensile strength and the Young's modulus, making the material more flexible and increasing the toughness. The change in properties can be as significant as 50% or more. This should therefore be considered during the installation and for the long-term performance of a PA CWP. The specific type of PA should be carefully tested how quickly and how significant the material properties change.

To assess the true performance of PA in the float and sink installation method, the Matlab optimization script is ran again. This script should return quite accurate results for PA as the materials properties of PA, mainly in terms of the Young's modulus, are very similar to HDPE.

For the optimization, the average material characteristics of the chosen grade of PA are again, as given in table 4.8. The maximum allowed stress is again assumed as the average yield strength divided by a safety factor of 1.5. This results in a maximum allowed stress of about 28.7 MPa. Furthermore, the same installation parameters are used again, as in the base case, aside from the PA material characteristics.

The results of the Matlab optimization study for PA type 6 are given in figure 4.9. From this figure it can be seen that when using PA, significantly larger pipe diameters can be installed than when using HDPE. The maximum pipe diameter which can now be installed is about 3.2 m, when a top tension of 350 t is used and an optimum air fill ratio of 0.25.

To again check these results, three pipe configurations are modelled in Orcaflex. The base case is modelled, the Matlab optimum at 350 t top tension and 3.2 m outer diameter is modelled and an extra case is again modelled indicating the limit of what can be installed according to Orcaflex. This extra case again uses 350 t top tension, an optimal air fill

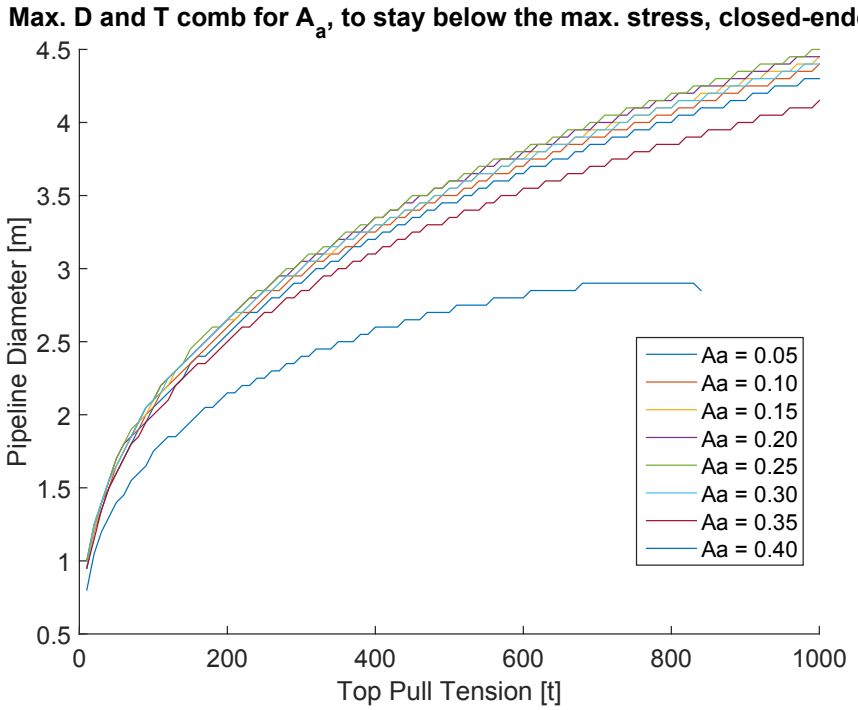

Figure 4.9: Maximum pipeline diameter which can be installed with respect to stress when varying the pull tension and air fill ratio, PA

ratio of 0.25 and furthermore the same parameters as used in the base case. The results of these three cases are given in table 4.9.

As can be concluded from table 4.9 and 3.7, significantly larger pipe diameters can be installed when using PA compared to HDPE, using the same SDR. According to the Orcaflex results, diameters up to about 4 meters are even possible.

In table 4.9 the Orcaflex results shows similar behaviour for PA near the upper limit as TPU did. The difference between the Matlab and Orcaflex results increases significantly close to the upper stress limit, where installation becomes critical. This is probably due to the low Young's modulus of PA and TPU as discussed in section 4.2.2.

	Max. Von Mises Stress [MPa]			% of Max. Stress	
	Matlab	Orcaflex	Difference	Matlab	Orcaflex
Base Case	22.346	20.481	-8.35 %	77.86 %	71.36 %
D = 3.2 m, T = 350 t	28.622	23.569	-17.65 %	99.73 %	82.12 %
D = 4.2 m, T = 350 t	54.884	28.932	-47.29 %	191.23 %	100.81 %

Table 4.9: Matlab, Closed-Ended Pipe vs Orcaflex Comparison for PA

4.3 Final Material Selection

In this section a final assessment will be made for the selected materials, to provide a good recommendation on materials suitable for large diameter CWP designs.

The preceding sections covered a detailed analysis of the performance of four materials (five including HDPE) during installation. From this analysis, it can be concluded that GFRP and ABS do not improve pipe installation capabilities. PA significantly increases installation capabilities and TPU practically increases installation capabilities infinitely.

To assess which of the four materials are good alternatives to HDPE, considering all relative aspects, a multiple criteria analysis (MCA) is performed. The multiple criteria analysis rates every material on a range of weighted criteria. The sum of the separate ratings, multiplied by the corresponding weight factor, of the criteria for each material makes up the total score for a material. All materials receive a score on a scale of 1 to 5 on all criteria, where higher is better. The material with the highest total score is considered most optimal as alternative CWP material.

The criteria by which the materials are judged are; *installation performance*, *price*, *thermal performance*, *durability*, *manufacturability*, *joinability*, *availability* and *environmental impact*. Most of these criteria have already been discussed in section 4.1.

The *installation performance* is based on sections 4.2.1 to 4.2.4 and is a combination of the material density, Young's modulus, and yield strength. For this criteria, the material that provides the largest pipe diameter installation capability receives the highest grade.

The criterion for material *price* is quite straight forward. If a material has a lower price and thus results in lower material costs for the pipeline, it receives a higher rating.

Thermal performance is determined by the thermal conductivity of a material. A lower thermal conductivity means that a material conducts less heat and thus the water will remain colder during transportation through the pipeline. A lower thermal conductivity will thus results in a higher grade for thermal performance.

Durability is determined by how well the material survives in the marine environment. For this criterion the salt water resistance and UV radiation resistance are considered.

How easily a material is made into a pipe is rated through the *manufacturability* criterion. Especially materials which can be extruded are very suitable for pipe production and will thus get a high rating on this criterion.

The criterion for *joinability* rates the materials on how easy and how well the material can be joined to create a long pipeline from separate pipe sections. Especially materials which can be welded in some way are favourable, as this is relatively quick and cheap and the strength of the material will remain largely unaltered.

Availability is used to rate how well a material is currently available at all and if it is already being fabricated into large diameter pipe. Materials which are widely used, with many suppliers and which are made into large diameter pipe sections already will receive a high rating.

	HDPE	GFRP	TPU	ABS	PA
Installation Performance WF = 0.214	3	3	5	2	4
Price WF = 0.107	5	2	2	4	3
Thermal Performance WF = 0.036	2	1	3	3	5
Durability WF = 0.161	4	4	4	3	4
Manufacturability WF = 0.089	5	2	5	5	4
Joinability WF = 0.036	5	2	5	5	4
Availability WF = 0.125	5	4	2	4	3
Environmental Impact WF = 0.232	5	1	5	4	2
Total	**4.303**	**2.518**	**4.071**	**3.5**	**3.34**

Table 4.10: CWP Material Multiple Criteria Analysis

Then finally, the *environmental impact* of a material is also very important. The environmental impact of a material is measured by the amount of CO_2 which is emitted during the production of the material, whether it is recyclable and/or biodegradable and whether it is not harmful to the marine ecosystem in which it will be installed (i.e. poisonous).

To ensure these eight criteria have an appropriate influence on the final material choice, weight factors are first determined for each criterion. This is done in appendix D.1, by comparing all criteria with each other and for each combination selecting the one which is more important. As a result, the criterion which is most important will gather the most points and this will be normalised into a weight factor for the multiple criteria analysis.

The multiple criteria analysis is performed and can be found in table 4.10. The ratings given to materials for the criteria are again based on the CES Edupack 2014 level 3 database. Except for availability, which is assessed through an internet enquiry for producers of large diameter pipe made out of the specific material. More information about the environmental impact of the selected materials can be found in appendix D.2.

From the multiple criteria analysis it can be concluded that thermoplastic polyurethane is the best alternative to HDPE. It performs better, has suitable characteristics for the fabrication of pipes and is relatively environmentally friendly. Downsides of TPU are that

it has a high material price and is currently not available in large diameters. Therefore, to be able to use TPU as alternative CWP material some steps have to be made. First, more elaborate modelling of the float and sink installation method using TPU is required. This will likely result in a more optimal pipe, probably with less wall thickness, which will decrease the costs of a TPU pipe. From this the economical feasibility of a TPU CWP can be studied. Additionally, a pipe manufacturer has to be found who is willing to start experimenting and investing in large diameter TPU pipe. This will help improve the availability of large diameter TPU pipe.

GFRP and ABS are not considered feasible alternatives for HDPE, as these materials don't improve the installation performance and score lower overall in the multiple criteria analysis.

Polyamides or nylons are interesting as they increase the installation capabilities into a range that is very interesting for large scale land-based OTEC plants. They don't score that well in the multiple criteria analysis however, as they are relatively expensive, are not available in large diameter pipes and have quite a significant environmental impact. Further research into the wide range of polymers available might yield another plastic with similar installation performance which improves the downsides of PA.

"The conclusion is that we have to develop new methods for the installation of marine PE pipes in diameter > OD 2,000 - 2,500 mm when installing the pipes in water depth > 12 m"

Prof. Ian Larsen [44]

5

Alternative Pipeline Installation Methods

This chapter focusses on alternative pipeline installation methods, to extend the range of diameters which can practically be installed. These methods should provide larger pipe diameter installation capabilities than the float and sink pipeline installation method. Furthermore, the pipe material which is used in these alternative method should preferably be HDPE. This is due to the fact that HDPE is a low cost, high performance material as has been indicated in section 4.3 and has a long history of usage for large diameter pipes. If other pipe materials are considered more optimal for a certain installation method, this will be noted.

Installation method characteristics which are assumed to significantly impact the installation performance, complexity and costs of a method are:

- The amount of bending encountered
- Specific installation method loads encountered
- Equipment required (Both in terms of size and amount)
- Weather window required
- Seabed profile

Some methods, such as the float and sink / S-lay method, require the pipe to be bent significant amounts to be able to be installed on the seabed. Other methods can be imagined where this does not have to be the case. For instance, a pipeline can be pulled down to the seabed gradually, while theoretically remaining perfectly straight. Or, the pipe sections can be lowered to the seabed and be connected to each other afterwards, which does not require any bending of the pipeline. However, bending is only one type of load which the pipe encounters.

Each specific installation method has a specific load profile on the pipe. The float and sink method mainly causes bending and axial tension in the pipe, combined with some loads due to internal pressure in part of the pipe. Other installation methods might

cause completely different load profiles. For instance, when pulling the pipeline down in a straight line, the lines with which the pipeline is pulled down will induce a completely different load profile on the pipe.

One aspect driving the costs and complexity of an installation method is the amount and size of equipment required for this specific installation method. Where some methods only require one tug boat and some ballasting, such as the float and sink installation method, others may require much more or complex equipment. Examples of equipment which alternative installation methods might require are: sub-sea anchors with pulleys, buoyancy tanks, a multitude of installation vessels, sub-sea connection/locking mechanisms and so on. Large amounts of equipment or equipment in sizes that are not commonly available will logically drive the costs and complexity of an installation method.

The second aspect which drives the costs and complexity of an installation method is the required weather window. The weather window indicates the time span required in which environmental conditions are mild enough for the installation to be completed. Installation times and allowed weather conditions will be different for every installation method. Installation methods with a small required weather window time frame and for which environmental conditions don't have to be as mild are thus more easy to plan and perform, which will results in lower costs and complexity.

Finally, the seabed profile also has a large influence on which installation method is most optimal. As discussed by Brewer, where for regular, smooth seabeds it is possible to install the pipeline lying on the seabed, for irregular, rough seabeds the pipeline might have to be installed floating some distance above the seabed [15]. Thus, the seabed profile dictates partly which installation methods can be used to start with. This of course is also influenced by the material choice, where a very flexible pipe can be installed lying on much rougher seabed profiles than a stiff pipe.

The purpose of this chapter is to introduce and shortly analyse a range of installation methods, some of which have been proposed by other authors before and some of which new. This chapter can therefore be used as a starting point for selecting alternative installation methods for the installation of a large diameter pipeline in deep water. This can then be used for further studies, to analyse these methods in detail and show whether they are truly both technically and economically feasible. The following sections are thus informative texts on alternative pipeline installation methods.

5.1 Sub-Sea Joining Installation Method

In this first alternative installation method, the pipe sections are not joined into one long pipeline before the installation but during the installation. This is done by sinking the separate sections to their target position and joining them to the other sections on location using some kind of connection/locking mechanism. Sinking the separate pipe sections to their target locations can be done by positioning them at sea level above their target location and then lowering the sections vertically using a deepwater installation vessel. This method has been used for the installation of the 18 foot diameter (about 5.5

m) pre-stressed concrete pipes for the cooling water system of the San Onofre nuclear plant [43][45].

A variation on this method would be to attach removable buoyancy and ballast chains to the separate sections and sink them to their target position along the seabed slope. This method would be much like the off-bottom tow or controlled depth tow as discussed in section 2.4, but then installing each section piecewise. A dead-man anchor (DMA) equipped with a pulley connected to a bottom pull winch on the shore would be used to pull the sections down to their target position and lock them into the connection with the other pipe sections. Additionally, guidelines and a deepwater installation vessel are used to control the position of the pipe segment more accurately. This second way to perform this installation method is shown in figure 5.1.

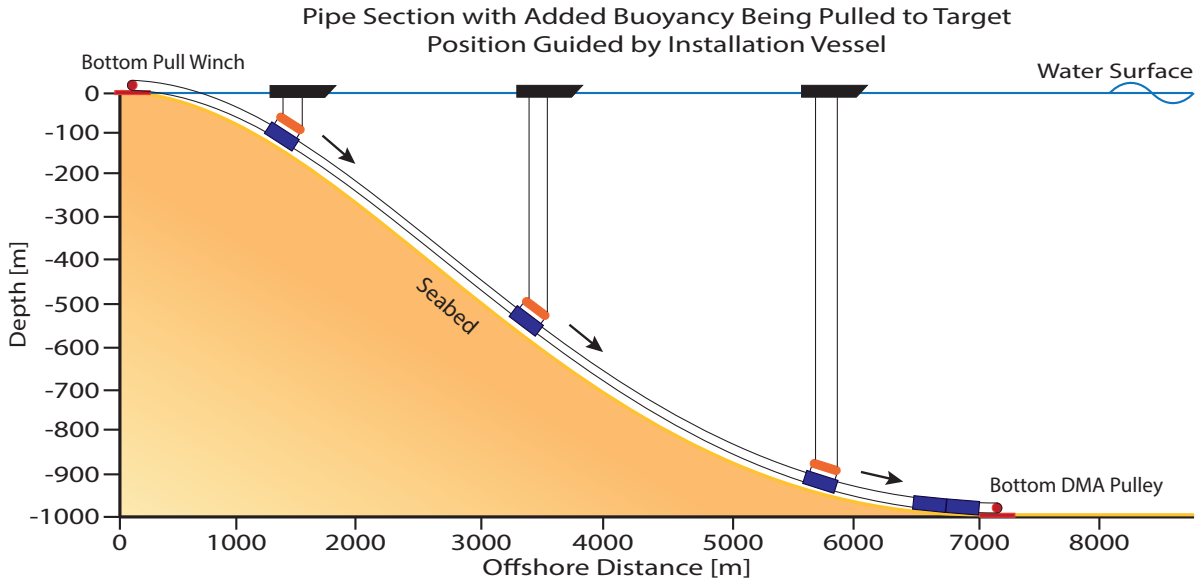

Figure 5.1: Bottom Pull Sub-Sea Joining Installation Method Procedure

This variation of the sub-sea joining installation method has been proposed by Brewer in combination with concrete pipe sections and a bottom pull using cable guidelines [43].

For this installation method concrete pipe segments do make more sense than HDPE, as concrete is much cheaper and flexibility is not required. Furthermore, industry has more experience with fabricating very large diameter concrete pipes. Though, for very irregular seabeds more flexible materials such as HDPE might be more viable than concrete. A proven locking mechanism used to join concrete pipe segments exists and this consists of conically fitting concrete pipe sections embedded with self-centring steel joint rings and a rubber O-ring to provide a water-tight seal. A downside of connecting the pipe segments like this is that it does not result in an inner pipe surface as smooth as can be achieved with welding. This, combined with the fact that concrete has a much rougher surface quality than HDPE will lead to a slightly less energy-efficient pipe for the transportation of water.

When this method is compared with the float and sink installation method, the pipe itself will likely be cheaper but the installation requires more equipment and much more time, resulting in higher installation costs. The weather window is not as much of a problem

however, as the majority of the work is done at a depth where waves and current have little influence.

A low installation risk for this method is anticipated as no great bending or other loads are encountered and similar installations in shallow water depth have been performed. Furthermore, no additional ballast is required as concrete is heavy enough once in place with the buoyancy module removed. This buoyancy module can be equipped with cameras and/or even thrusters for additional control and can be reused for every pipe segment.

5.2 Straight Line Pull-Down Installation Method

The second alternative large diameter pipeline installation method introduced is the straight line pull-down method. This method is performed by first floating the complete pipeline over its target position at sea level, as is done for the float and sink installation method. The floating pipeline is then connected to a number of anchored pulleys on the seabed. The pipe is connected with cables through these pulleys to buoys, providing a downward force on the pipe. The offshore pipe end is not connected to a buoy through the pulley, but to an installation vessel equipped with a winch. This configuration is given in figure 5.2.

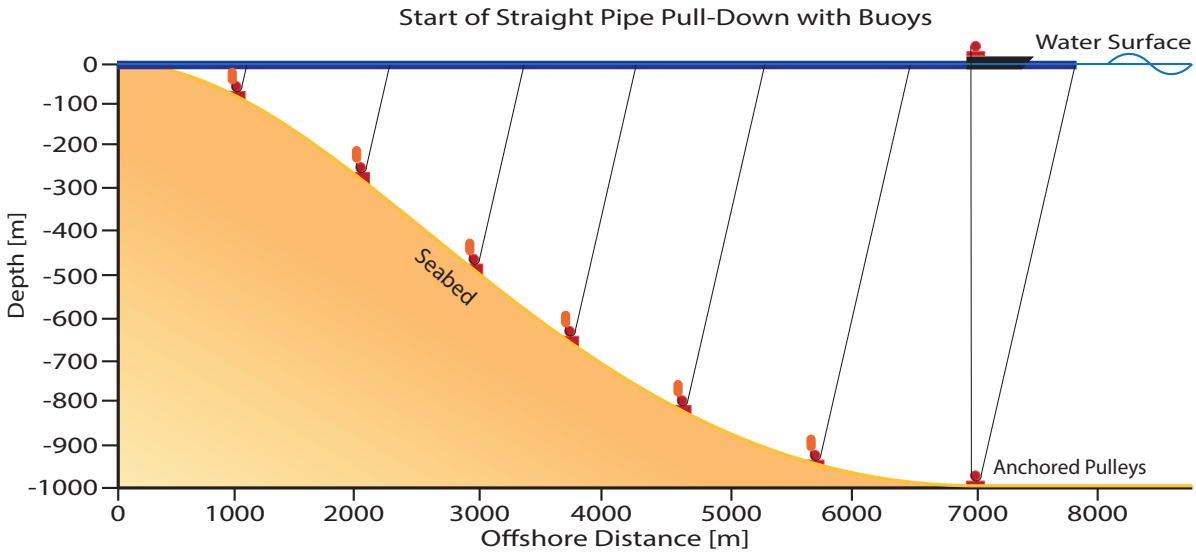

Figure 5.2: Start of the Straight Line Pull-Down Installation Method Procedure

To start the sinking of the pipeline, the winch starts pulling the pipe end down. If the buoys and pipeline weight are dimensioned correctly, the rest of the pipeline will follow the pipe end down to the seabed. During the sinking the pipeline should remain relatively straight as the downward force from the buoys decreases the moment due to the buoyancy of the pipe. When the pipe has reached the desired depth, as illustrated in figure 5.3, the cables can be locked in the pulleys and the buoys can be removed. The pipe installation is now finished and thus, the pipe will remain floating some distance above the seabed through its entire lifetime. This is especially useful for pipeline installation in areas with a very rough seabed.

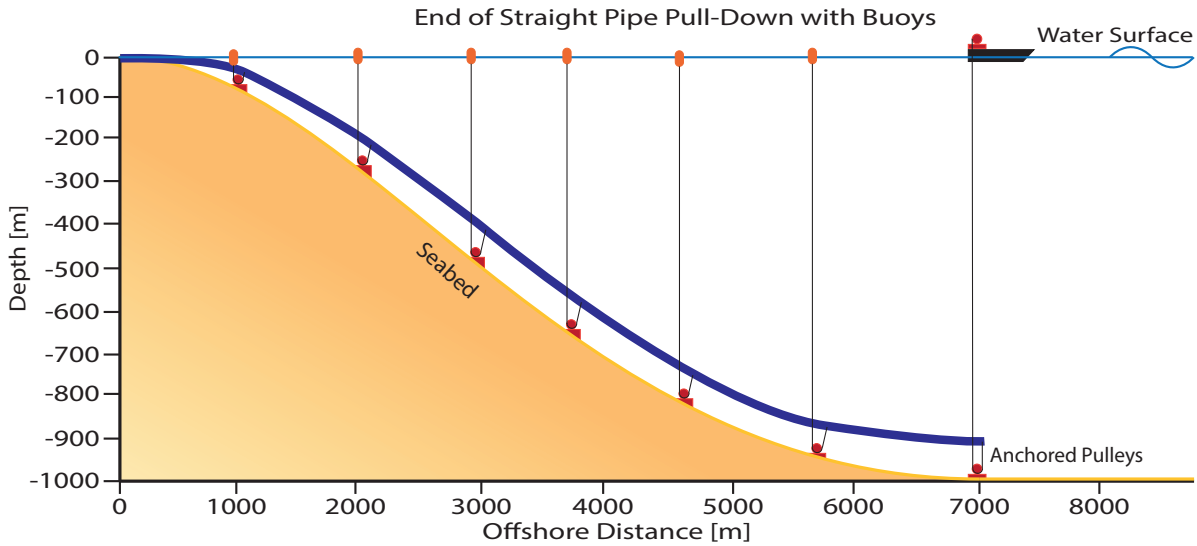

Figure 5.3: End of the Straight Line Pull-Down Installation Method Procedure

As the pipeline will remain floating and thus will move during its entire lifetime, a relatively flexible material with a high fatigue lifetime is required. HDPE is suitable for this as has been shown by a similar installation of a 1 m diameter CWP on Hawaii [26]. A FRP pipe design has been proposed for this installation method by Brewer [43].

The pipeline, flooded with seawater, will have to provide sufficient buoyancy so that it is relatively stable once installed. If insufficient buoyancy is available, the anchor lines will not be under sufficient tension and the pipeline will be displaced easily by for instance currents. Therefore, material density is also an important factor for choosing a material for this installation method. If a material can not provide sufficient buoyancy, additional buoyancy has to be added which is expensive.

For this installation method an acceptable level of risk is anticipated. A similar pipe installation has been performed before on Hawaii and this pipe has significantly exceeded its design lifetime. Careful engineering of the mooring forces is however required, combined with a pipe material with a long fatigue lifetime, as the environmental/dynamic loading over time on a sub-sea floating structure can be significant.

Two Delft University of Technology civil engineering students have performed a bachelors graduation study on this method. This study was partly commissioned by Bluerise, from which the students also received assistance. The aim of this study was to analyse the feasibility of large diameter HDPE pipe installations with the buoy assisted straight line pull-down installation method. Furthermore, they have tried to minimize the amount of anchors required and checked the sensitivity of the method to inaccuracies in buoy sizes [46].

A conclusion of this report is that the method is only feasible for very large diameters of more than 6 m, due to the high bending moments encountered. Smaller diameters would require very large numbers of anchors and buoys with a very accurate amount of buoyancy to stay within allowed bending moment limits. Large diameters would require less amounts of anchors but unrealistically large buoy sizes. Therefore, it is advised to use multiple pipe lowering vessels instead of buoys.

In reality, this method might result in less severe loads on the pipe than anticipated by these students. This is due to the way in which the installation has been modelled. In the report the pipe has been modelled as a beam on two supports, where the onshore end is on the second support and the offshore end is free. As a result the onshore end of the pipe encounters a large moment for static equilibrium to hold, in fact the largest moment in the pipe. The onshore end op the pipe is thus secured in position in this model, but can rotate resulting in a large moment. In reality, the onshore end might not have to be secured during the installation, keeping the complete pipeline floating, moored to the anchors. This will result in significantly lower moments in the pipe as it is not unnecessarily bent. Therefore additional modelling would be interesting to see what the limits of this method are if both pipe ends are kept floating, with zero bending moment on both these ends.

A variation on the buoy assisted straight line pull-down installation method would be to replace the buoys by small ships equipped with winches as stated before. In this way the pipe can be lowered in a more controlled way. Furthermore, unrealistically large buoyancy units are no longer required. A multitude of ships will however result in significant costs.

Another variation of this method has been proposed for an experimental OTEC plant on Tahiti. In this method anchored rings or hawse pipes would be pre-installed at the target water depths of the pipe, after which the pipe would be pulled through these rings to install it [47]. This method appears rather impractical, due to the difficulty of pulling a buoyant pipe through rings at considerable depth.

5.3 Off-Bottom Pull Installation Method

A third alternative method is the off-bottom pull installation method, which is very closely related to the off-bottom tow method as discussed in section 2.4. Off-bottom towing has been used for years to install complete pipelines for both offshore and other types of projects [28]. The off-bottom pull installation method has also been introduced shortly in a feasibility study by Brewer [43].

In the off-bottom pull method the entire pipe is fitted with sufficient buoyancy to make it slightly buoyant. Then, chains or another type of hanging ballast is added to make the overall assembly heavy enough to sink. As the assembly sinks the chains will hit the seabed and as more length lays down on the seabed the weight from this length of chain is removed from the overall assembly. If the amount of buoyancy and ballast weight is balanced correctly the pipeline can be made to constantly float a predetermined distance above the seabed in this manner. The pipeline can then be pulled from the shore, floating just off the bottom following the seabed profile, down to its target location using a sub-sea dead man anchored pulley. Once the pipeline is in position the buoyancy units can be removed/flooded and the pipe will settle on the seabed. This installation method is illustrated in figure 5.4.

As can be noted, this method is very similar to the installation method described in section 5.1, only now using a long length.

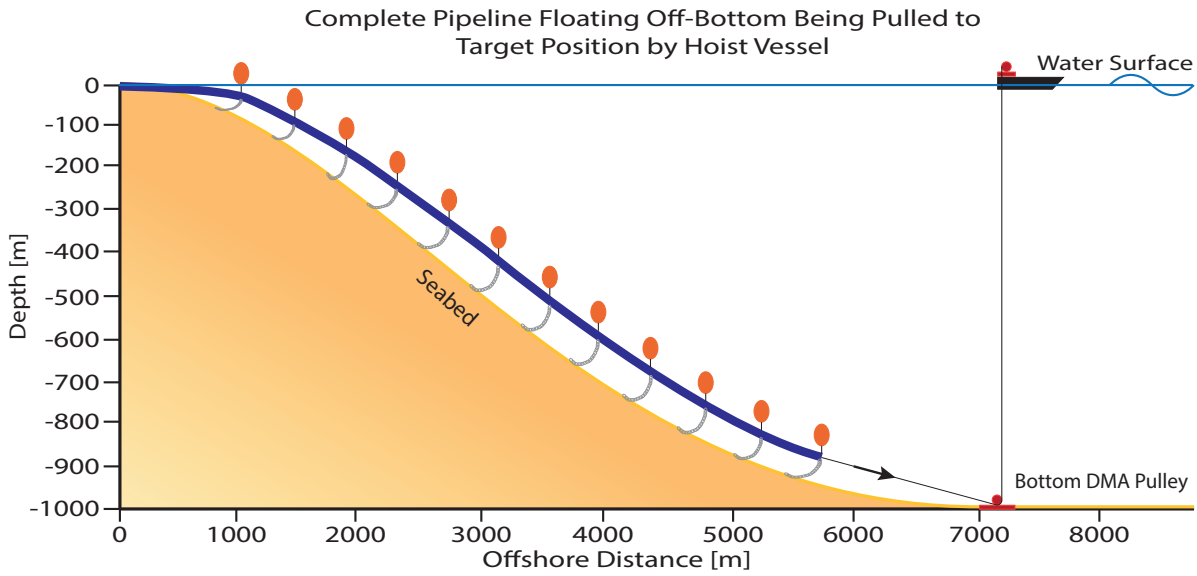

Figure 5.4: Full Pipeline Length Off-Bottom Pull Installation Method Procedure

HDPE would be suitable for this type of installation due to its density close to that of water. This indicates that less added buoyancy is required than for a heavier material such as steel or concrete. Care should be taken however that after the installation, once the buoyancy is removed and the pipe has settled on the seabed, it has sufficient weight to remain stable. Furthermore, HDPE should be able to relatively easily follow the contours of the seabed during the installation due to its flexibility.

A benefit of this method is that the pipe sections can be welded onshore, which saves a lot of costs. A downside is that a very large amount of buoyancy modules and chains is required to perform off-bottom tow of a long length of large diameter pipe. This will result in high costs.

An acceptable installation risk is anticipated for this method as no great loads are expected on the pipe except for the axial pull force. This axial pull force can be limited if the installation is performed slowly. A proper weather window is required to submerge the pipe from the shore and to attach the buoyancy and chains in shallow water. Furthermore, care should be taken that the chains do not get stuck at the seabed and can slide freely.

5.4 Drilled Tunnel Installation Method

A final, more out-of-the-box method to establish a CWP would be to drill a tunnel from the shore down to 1000 m depth through the seabed. This would be done using a technique similar to horizontal directional drilling (HDD), as used often for oil wells or for instance for (waste)water or cable tunnels below occupied areas. Another option would be to use a tunnel drilling machine as used for traffic or train tunnels. Establishing a CWP in stable rock ground would mean simply drilling a tunnel, where for less stable, softer grounds a liner would have to be inserted in the tunnel.

A drilled CWP tunnel is illustrated in figure 5.5

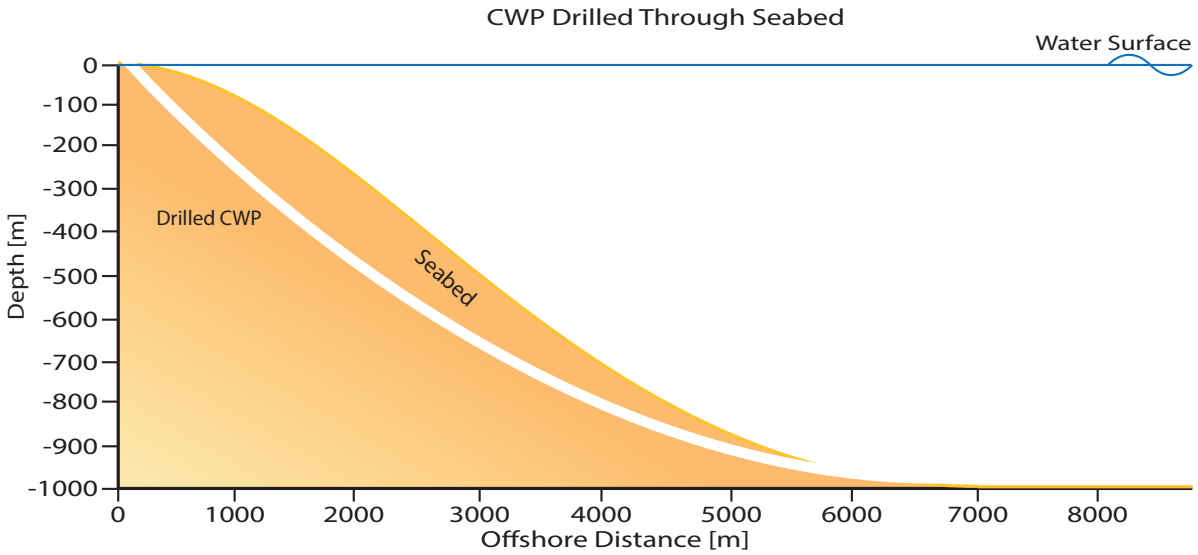

Figure 5.5: A Drilled CWP tunnel

The current state of art of drilling tunnels using HDD in terms of length is in the range of several kilometres, which should be enough for a sufficiently steep seabed slope. However, HDD has never been used for diameters as large as required for large scale OTEC [48]. Large tunnel drilling machines have been used to drill tunnels of much larger diameter and length than required for OTEC. These projects where however mainly horizontal tunnels for traffic or waterways instead of the more vertical/diagonal tunnel required for a CWP, which increases the difficulty. Furthermore, tunnels drilled using such tunnel drilling machines often cost several tens to hundreds of millions. Therefore, drilling a tunnel for a CWP might not be one of the most realistic options although is worth considering for very large scale OTEC projects.

The geophysical characteristics of the seabed are very important to determine whether drilling a large diameter tunnel is possible. Very hard rock might make the drilling very expensive, while very soft grounds are unstable and require reinforcement of the tunnel. Furthermore, a drilled tunnel will result in a relatively rough pipe wall surface quality which results in less energy-efficient pumping of the cold seawater.

5.5 Review of the Alternative Installation Methods

To provide a better overview of the proposed installation methods, they are reviewed against a set of criteria. These criteria are: *expected installation capabilities*, *overall expected costs*, *installation time*, *seabed dependence*, *weather dependence* and *anticipated installation risk*. Each installation method will receive a rating on each of these criteria of either two crosses for very bad, one cross for bad, one check mark for acceptable or two check marks for very good. A full multiple criteria analysis as was done for the material selection in section 4.3 is thought inappropriate here. This is due to the fact that currently only very limited information is available for the proposed installation methods.

The *expected installation capabilities* are assessed by the loads which are expected on the pipe when using the specific installation method. Furthermore, the availability of equipment required to install large diameter pipes using a certain method is also taken into account. When little loads are expected and equipment is widely available a method will receive a good rating on this criteria.

The *overall expected costs* are estimated based on the costs of the pipe material required, equipment required, expected amount of engineering required and time required to perform a certain installation method. When the overall expected costs of a method are low, this method will receive a good rating on this criteria.

Installation time is estimated by the amount of actions that are required to install the complete pipeline using a certain installation method and the amount of time that each of these actions take. When a long installation time is expected, the specific method will receive a bad rating on this criteria.

The *seabed dependence* of a method is determined by the fact whether a method requires the seabed to be smooth and regular or not for the installation of a large diameter pipe. If the type of seabed does not matter for the installation capabilities of a certain method, it will receive a good rating on this criteria.

The *weather dependence* of an installation method is assessed by whether a lot of installation time is required at the sea surface or in shallow water. How sensitive the method is to more severe environmental conditions is also taken into account. If the weather is of no influence on the installation capabilities of a certain installation method, this method will receive a good rating on the criteria for weather dependence.

The amount of past experience with installations similar to the installation method and the engineering challenge caused by the dynamics of a certain installation method determine the *anticipated installation risk*. When a method is proven before in other similar projects and dynamics/risk of unwanted events are limited an installation method will receive a good rating on this criteria.

The ratings for all proposed installation methods on each criteria can be found in table 5.1. In this table, double crosses XX indicate that a method scores very bad at a certain criteria, a single cross X indicates poor performance, a single checkmark ✓indicates acceptable ratings and double checkmarks ✓✓are used to indicate very good scores. Ratings given here are just based on expectations based on engineering insights. For a better comparison of methods, more thorough analysis of the separate methods, both technical and economical, is required.

	Float & Sink	Sub-Sea Joining	Pull-Down	Off-Bottom	Drilling
Expected Installation Capabilities	X	✓✓	✓	✓	✓✓
Overall Expected Costs	✓✓	✓	✓	XX	XX
Installation Time	✓✓	X	✓	✓	XX
Seabed Dependence	X	XX	✓✓	X	✓✓
Weather Dependence	X	✓	X	XX	✓✓
Anticipated Installation Risk	✓	✓	X	✓	✓

Table 5.1: Review of Installation Methods

"Our imagination is the only limit to what we can hope to have in the future."

Charles F. Kettering

6 Conclusion & Recommendations

6.1 Conclusion

Large diameter deep water cold water pipelines (CWPs) can be used to provide a valuable supply of cold seawater. Some applications of this cold seawater are the base load clean electricity generation with OTEC and the very energy-efficient SWAC technology. One of the greatest remaining challenges for land-based large scale OTEC is the installation of the required very large diameter CWPs in deep water.

Therefore, the aim of this thesis has been to find and expand the limits of the installation of very large diameter deep water CWPs.

Relevant past installations of CWPs and other large diameter marine pipes have initially been researched, to establish the current proven installation capabilities. These have shown to be insufficient for large scale OTEC, which requires CWPs with diameters of more than 2.5 m to be installed down to depths of 1000 m. The largest CWP diameter found, installed in deep water, was 1.4 m. Furthermore a paper was found, stating that a validated design for the installation of HDPE CWPs in deep water existed for pipes with a diameter up to 1.6 m. After this, analysis was commenced to further expand these established installation capabilities.

The conventional float and sink installation method, often used for large diameter HDPE pipe installations in shallow water, was first analysed. Both analytical modelling using the natural catenary theory and FEM modelling using Orcaflex have proven that this conventional method does not provide good enough installation capabilities for large scale OTEC CWPs. The installation limit found in static analysis was a maximum outside diameter of about 2.3 m for HDPE pipe, when a pull tension of 350 t was used. Here, 350 t is already quite a significant pull tension which requires a very strong tug/installation vessel.

This result has been achieved after optimizing the float and sink installation method

with respect to the air fill ratio of the pipe, the pull tension, the pipe outer diameter and to a lesser extend the pipe wall thickness. This optimization has been performed in the context of some set maximum stress and minimum bending radius limits using the analytical natural catenary model. These results were compared with Orcaflex results, which indicated some expected conservativeness in the natural catenary model.

Furthermore, as this result was achieved with static analysis, the true limit will be even lower as dynamic effects will increase the loads on the pipeline. Examples of dynamic loads are for instance waves and current. Additionally, the offshore industry recommends the use of significant safety factors, as indicated by many engineering design codes. This will further lower the installation limit, as no safety factor (aside from some conservativeness in the model and chosen material limits) has been included in the limit analysis.

Three manners in which installation capabilities can possibly be increased were proposed:

- Adjustments to the float and sink installation method
- Alternative pipe material choice for the float and sink installation method
- Alternative pipe installation method

Some ways to perform the first option where shortly introduced. Installation capabilities can for instance be increased by decreasing the pipeline weight during the installation, which possibly decreases the amount of stress, amount of bending and required top pull. Another option would be to use bending restrictors, to prevent excess bending op the pipeline during installation.

Second, four alternative pipe materials where proposed and analysed for use in the float and sink installation method. Two of these materials, TPU and PA, are promising to significantly increase the pipe installation capabilities of the float and sink installation method. Especially the very flexible TPU, which received the highest score in a multiple criteria analysis performed on the alternative pipe materials, is very promising. Several aspects of the nominated alternative materials, such as the higher price compared to HDPE and limited availability in large diameter pipe, might however prove to be a problem. Furthermore, additional more in depth technical analysis is required to check whether these materials would actually perform well as deep water pipe materials. This is due to the fact that these materials are very different to for instance HDPE or steel and thus might show unexpected material behaviour.

Finally, four completely different large diameter CWP installation methods have been proposed and discussed. These methods are all very different and thus, the expected loads on the pipe during installation are also very different. To provide some clarity, these four alternative installation methods have been roughly rated on some important criteria. From this it can be concluded that each of these methods has some promising aspects. However, both technical and economical feasibility of these methods is still very unclear at this point. Therefore, detailed analysis is required to be able to assess the full potential of these installation methods.

Concluding, current installation capabilities are insufficient for the installation of large diameter CWPs required for large scale OTEC. There are however, many promising

options open for further research which might significantly improve the installation capabilities, up to the standards required for large scale OTEC.

6.2 Recommendations

This thesis has provided a broad range of possibilities to expand the installation capabilities of very large diameter CWPs. Further research in these provided directions is required to expose the most feasible option.

Firstly, it is likely possible to slightly stretch the installation limits of the conventional float and sink installation method further, using one of the proposed adjustments. Therefore, it is required that these are further investigated for the installation of CWPs with slightly larger diameters than the currently proven installation capabilities. Additionally, installing multiple smaller parallel pipes using the proven and relatively cheap float and sink installation method, instead of one large diameter pipe, might also be a viable solution worth further investigation.

Continuing, for very large diameter CWPs it is very interesting to further investigate both the alternative materials as well as the alternative installation methods. Especially the very flexible material TPU shows very promising installation capabilities. The suitability of elastomers like TPU for a deep water CWP should however also be further investigated, as these have quite peculiar characteristics. For instance, whether this material is actually rigid enough as a pipe with reasonable wall thickness to suck water through at 1000 m depth. Furthermore, an economical feasibility and market study for large diameter TPU pipe is also recommended. This is required, to assess whether a manufacturer can be found who is actually able and willing to produce large diameter TPU pipe and at what cost.

Furthermore, the influence of not only statics but also dynamics on installation methods should be investigated, to establish a reliable design and corresponding reasonable safety factors. Especially for completely new installation methods, lots of careful analysis and experiments will be required to decrease the risks and gain confidence from for instance investors and marine warranty surveyors.

A final recommendation is made regarding the modelling of pipeline installations. It would be very useful to develop a model, able to both generate more accurate results than the natural catenary model and optimize the design/installation for a range of parameters. In the current set-up optimizing was performed using the Matlab natural catenary model, which might not have resulted in very accurate optimums for specific pipes. The more accurate Orcaflex model was sadly not readily usable for optimization studies.

The author of this thesis is confident that with the range of presented solutions, a solid base has been provided for solving one of the decreasing amount of challenges for the large scale implementation of OTEC.

References

[1] A. N. Menegaki, "On energy consumption and GDP studies; A meta-analysis of the last two decades," *Renewable and Sustainable Energy Reviews*, vol. 29, pp. 31–36, 2014.

[2] ExxonMobil, "The Outlook for Energy: A View to 2040," tech. rep., 2015.

[3] Ipcc, "Climate Change 2014, Mitigation of Climate Change. Contribution of Working Group III to the Fifth Assessment Report of the Intergovernmental Panel on Climate Change," tech. rep., 2014.

[4] Ipcc, "Renewable energy sources and climate change mitigation: special report of the Intergovernmental Panel on Climate Change," tech. rep., 2012.

[5] J. C. War, "Seawater Air Conditioning (SWAC) A Renewable Energy Alternative," pp. 1–9, 2011.

[6] Bluerise BV, "Schematic of OTEC working Principle," 2014.

[7] H. Knight, "20,000 megawatts under the sea: Oceanic steam engines," *New Scientist March 1-7*, pp. 48–51, 2014.

[8] Bluerise BV, "Offshore ocean thermal energy conversion; Feasibility study of a 10 MW installation," tech. rep., 2014.

[9] Bluerise BV, "Schematic of Different OTEC Implementations," 2014.

[10] T. Mitsui, F. Ito, Y. Seya, and Y. Nakamoto, "Outline of the 100 kW OTEC Pilot Plant in The Republic of Nauru," *IEEE Transactions on Power Apparatus and Systems*, vol. PAS-102, N, pp. 3167–3171, 1983.

[11] R. Pelc and R. M. Fujita, "Renewable energy from the ocean," *Marine Policy*, vol. 26, no. 6, pp. 471–479, 2002.

[12] B. J. Taylor and F. A. McHale, "An OTEC Slope-Mounted Cold Water Pipe Experiment," pp. 345–348, 1984.

[13] J. Vadus and B. Taylor, "OTEC cold-water pipe research," *IEEE Journal of Oceanic Engineering*, vol. 10, no. 2, 1985.

[14] J. R. Chiles, "The Other Renewable Energy," *Invention & Technology*, pp. 24–35, 2009.

[15] J. H. Brewer, "Land-Based OTEC Plants - Cold Water Pipe Concepts," in *6th Proceedings of OTEC, Washington*, 1979.

[16] T. Nakasone and S. Akeda, "The application of deep sea water in Japan," tech. rep., 1999.

[17] T. H. Daniel, "Operational Experience With The Cold Water Pipe At The Natural Energy Laboratory Of Hawaii," 1986.

[18] Makai Ocean Engineering, "Makai Ocean Engineering, Installed Pipelines."

[19] M. G. Brown, M. Gauthier, and J. Meurville, "George Claude's Cuban OTEC Experiment: A Lesson Of Tenacity For Entrepreneurs.," 2002.

[20] Makai Ocean Engineering, "Makai Ocean Engineering, Deep Pipelines for Aquaculture."

[21] Makai Ocean Engineering, "Makai Ocean Engineering Brochure, OTEC Test Facility," 2012.

[22] L. a. Vega, "Ocean Thermal Energy Conversion Primer," *Marine Technology Society Journal*, vol. 36, no. 4, pp. 25–35, 2002.

[23] Pipelife Norge AS, "Technical Catalogue for Submarine Installations of Polyethylene Pipes," tech. rep., Pipelife Norge AS, 2002.

[24] Cambridge University Engineering Department, "Materials data book," pp. 1–39, 2003.

[25] L. H. Gabriel, *Corrugated Polyethylene Pipe Design Manual & Installation Guide*.

[26] L. F. Lewis, J. V. Ryzin, and L. Vega, "Steep Slope Seawater Supply Pipeline," *Coastal Engineering*, pp. 2641–2654, 1988.

[27] Det Norske Veritas (DNV), "DNV-OS-F101 Submarine Pipeline Systems," Tech. Rep. October, 2013.

[28] B. Guo, S. Song, A. Ghalambor, and T. R. Lin, *Offshore Pipelines; Design, Installation and Maintenance*. Gulf Professional Publishing / Elsevier, second edi ed., 2014.

[29] Allseas Engineering, "Allseas Pioneering Spirit Pipeline installation."

[30] T. Blomster, "Advantages and Experiences of the Use of Long Length PE Pipes for Marine Pipeline Construction & Installation Techniques for Flexible PE Pipes," 2012.

[31] C. P. Sparks, *Fundamentals of Marine Riser Mechanics: Basic Principles and Simplified Analyses*. Penwell Books, first edit ed., 2007.

[32] Orcina Ltd, "OrcaFlex Manual; Version 9.8a," tech. rep., 2014.

[33] J. Journée and W. W. Massie, *Offshore hydromechanics*. No. January, Delft University of Technology, first edit ed., 2001.

[34] E. J. Routh, *A Treatise On Analytical Statics*. Cambridge At The University Press, volume i ed., 1891.

[35] M. Kashani and R. Young, "Hoop stress approximation in offshore design codes," *Marine Structures*, vol. 21, no. 2-3, pp. 224–239, 2008.

[36] M. G. Jenkins, "Course Notes Mechanical Engineering 354; Mechanics of Materials Laboratory," tech. rep., University of Washington, 2001.

[37] V. Polenta, S. D. Garvey, D. Chronopoulos, A. C. Long, and H. P. Morvan, "Effects of Pipe Curvature and Internal Pressure on Stiffness and Buckling Phenomenon of Circular Thin-Walled Pipes," *International Journal of Mechanical, Aerospace, Industrial, Mechatronic and Manufacturing Engineering*, vol. 9, no. 2, pp. 278–282, 2015.

[38] Maritime Journal News, "'KL Sandefjord' breaks bollard pull record," 2011.

[39] S. Miroslav (Pipelife), "Email Conversation with Pipelife; SV Large Diameter OTEC Pipe Installation Thesis Bluerise," 2015.

[40] M. F. Ashby, *Materials Selection in Mechanical Design*. Elsevier, fourth edi ed., 2011.

[41] Unique Seaflex, "Floating a Pipeline with Air Filled Bags," 2014.

[42] Granta Design, "CES Edupack," 2014.

[43] J. H. Brewer, J. Minor, and R. Jacobs, "Feasibility Design Study Land-Based OTEC Plants," tech. rep., 1979.

[44] I. Larsen, "On installation of very large diameter marine PE pipes," in *Marine Waste Water Discharge Conference*, 2014.

[45] Ameron International, "Ameron Prestressed Concrete Cylinder Pipe Brochure," 2002.

[46] M. I. Kelkitli and F. J. Koppes, *The Feasability of BrewerâĂŹs Installation Method for CWP Laying for Land-Based OTEC Plants*. Bachelor thesis, Delft University of Technology, 2015.

[47] R. H. Vilain, M. A. Spielrein, and J. P. Miquel-Elcano, "Structure and Material for the CWP OTEC Tahiti Experimental Plant," in *OCEANS '85 - Ocean Engineering and the Environment*, pp. 1217 – 1221, Ifremer & Ergocean, 1985.

[48] G. M. Duyvestyn, "Considerations for Large Diameter or Long Length HDD Installations," *Horizontal Directional Drilling Guide*, pp. 40–41, 2011.

A

Appendix: Hydraulic Efficiency

In this appendix the benefits of using a large diameter pipe with low flow velocities is shown. Firstly, by showing how a large diameter pipe with low flow velocities is more efficient than a set/bundle of multiple smaller diameter pipes with equally low flow velocities, providing the same net volume of cold water. Secondly, by showing how a large diameter pipe with low flow velocities is significantly more efficient than a smaller diameter pipe with higher flow velocities providing the same net volume of cold water.

For the purpose of this comparison, the base case of a 4 m inner diameter HDPE pipe is used with a constant flow velocity of 2 m/s. This pipe will thus provide 25.13 m^3/s cold deep seawater. The pipeline has a length of 7 km.

A set of three HDPE pipes, which each have an inner diameter of 2.31 m, is able to provide about the same volume of water, if the same flow velocity of 2 m/s is used.

A single 2.3 m inner diameter will have to transport water with flow speeds of about 6.05 m/s to provide the same volume of water.

The efficiency of a pipeline is determined here by the amount of friction losses which occur along the length of the pipe. As we are dealing with a very long pipeline other minor losses, such as those due to entries and exits, are neglected. The pipes are assumed to be straight and with circular cross-section.

The amount of head lost in a pipe due to friction losses can be determined using the Darcy-Weisbach formula for fully developed, turbulent flow. This formula is given in equation A.1.

$$\delta h_f = f \frac{L}{D} \frac{V^2}{2g} \tag{A.1}$$

where;

Δh_f = Hydraudynamic head losses due to friction [m]
f = Darcy friction coefficient [-]
L = Total length of pipe [m]
D = Inner pipe diameter [m]
V = Flow velocity [m/s]
g = Gravitational constant [m/s^2]

The Darcy friction coefficient is a function of the dimensionless Reynolds number, relative roughness of the pipe and the pipe cross-section. For a circular pipe cross-section the Moody diagram can directly be used to find the Darcy friction coefficient, using the Reynolds number as calculated in equation A.2 and the relative roughness of the pipe.

$$Re = \frac{VD}{\nu} \tag{A.2}$$

where;

Re = Reynolds number [-]
ν = Kinematic viscosity [m^2/s]

The relative roughness of a pipe is calculated by dividing the absolute roughness of a pipe of specific material by the inner diameter of the pipe. For a HDPE intake pipe, the absolute roughness should be assumed to be 2 mm according to Pipelife. This is relatively high, as a completely clean HDPE pipe can theoretically have a much lower absolute roughness (as low as 0.05 mm). The absolute roughness is assumed this high for HDPE intake design, as some biofouling will occur during the lifetime of the pipe which will increase the pipe surface roughness.

The head losses due to friction for the three pipe configurations are now given in table A.1. From this table, it can be concluded that the losses in a set of bundled pipes of smaller diameter, or in a single smaller diameter pipe with higher flow velocities are significantly higher than the losses in a large diameter, low flow velocity pipe. Therefore, a large diameter pipe with low flow velocities is the most energy efficient solution.

		Single Large Pipe	Bundle of Smaller Pipes	Single Smaller Pipe
L	[m]	7000	3 x 7000	7000
D	[m]	4	2.31	2.3
V	[m/s]	2	2	6.05
ν	[m^2/s]	1.6*10^{-6}	1.6*10^{-6}	1.6*10^{-6}
Re	[-]	1.6000*10^{-6}	2.8875*10^{-6}	8.6969*10^{-6}
$\frac{\epsilon}{D}$	[-]	5.00*10^{-4}	8.66*10^{-4}	8.70*10^{-4}
f	[-]	0.017	0.019	0.019
$\mathbf{\Delta h_f}$	**[m]**	**6.065**	**35.215**	**107.879**

Table A.1: Hydraulic Efficiency Comparison

B

Appendix: Sensitivity Study

B.1 Air Fill Ratio A_a

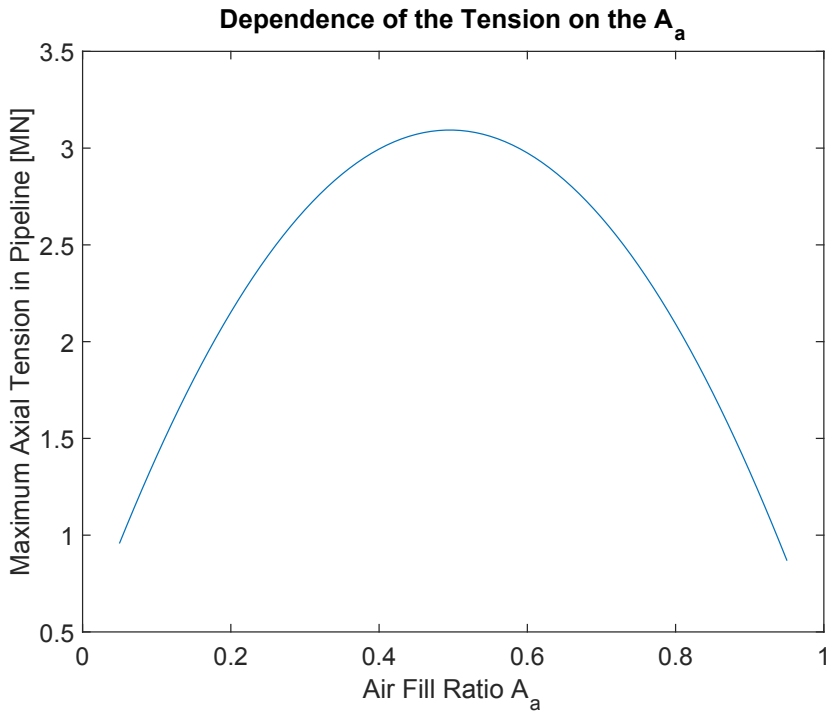

Figure B.1: Dependence of the axial tension along the pipe catenary on the air fill ratio A_a

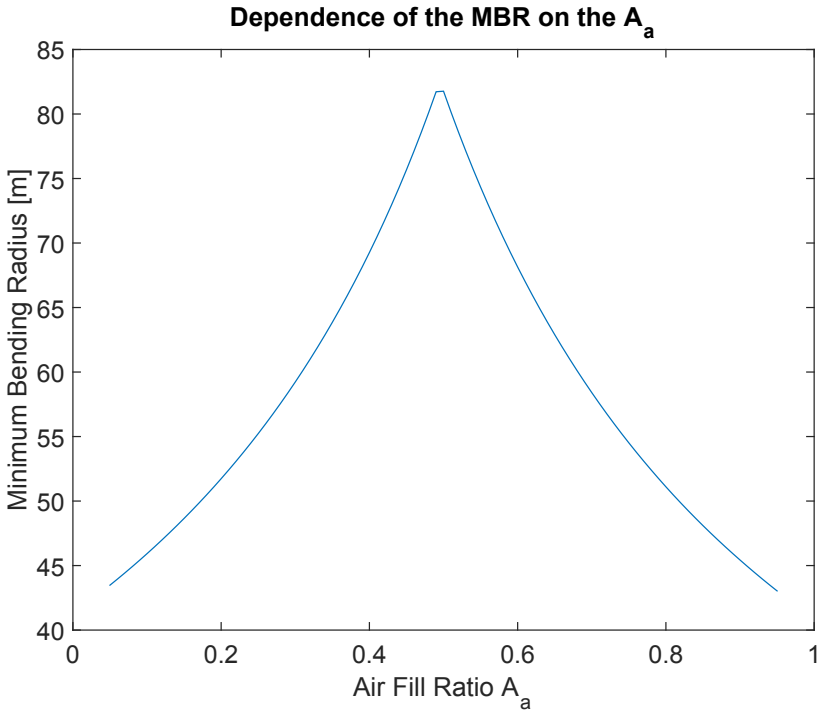

Figure B.2: Dependence of the minimum bending radius along the pipe catenary on the air fill ratio A_a

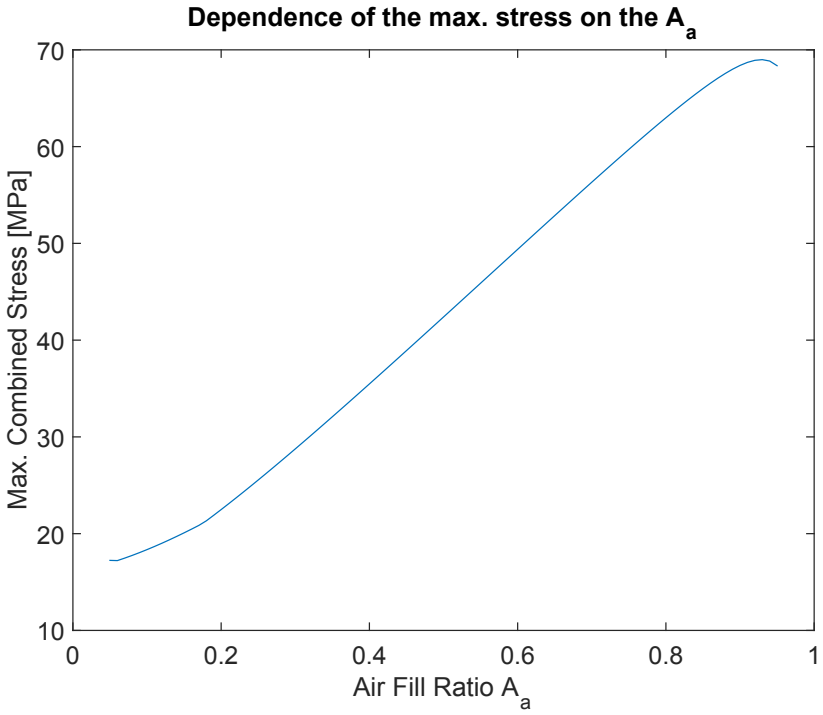

Figure B.3: Dependence of the maximum combined stress (Von Mises) along the pipe catenary on the air fill ratio A_a

B.2 Target Installation Depth

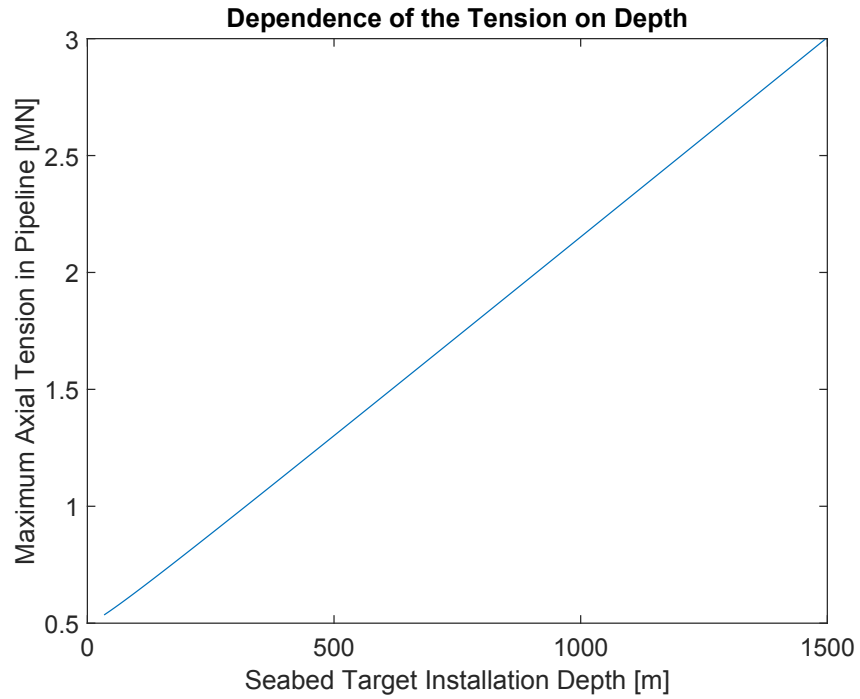

Figure B.4: Dependence of the axial tension along the pipe catenary on the target installation depth

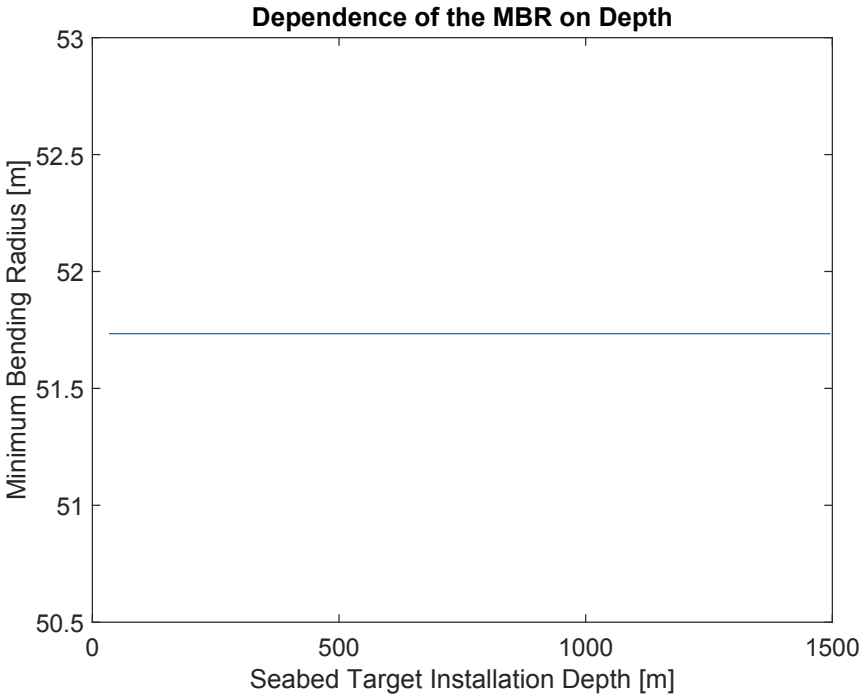

Figure B.5: Dependence of the minimum bending radius along the pipe catenary on the target installation depth

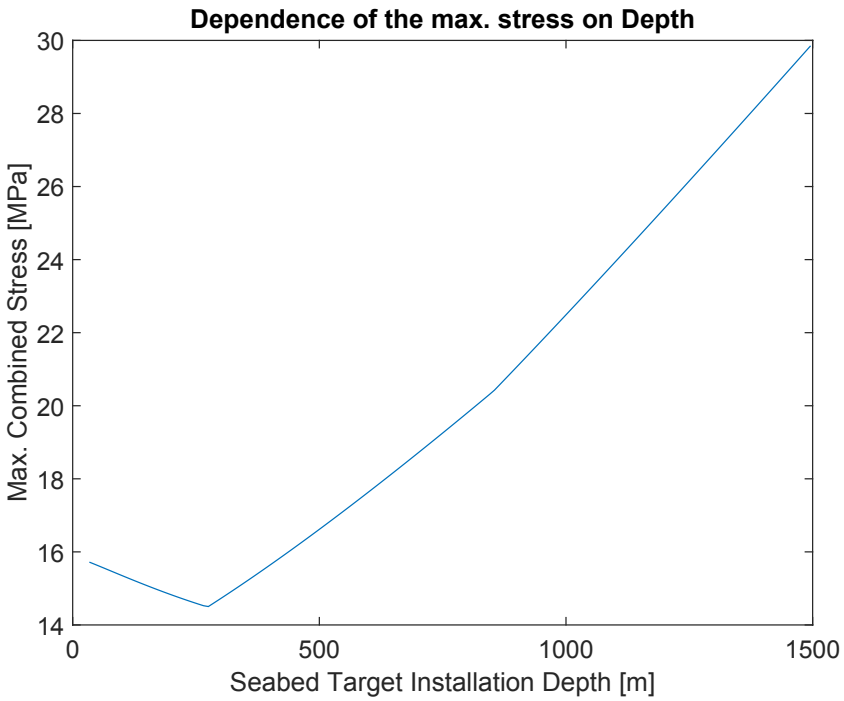

Figure B.6: Dependence of the maximum combined stress (Von Mises) along the pipe catenary on the target installation depth

B.3 Pipeline Outer Diameter

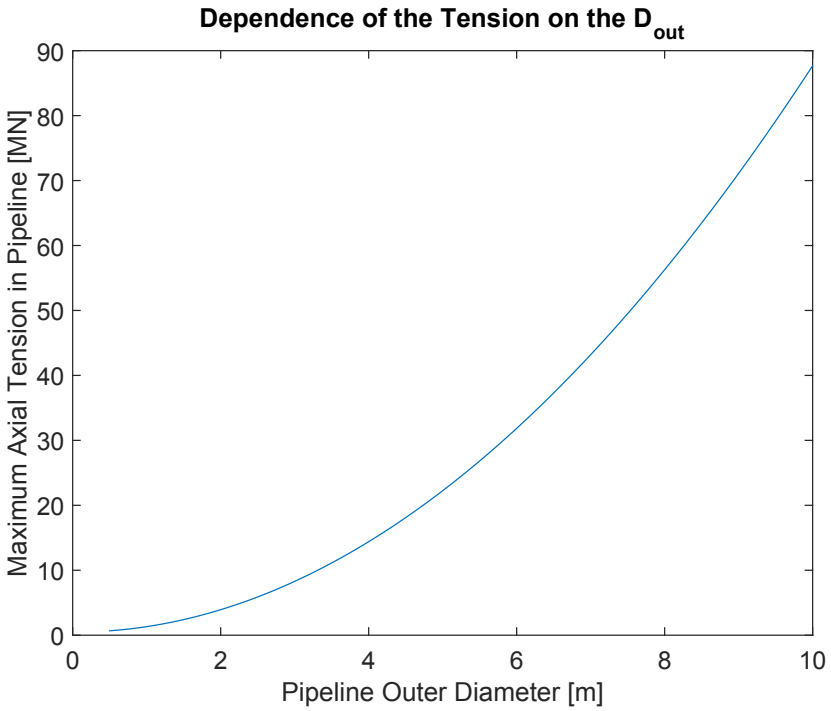

Figure B.7: Dependence of the axial tension along the pipe catenary on the pipeline outer diameter

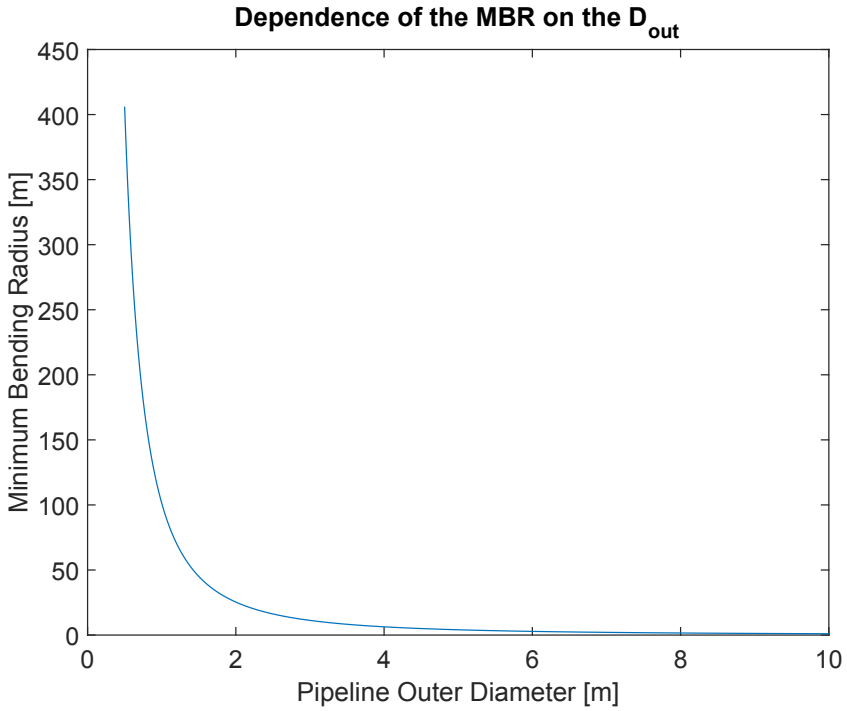

Figure B.8: Dependence of the minimum bending radius along the pipe catenary on the pipeline outer diameter

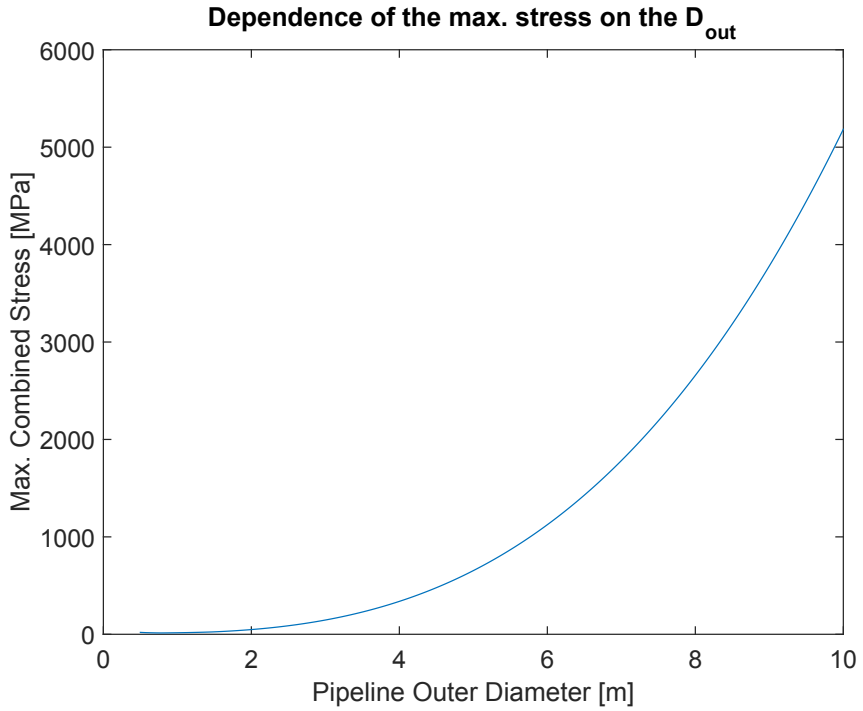

Figure B.9: Dependence of the maximum combined stress (Von Mises) along the pipe catenary on the pipeline outer diameter

B.4 SDR

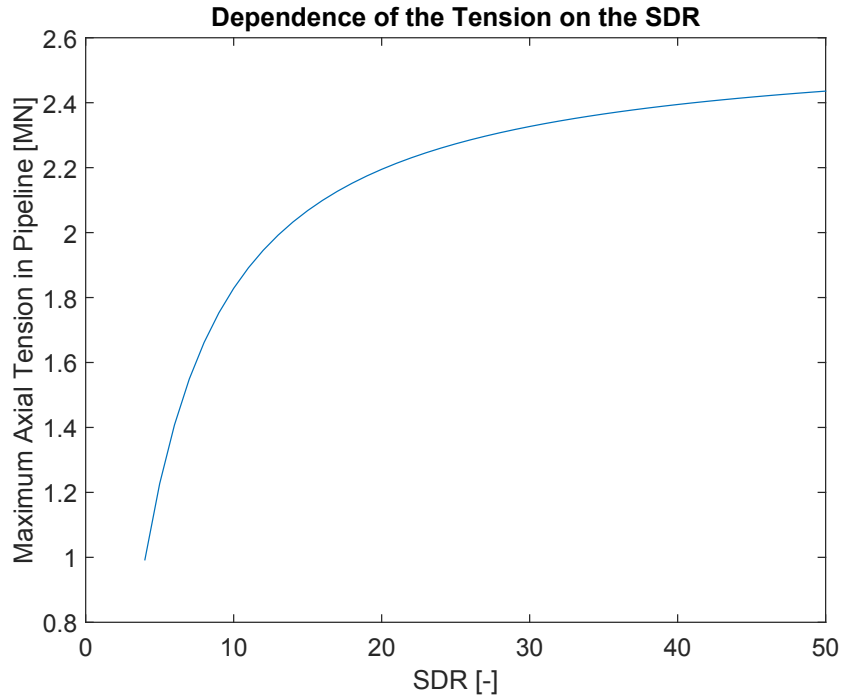

Figure B.10: Dependence of the axial tension along the pipe catenary on the pipeline diameter to wall thickness Ratio SDR

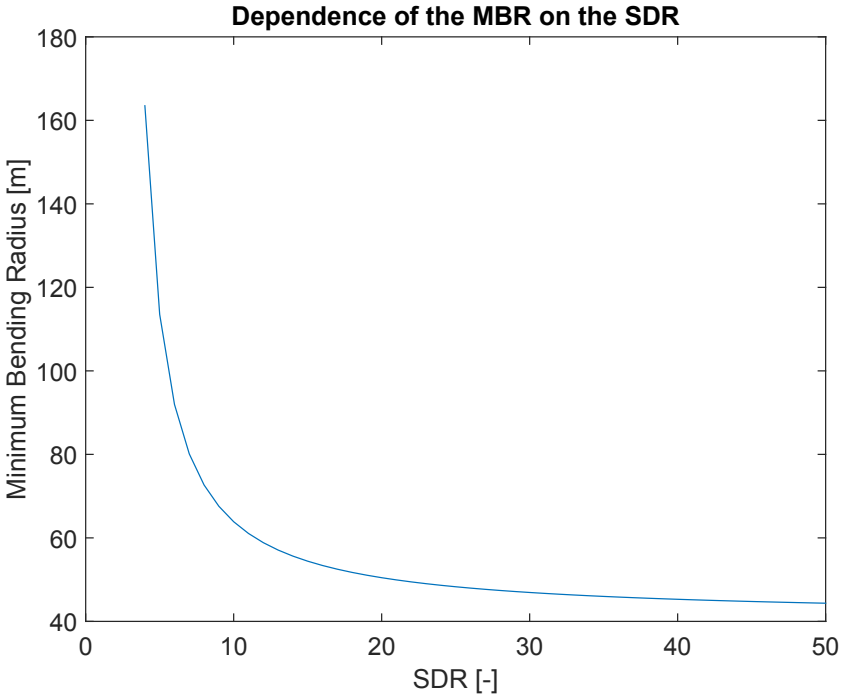

Figure B.11: Dependence of the minimum bending radius along the pipe catenary on the pipeline diameter to wall thickness Ratio SDR

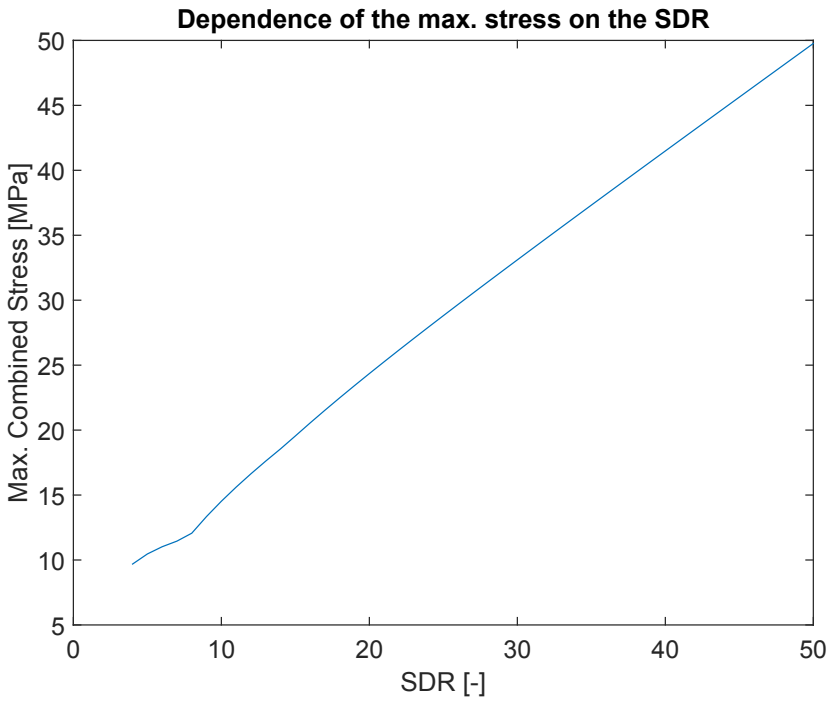

Figure B.12: Dependence of the maximum combined stress (Von Mises) along the pipe catenary on the pipeline diameter to wall thickness Ratio SDR

B.5 Seabed Slope

Figure B.13: Dependence of the axial tension along the pipe catenary on the seabed slope steepness

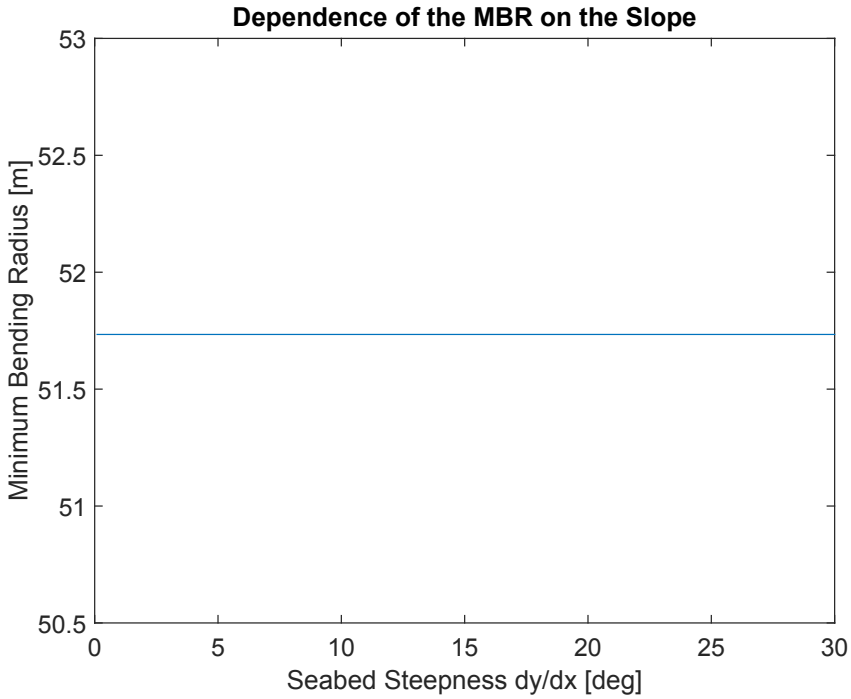

Figure B.14: Dependence of the minimum bending radius along the pipe catenary on the seabed slope steepness

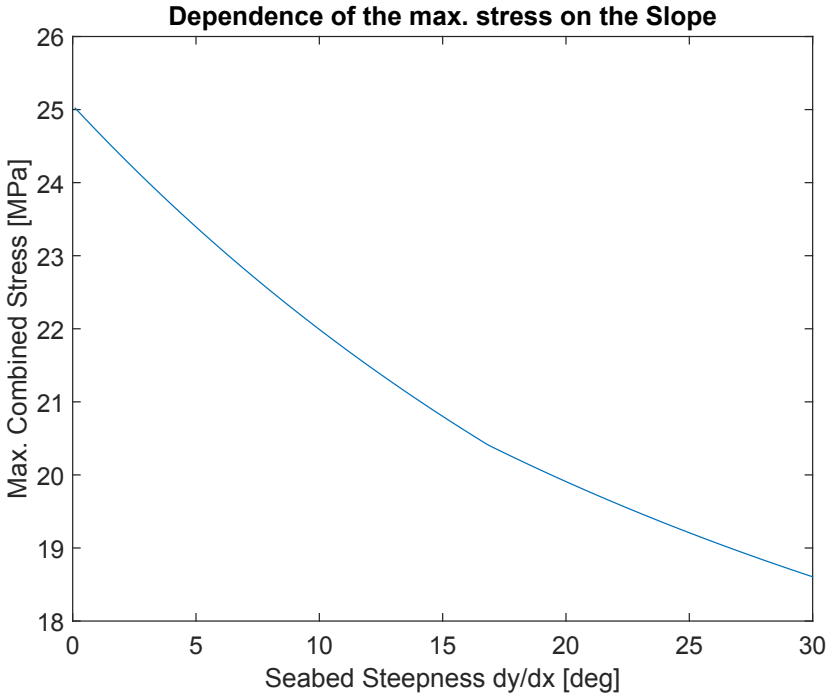

Figure B.15: Dependence of the maximum combined stress (Von Mises) along the pipe catenary on the seabed slope steepness

B.6 Horizontal Top Pull Force

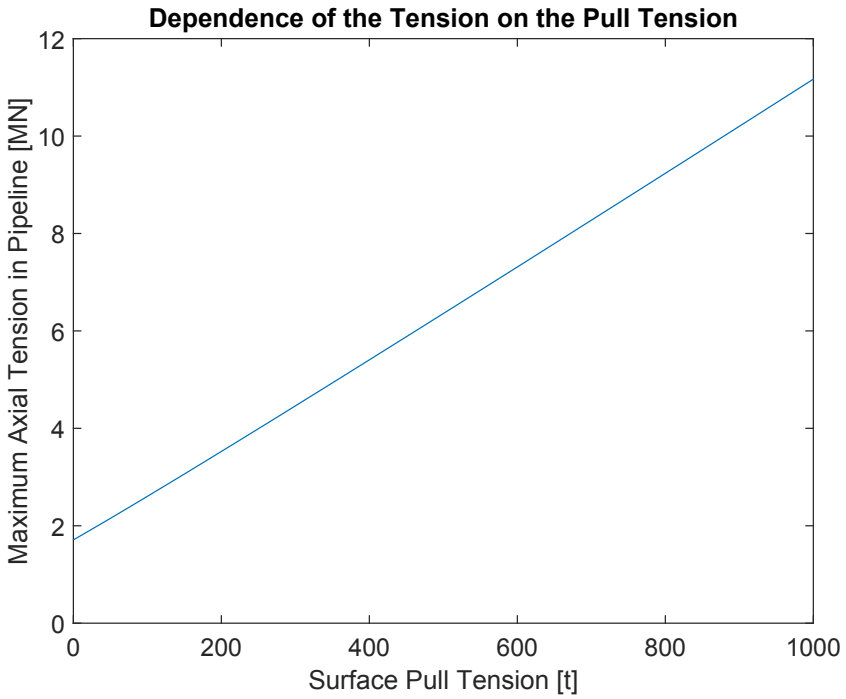

Figure B.16: Dependence of the axial tension along the pipe catenary on the horizontal surface pull tension

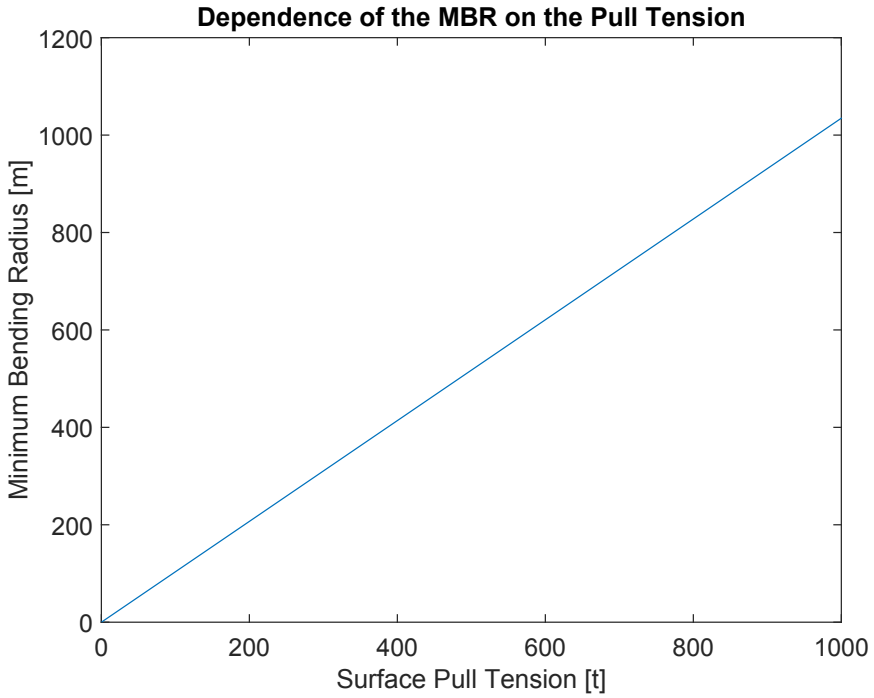

Figure B.17: Dependence of the minimum bending radius along the pipe catenary on the horizontal surface pull tension

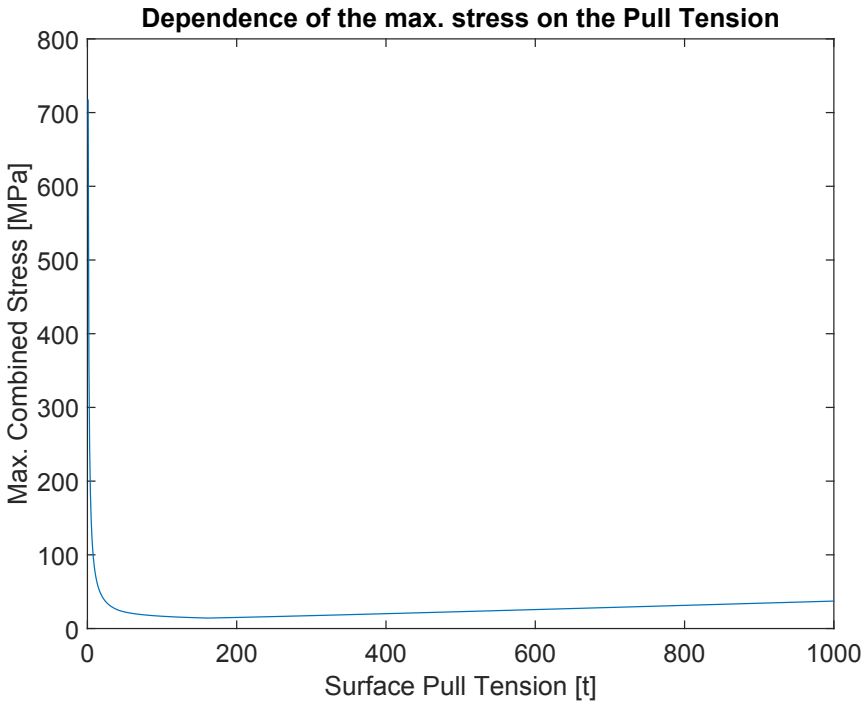

Figure B.18: Dependence of the maximum combined stress (Von Mises) along the pipe catenary on the horizontal surface pull tension

C

Appendix: Optimization of the Improved Analytical Model

C.1 Sensitivity Study of the Model with Closed-Ended Pipe

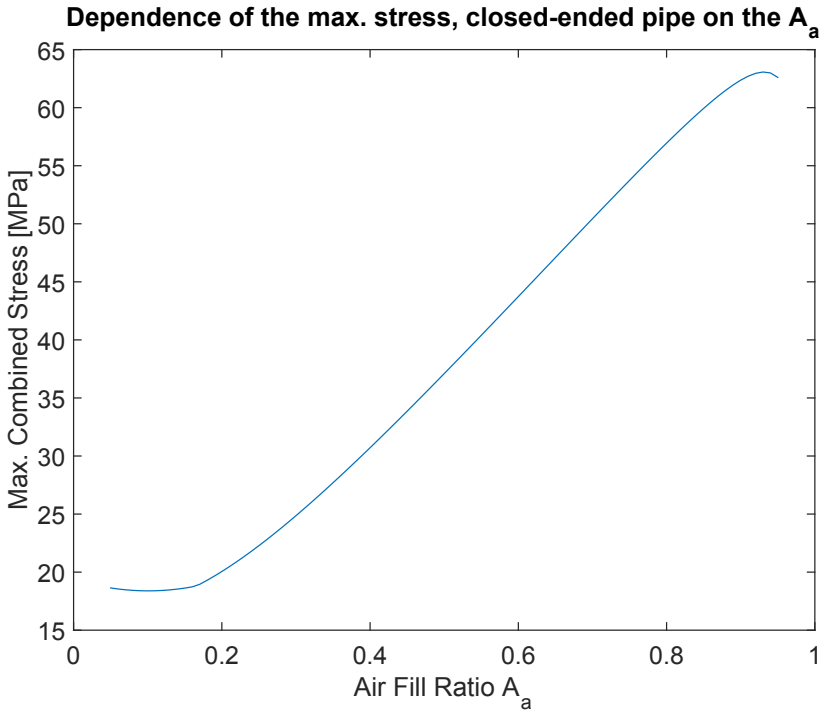

Figure C.1: Dependence of the maximum combined stress (Von Mises) with closed-ended pipe along the pipe catenary on the air fill ratio A_a

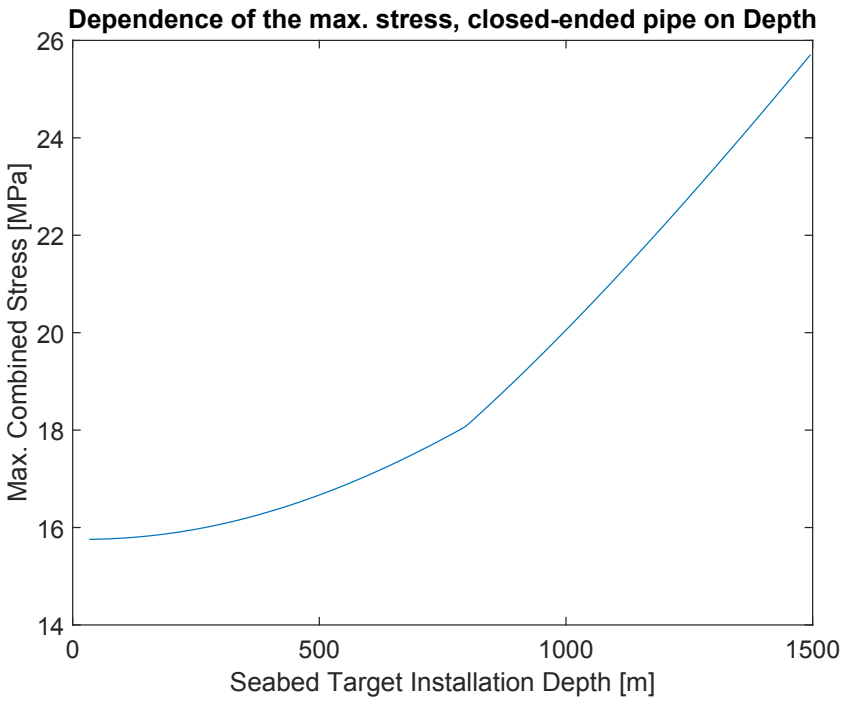

Figure C.2: Dependence of the maximum combined stress (Von Mises) with closed-ended pipe along the pipe catenary on the target installation depth

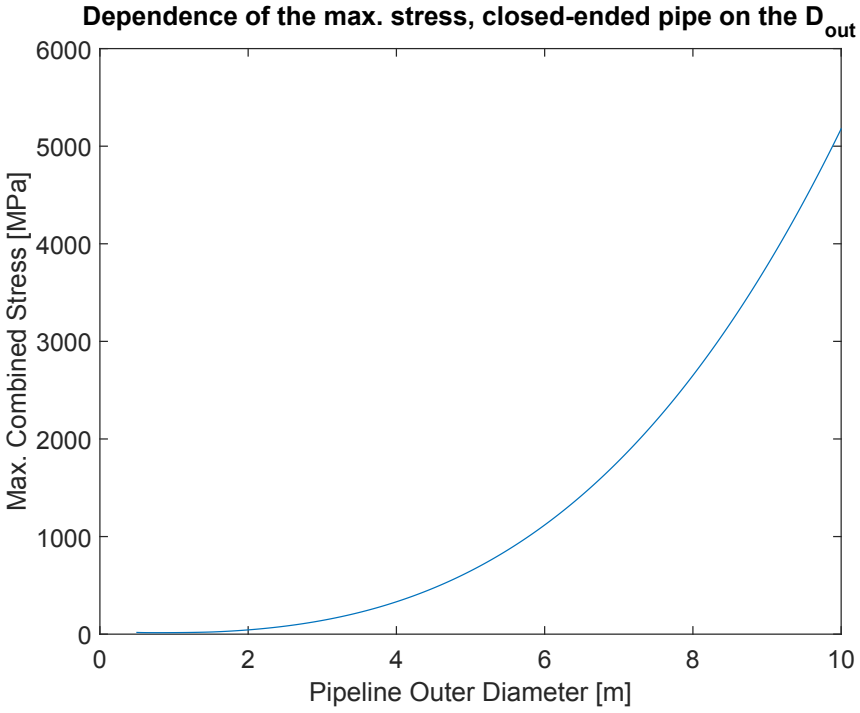

Figure C.3: Dependence of the maximum combined stress (Von Mises) with closed-ended pipe along the pipe catenary on the Pipeline Outer Diameter

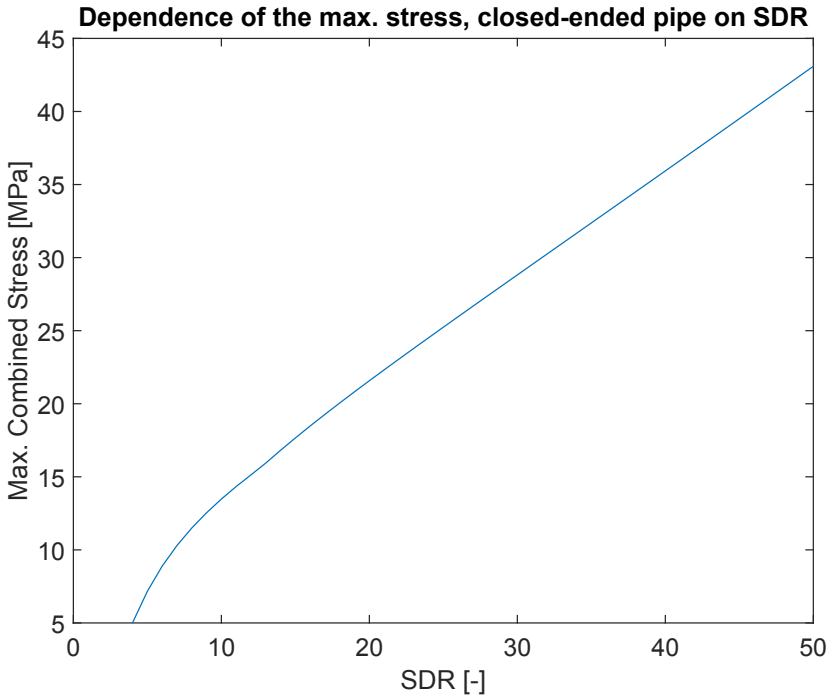

Figure C.4: Dependence of the maximum combined stress (Von Mises) with closed-ended pipe along the pipe catenary on the SDR

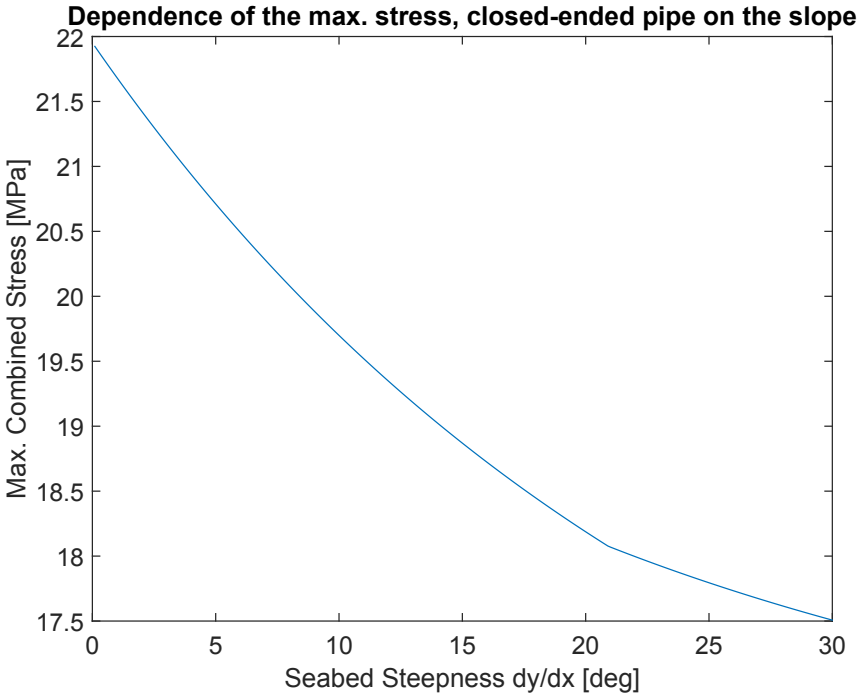

Figure C.5: Dependence of the maximum combined stress (Von Mises) with closed-ended pipe along the pipe catenary on the seabed slope steepness

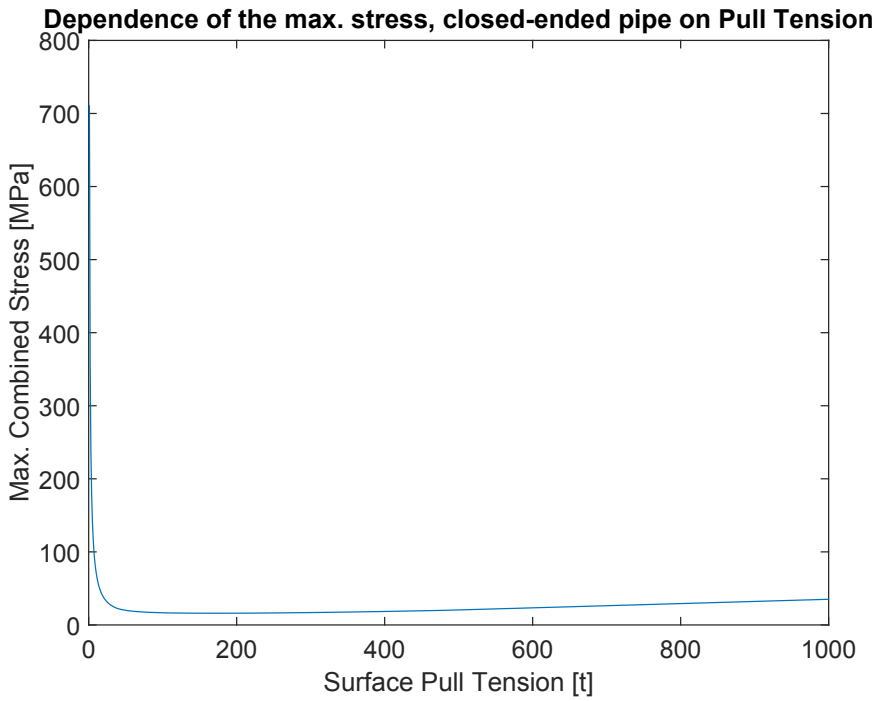

Figure C.6: Dependence of the maximum combined stress (Von Mises) with closed-ended pipe along the pipe catenary on the Horizontal Top Pull Force

C.2 Optimization with Closed-Ended Pipe

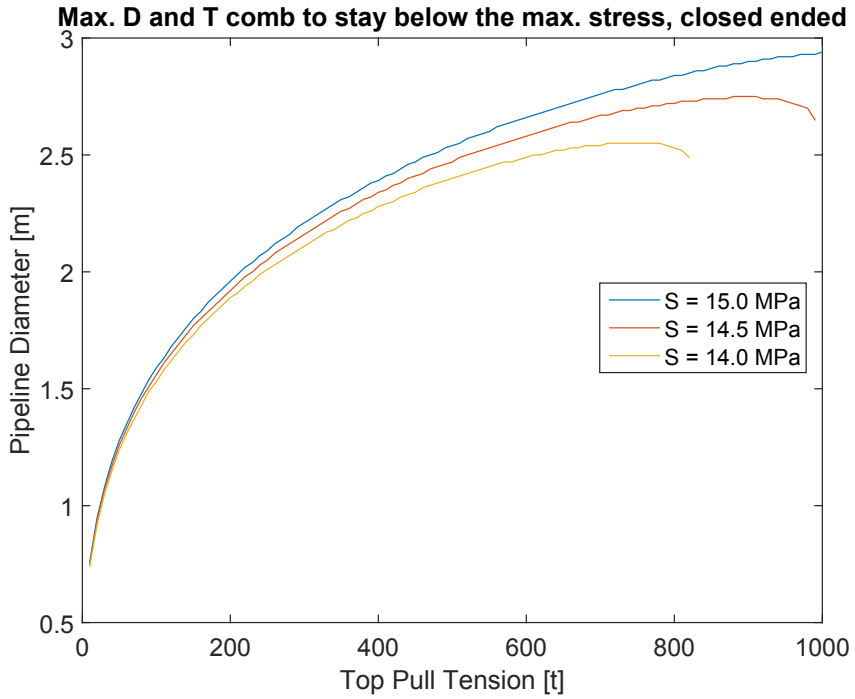

Figure C.7: Maximum pipeline diameter which can be installed with respect to stress when varying the pull tension using A_a=0.06, SDR=18, including closed-ended pipe

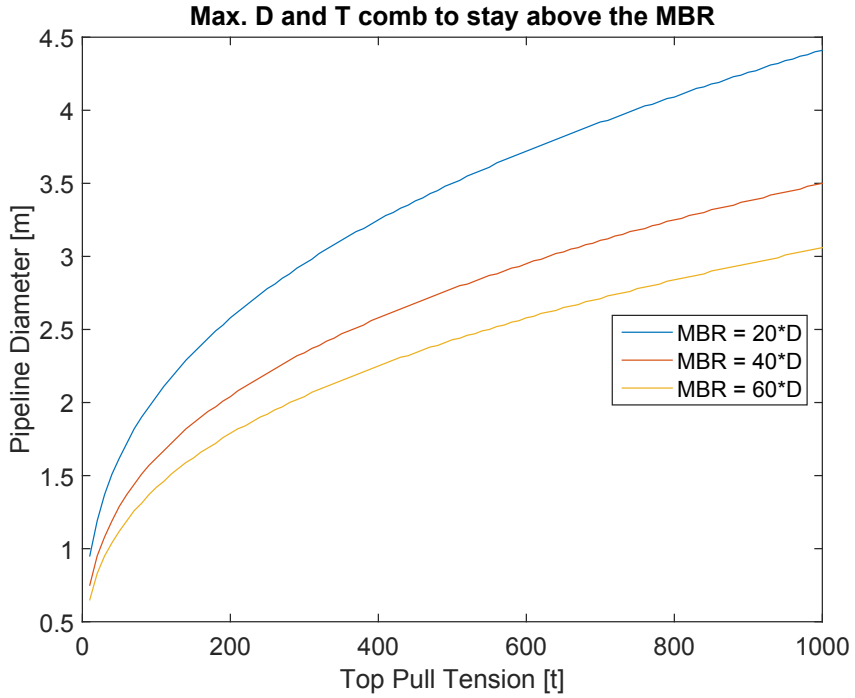

Figure C.8: Maximum pipeline diameter which can be installed with respect to the MBR when varying the pull tension using A_a=0.06, SDR=18, including closed-ended pipe

When the SDR is decreased and thus the pipe wall thickness is increased, it can be noticed that the optimal air fill ratio shifts. Due to the added thickness bending stress becomes more significant than stresses due to internal pressure. This can be seen in figure C.9. Here the large air fill ratio's are positioned at the top and thus allow for the largest pipeline diameter to be installed. The difference in installation capability using low and high air fill ratio is very low though, as the limit lines are bundled closely.

The maximum pipe diameter which can now be installed is about 3.5 m when using 1000 t top tension or 2.65 when using 350 t top tension.

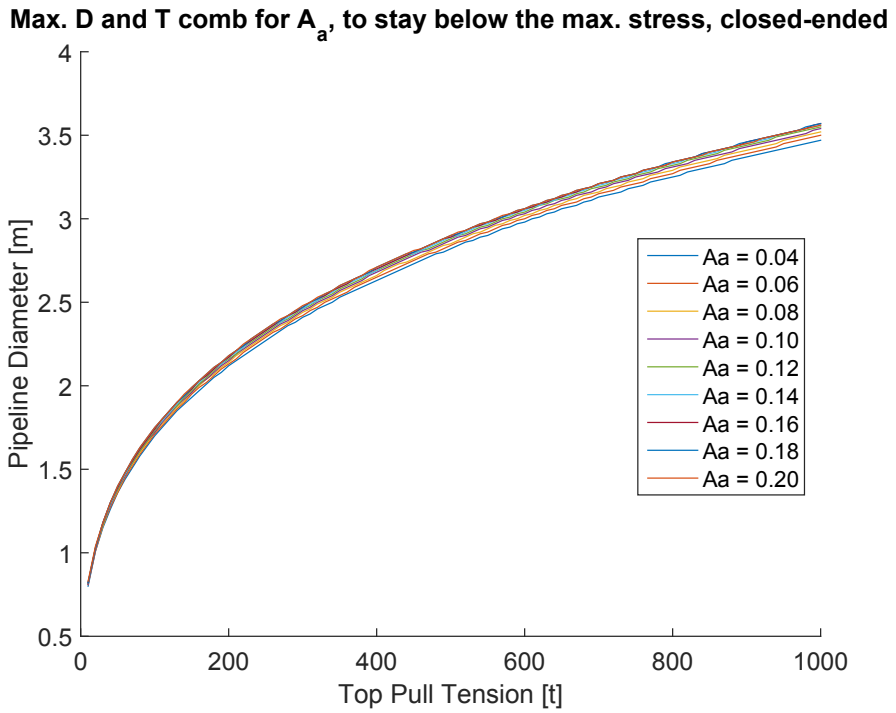

Figure C.9: Maximum pipeline diameter which can be installed with respect to stress when varying the pull tension and air fill ratio, including closed-ended pipe

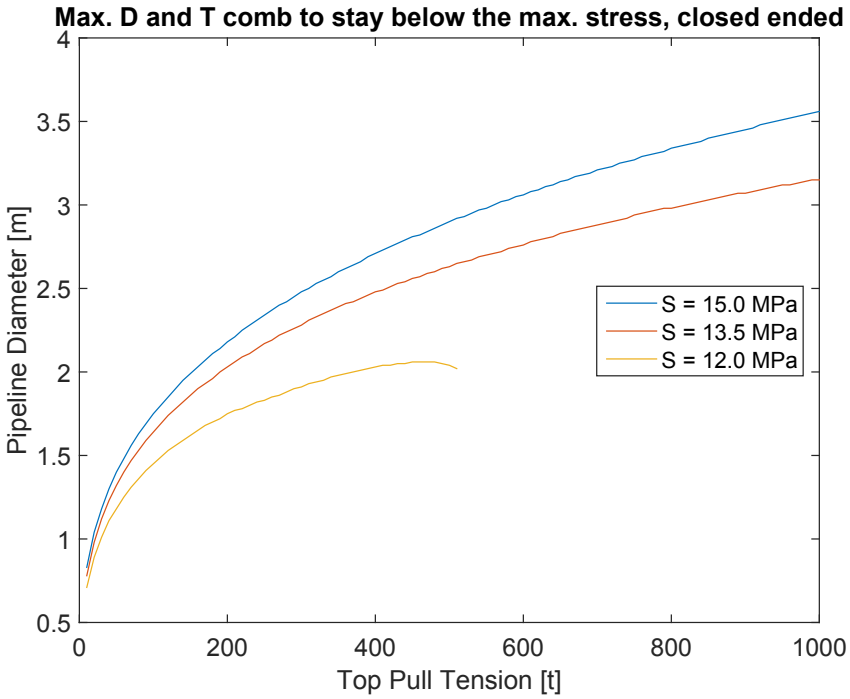

Figure C.10: Maximum pipeline diameter which can be installed with respect to stress when varying the pull tension using A_a=0.2, SDR=12, including closed-ended pipe

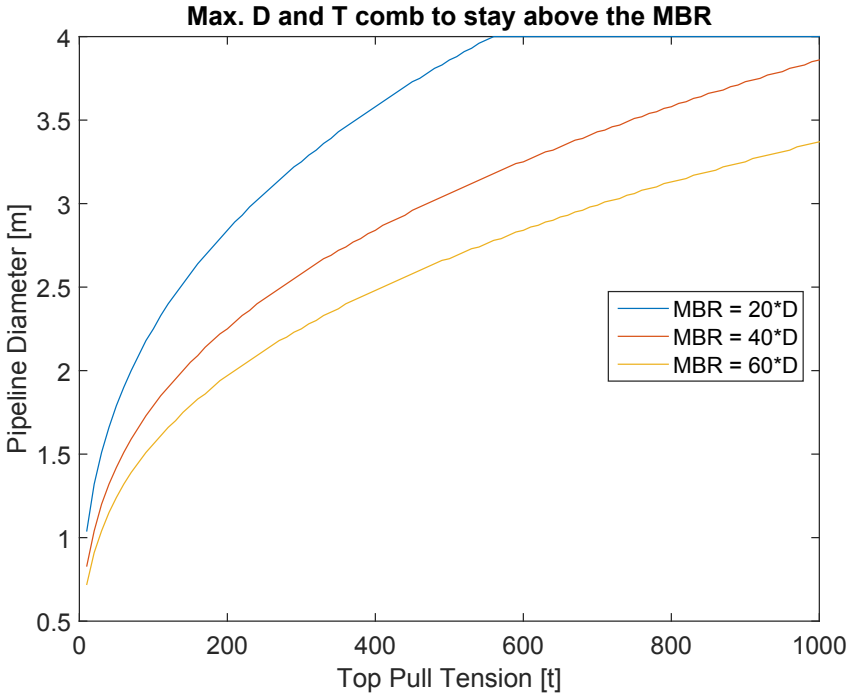

Figure C.11: Maximum pipeline diameter which can be installed with respect to the MBR when varying the pull tension using A_a=0.2, SDR=12, including closed-ended pipe

D

Appendix: MCA Additional Information

D.1 MCA Weight Factor Determination

In table D.1 the weight factor for each criterion is calculated. To do so, the criterion in the first column is compared to the criterion in the second, third, fourth, and so on, column. If the criterion in the first column is found to be more important, a 1 will be noted in the corresponding box. If the criterion in the first column is found to be less important than the criterion in the top row a 0 is noted in the corresponding box. For instance, if the price (column one, row three) of a CWP material is considered more important than the Durability (column five, row one) a 1 will be noted in the corresponding box of price vs durability (column five, row three). Consequently, a 0 will be noted in the opposing box of durability vs price (column three, row five). Additionally, a .5 can be noted for combinations of criteria which are closely linked and where it is thus very hard to decide which is more important.

The points for each criterion are then horizontally summed and divided by the total amount of points, which is 28 for 8 criteria, to obtain the weight factor.

From table D.1 it can be concluded that great emphasis is put on the environmental impact of a CWP material. This is due to the clean/sustainable energy image that OTEC/SWAC has and will have to maintain. When the CWP material is poisonous and endangers marine wildlife or people, OTEC/SWAC will not be accepted as a clean energy source. Furthermore, it is also important that the amount of CO_2 emitted during the creation of the complete OTEC plant will be significantly less than the amount of CO_2 saved by that same OTEC plant. Otherwise, the technology will cause more harm than it can ever prevent.

The second-most important criterion is the installation performance of a CWP material. This makes sense as when selecting an alternative CWP material to mainly increase the installation capabilities, it will only be useful to do so if the installation performance actually increases.

	1)	2)	3)	4)	5)	6)	7)	8)	Total	**Weight Factor**
Installation Performance 1)	x	1	1	1	1	1	1	0	6	**0.214**
Price 2)	0	x	1	.5	.5	.5	.5	0	3	**0.107**
Thermal Performance 3)	0	0	x	0	.5	.5	0	0	1	**0.036**
Durability 4)	0	.5	1	x	1	1	.5	.5	4.5	**0.161**
Manufacturability 5)	0	.5	.5	0	x	1	.5	0	2.5	**0.089**
Joinability 6)	0	.5	.5	0	0	x	0	0	1	**0.036**
Availability 7)	0	.5	1	.5	.5	1	x	0	3.5	**0.125**
Environmental Impact 8)	1	1	1	.5	1	1	1	x	6.5	**0.232**

Table D.1: MCA Weight Factor Determination

Furthermore, it can be noted that durability also has received a high weight factor. This is due to the fact that the pipe material will have to be able to atleast span the long lifetime of the OTEC plant. This is very important as the CWP accounts for a large portion of the total CAPEX of an OTEC plant. Additionally, a durable pipe will also be much more environmentally friendly than a non-durable pipe. This is because a non-durable pipe might have to be replaced once or more, likely resulting in a higher carbon footprint. Also, a non-durable pipe might cause more pollution, due to for example corrosive effects.

Price, Thermal performance, manufacturability, joinability and availability are all more or less economical aspects and thus combined, economics has also received a very significant weight factor. Thermal performance can for instance be enhanced with coatings or liners. Manufacturability, joinability and availability are aspects which are not necessarily technical deal breakers and more economical deal breakers. As most problems caused by a bad performance on one of these aspects can technically be overcome, but at an expense.

D.2 MCA Environmental Impact

In table D.2 some environmental impact data for the chosen alternative materials is given. This data is according to the CES Edupack 2014 level 3 Eco Design database [42] and belongs to the specific material grades as used in the detailed performance analysis of sections 4.2.1 to 4.2.4. From this table it can be seen that all five materials are available in relatively safe grades in terms of toxicity. Furthermore, GFRP is not recyclable, probably due to the fact that it is a cured composite which makes it hard to separate materials, and has the largest carbon footprint per kg of produced and formed material. HDPE and TPU have the lowest carbon footprint.

	HDPE	GFRP	TPU	ABS	PA
RoHS (EU) Compliant	✓	✓	✓	✓	✓
CO_2 footprint [kg/kg], Primary Production	2.46 – 2.92	10.6 – 11.7	2.56 – 2.83	3.64 – 4.03	7.58 – 8.38
CO_2 footprint [kg/kg], Forming	.442 – .489	1.48 – 1.63	.434 – .480	.434 – .480	.442 – .489
Recyclable	✓	X	✓	✓	✓
CO_2 footprint [kg/kg], Recycling	.897 – .991		.869 – .961	1.24 – 1.37	2.57 – 2.85
Landfill	✓	✓	✓	✓	✓
Biodegrade	X	X	X	X	X

Table D.2: Detailed Alternative Material Environmental Impact [42]